Enhanced Methanogenic Degradation of Propionate/Butyrate with Conductive Additives

By

Sajib Barua

A thesis submitted in partial fulfillment of the requirements for the degree of

Master of Science

In

Environmental Engineering

Department of Civil and Environmental Engineering

University of Alberta

Abstract

Direct interspecies electron transfer (DIET) is the recently discovered microbial syntropy between bacteria and methanogens in anaerobic digestion process that can accelerate the syntrophic conversion of various reduced organic compounds into methane through cell-to-cell electron transfer coupled with the reduction of carbon dioxide. DIET-based syntropy can occur via conductive pili and outer membrane c-type cytochromes, or through the addition of various conductive materials. In recent years, understanding and engineering DIET-based syntropy have emerged in improving methanogenesis kinetics to increase the robustness and decrease the footprint of the anaerobic digester. This study examined the effectiveness of conductive carbon fiber (CF) and magnetite doped granular activated carbon (GAC) in promoting DIET during syntrophic methanogenic conversion of propionate/butyrate. Carbon fiber enhanced specific methane production (mL-CH_4/g $COD_{Initial}$) by 2.4 folds than the unamended control bioreactor from propionate and butyrate as co-substrate, whereas propionate accumulated in the control. Various electroactive bacteria were abundant in the carbon fibers-amended bioreactor, while various fermentative bacteria were abundant in control. Likewise, magnetite doped-GAC particles stimulated specific methane production (mL-CH_4/g $COD_{Initial}$) by 1.5 times the unamended control bioreactor from propionate as sole substrate. Moreover, magnetite doped GAC performed better than GAC. In a nutshell, this study first demonstrates that CF and magnetite doped GAC particles can significantly stimulate methanogenesis rate through DIET based syntropy in the anaerobic digester.

Preface

Chapter 2 of this thesis has been published as S. Barua, B.R. Dhar, (2017) "*Advances Towards Understanding and Engineering Direct Interspecies Electron Transfer in Anaerobic Digestion*" in Bioresource Technology, vol. 244 part 1, 698-707. S. Barua was responsible for the data collection from the literature. B.R. Dhar planned and directed the study. All authors contributed to the manuscript preparation.

Chapter 3 of this thesis has been published as S. Barua, B.S. Zakaria, B.R. Dhar, (2018) "*Enhanced Methanogenic Co-degradation of Propionate and Butyrate by Anaerobic Microbiome Enriched on Conductive Carbon Fibers*" in Bioresource Technology, vol. 266, 259-266. S. Barua was responsible for experimental design, laboratory experiments, data interpretation and analyses. B.S. Zakaria conducted microbial community analysis, microscopic characterization, and data analysis. B.R. Dhar planned and directed the study. All authors contributed to the manuscript preparation

Chapter 4 of this thesis will be submitted as S. Barua, B.S. Zakaria, L. Lin, B.R. Dhar, (2019) "*Syntrophic Degradation of Propionate with GAC and Magnetite Doped GAC*". S. Barua was responsible for experimental design, laboratory experiments, data interpretation and analyses. L. Lin and B.S. Zakaria assisted in microbial community analysis and data analysis. B.R. Dhar planned and directed the study. All authors contributed to the manuscript preparation

Dedication

To my parents, and sister.

Acknowledgements

I would like to express my sincere gratitude to my supervisor Dr. Bipro Dhar, for the opportunity I got working with him. His constant guidance, valuable suggestions, constructive criticism, and meticulous help inspired me to dig the fundamentals of anaerobic digestion process through continuous improvement of my skills and knowledge. My sincere thanks also go to my M.Sc. thesis defence committee members (Dr. Zaher Hashisho, Dr. Mohamed Gamal El-Din, and Dr. Huazhou (Andy) Li) for their time and valuable comments on my thesis work.

I express my warm thanks to all my past and present friends, colleagues, and mentors for their support and help. My profound thanks go to Basem S. Zakaria and Dr. Long Lin for their assistance in microbial analysis for this project. I also thank Mrs. Chen Liang, and Mr. Yupeng (David) Zhao for their logistical and laboratory related training. I sincerely appreciate the help from Dr. Xihua Wang's lab in biomass conductance measurement. I would also like to thank Mr. Abdul Mohammed for his assistance in collecting anaerobic sludge for this project.

I express my gratitude to the donors of the scholarship (Alberta Innovates Graduate Student Scholarship) and awards (The Gordon R Finch Memorial Graduate Scholarship in Environmental Engineering, and Dr Donald R Stanley Graduate Scholarship in Environmental (Civil) Engineering) I received during my M.Sc. program at University of Alberta. I am also thankful to Natural Sciences and Engineering Research Council (NSERC) of Canada and Future Energy Systems at University of Alberta to support this research project.

Last but not least, I am grateful to my parents and sister for their continuous encouragement and support.

Table of Contents

List of Tables

List of Figures

Chapter 1

Introduction

1.1. Background

In recent years, waste biorefinery has become a popular concept for sustainable management of waste biomass that can significantly promote circular economy through the recovery of renewable energy, and various bio-based value-added products, including biogas, syngas, biohydrogen, biodiesel, bioplastics, alcohols, organic acids, etc. (Cherubini, 2010; De Corato et al., 2018; Rajendran et al., 2018; Sauvée and Viaggi, 2016). Anaerobic digestion (AD) is one of the most widely adopted biorefinery processes for various organic waste and high strength wastewater because AD produces biogas and nutrient-rich digestate (Appels et al., 2011; Carrere et al., 2016). Biogas can be used for on-site heat and electricity production through combined heat and power system (CHP), while digestate can be used as biofertilizer.

Anaerobic digestion of complex organics consists of three major steps: hydrolysis, fermentation, and methanogenesis. Among these steps, hydrolysis can be the rate-limiting step for lignocellulosic biomass (e.g., agricultural and forestry waste), whereas methanogenesis becomes rate-limiting step for readily biodegradable biomass (e.g., food waste, high strength wastewater, etc.) (Bouallagui et al., 2005; Hansen et al., 1998; Ren et al., 2018). During methanogenesis step, methanogens or methanoarchaea can only metabolize simple organic substrates (e.g., acetate, CO_2/H_2, methanol, formate, etc.) to produce methane (De Bok et al., 2004; Gujer and Zehnder, 1983). For instance, acetoclastic methanogens metabolize acetate, while hydrogenotrophic methanogens metabolize H_2/CO_2 to produce methane. Therefore, during AD process, methanogens build a syntrophic association with fermentative bacteria that can degrade volatile fatty acids (VFAs) and alcohols into acetate and CO_2/H_2. This syntrophic balance between fermentative bacteria and methanogens can easily be disrupted due to faster hydrolysis and fermentation step which results in irreversible acidification of digester (Cruz Viggi et al., 2014; Schmidt and Ahring, 1993). However, increasing the metabolite exchange rate between these syntrophic partners via microbial aggregates, such as granules, flocs, or biofilm, can prevent digester from acidification (Thiele and Zeikus, 1988). Interspecies H_2 transfer between methanogens and their syntrophic fermentative bacteria, known as interspecies hydrogen transfer (IHT), was believed to be putatively essential for the growth and metabolism of methanogens in

digester regardless of their association (e.g., close aggregation) with syntrophic partner (Iannotti et al., 1973; Thiele and Zeikus, 1988). However, some syntrophic bacteria have recently been discovered to transfer electrons directly towards methanogens through conductive nanowires and extracellular redox cofactors (e.g., c-type cytochrome) in the anaerobic aggregate of an up-flow anaerobic sludge blanket (UASB) reactor (Liu et al., 2012; Morita et al., 2011; Rotaru et al., 2014a, 2014b). This cell-to-cell electron transfer mechanism is termed as "direct interspecies electron transfer" (DIET) which is thermodynamically and metabolically faster than IHT (Cheng and Call, 2016; Lovley, 2011a, 2011b). Close aggregation of syntrophic partners like anaerobic aggregate might be difficult in reactors, such as continuous stirred tank reactor (CSTR). Nonetheless, recent findings have shown that DIET can be engineered in CSTRs simply deploying non-biological conductive materials, such as granular activated carbon (GAC), biochar, carbon cloth, iron nanoparticles, carbon nanotubes, etc. (Cheng and Call, 2016; Park et al., 2018; Sasaki et al., 2018).

The impact of conductive additives on the methanogenic degradation of various types of substrate (e.g., ethanol, acetate, glucose, dog food, etc.) have been reported in the literature (Cheng and Call, 2016; Lovley, 2017; Park et al., 2018; Sasaki et al., 2018). However, limited information is available in the literature on how the addition of conductive materials can influence the syntrophic degradation of propionate and butyrate in anaerobic digesters. Propionate and butyrate are one of the intermediates that is produced during the anaerobic digestion process and often detected in the acidified digester (Lin et al., 1986; Schmidt and Ahring, 1993). Thus, more insights into the role of conductive additives on propionate/butyrate degradation can improve the robustness of AD process. Additionally, further development of conductive additives would be essential for effectively engineering DIET in various configurations of anaerobic bioreactors. Studies have suggested that various conductive additives primarily promote the enrichment of electroactive bacteria as well as electrotrophic methanogens, and thereby enable DIET-based syntropy. Among various non-biological conductive materials examined for promoting DIET, only GAC and magnetite nanoparticles have been broadly studied for enhancing anaerobic digestion (Cheng and Call, 2016; Lovley, 2017; Park et al., 2018; Sasaki et al., 2018). Interestingly, various conductive materials are already being used as anode electrodes in microbial electrochemical systems, where enrichment of electroactive bacteria is a vital feature (Butti et al., 2016; Dhar et al., 2017a). Studies have shown that carbon fibers as an anode electrode could provide high surface area per unit volume for the enrichment of electroactive bacterial biofilms (Dhar et al., 2019,

2016b; Lee et al., 2019; Matsumoto et al., 2012; Yue et al., 1999). Furthermore, GAC surface doped with the iron particle is reported to boost electroactive bacteria enrichment in microbial electrochemical systems (Yasri and Nakhla, 2017, 2016). However, the effectiveness of carbon fiber and GAC doped with magnetite particles in stimulating DIET kinetics in anaerobic digester has yet to be examined.

1.2. Scope and Objectives

The overall goal of this study was to investigate the effects of conductive carbon fibers (CF) and magnetite doped granular activated carbon (GAC) in promoting methanogenesis from propionate/butyrate that are not readily biodegradable by methanogenic communities. Two specific objectives of this study were:

a) To study the impact of conductive carbon fibers on methanogenic co-degradation of propionate and butyrate.
b) To examine the effect of magnetite doped GAC on the methanogenic degradation of propionate.

Bench-scale studies were conducted to understand the effect of conductive materials on (i) methane productivity and kinetics, (ii) accumulation of volatile fatty acids, (iii) microbial communities and their syntrophic interactions.

1.3. Thesis Outline

This thesis is divided into five chapters. Chapter 1 (current chapter) highlights the background of the topic under investigation and summarizes the specific objectives of the proposed research. Chapter 2 presents a comprehensive literature review related to the proposed research. Chapter 3, and 4 present the findings from this thesis research in article format. Chapter 5 summarizes the results with their scientific and engineering implications and provides recommendations for future research.

Chapter 2

Literature Review

A version of this chapter was published in Bioresource Technology, vol. 244 part 1, pp. 698-707.

2.1. Introduction

Methanogenesis represents a significant portion of carbon flow in both natural and engineered anaerobic environments. Methanogenesis in engineered systems, such as anaerobic digester and microbial electrolysis cell, is of great importance in sustainable management and bioenergy recovery from organic waste and high strength wastewater. Among these two engineered systems, anaerobic digestion for methane production has already been widely adopted at full-scale for stabilization of various organic waste streams (Carrere et al., 2016; Cavinato et al., 2013). The microbes mediating methane-forming reactions in anaerobic digestion are known as methanogens or methanoarchaea (Thauer, 1998). Methanogens can utilize simple organic substrates, such as acetate, CO_2/H_2, methanol, and formate (De Bok et al., 2004; Gujer and Zehnder, 1983; Thauer, 1998). Hence, methanogens build syntrophic associations with other microorganisms for methane production from short-chain volatile fatty acids and alcohols, such as ethanol, propionate, butyrate, etc., produced from biodegradation of complex organic compounds (De Bok et al., 2004; Shin et al., 2010). These reduced organic compounds are usually found to be degraded to acetate and H_2/CO_2 by syntrophic microorganisms (mainly fermentative bacteria), and then consumed by methanogens. Acetoclastic methanogens utilize acetate; H_2 is consumed by H_2-utilizing or hydrogenotrophic methanogens for methane production via CO_2 reduction. Thus, hydrogenotrophic methanogens maintain low H_2 partial pressures that provide a thermodynamically feasible condition for fermentative bacteria to continue fermentation of the reduced organic compounds, such as ethanol, propionate, butyrate, etc. (De Bok et al., 2004; Gujer and Zehnder, 1983; Shin et al., 2010). In some methanogenic environments, formate has also been identified as an electron carrier between methanogens and fermentative bacteria (Boone et al., 1989). For many years, H_2 and formate transfer between methanogens and their syntrophic partners were thought to be the most sustainable mechanisms for interspecies electron transfer between methanogens and fermentative bacteria. Recent discoveries revealed that some bacteria

could directly transfer electrons to methanogens instead of interspecies H_2/formate transfer (Morita et al., 2011; Rotaru et al., 2014a, 2014b). This unique cell-to-cell electron transfer mechanism allows the methane production from the reduced organic compounds in a thermodynamically and metabolically more efficient manner (Cheng and Call, 2016), which ultimately provides rapid conversion of organic wastes to methane. This newly discovered mechanism of electron transfer between species has been recognized in the literature as "direct interspecies electron transfer (DIET)" (Cheng and Call, 2016; Dubé and Guiot, 2015; Lovley, 2011b, 2011a; Morita et al., 2011; Summers et al., 2010). Methanogens that can directly accept electrons from other species are called "electrotrophic methanogen" (Lovley, 2011a, 2011b).

Studies have shown that a wide variety of electron donating bacteria and electrotrophic methanogens can build a DIET-based syntrophic partnership, possibly driven by digester operating conditions, such as substrate type, organic loading rate, reactor configuration, and so on (Dang et al., 2017, 2016; Shrestha et al., 2014; Wang et al., 2016; Zhao et al., 2016a, 2015). As shown in Table 2-1, various DIET-active electron donating bacteria have been isolated from methanogenic digesters (Chen et al., 2014b, 2014a, Dang et al., 2017, 2016; Jing et al., 2017; H.-S. Lee et al., 2016; J.-Y. Lee et al., 2016; Lei et al., 2016; Lin et al., 2017; Rotaru et al., 2014a, 2014b; Zhuang et al., 2015). Among them, *Geobacter* and *Pseudomonas* species are known as "exoelectrogen" or "electrochemically active bacteria (EAB)" for their ability to produce electricity in microbial electrochemical systems via extracellular electron transfer (EET) (Chang et al., 2006; Logan, 2009). In comparison, other species, such as *Sporanaerobacter*, *Bacteroides*, *Streptococcus*, and *Syntrophomonas* are typically known as fermentative bacteria (Dang et al., 2017, 2016; Lei et al., 2016), and their ability to conduct EET is not yet conclusive.

An interspecies electrical connection between species has been found to be critical for DIET. *Geobacter* species can make a biologically wired connection to methanogens by producing filamentous protein appendages called electrically conductive pili or microbial nanowire (Rotaru et al., 2014b, 2014a; Shrestha et al., 2014). However, aggregation of species would be essential for such electrical connection, which may be possible in some specific configuration of anaerobic digesters, such as up-flow anaerobic sludge blanket (UASB) reactor. It has now been shown that the addition of non-biological conductive materials, such as granular activated carbon (GAC), biochar, carbon cloth, iron nanoparticles, carbon nanotubes, etc., in methanogenic bioreactors can

induce DIET-ability within a wide range of bacteria that can not produce conductive pili or nanowires like *Geobacter* species (Chen et al., 2014b, 2014a; Liu et al., 2012). Syntrophic partners can attach to the surface of these conductive materials and utilize them as electrical conduits for electron exchange. This approach can be metabolically more favorable since these conductive additives may alleviate the energy investment by microbes for the synthesis of these conductive pili (Zhao et al., 2015). Furthermore, this approach will allow sustainable engineering of DIET-based syntrophy in many configurations of anaerobic digesters.

Several studies have shown that facilitating DIET in anaerobic digestion can significantly enhance methanogenesis kinetics, thus, increases methane production rates (Chen et al., 2014b; Dang et al., 2016; Liu et al., 2012; Rotaru et al., 2014b, 2014a; Zhao et al., 2015). It was also apparent from these studies that a significant portion of electrons from reduced organic compounds (mainly volatile fatty acids and alcohols) can be efficiently recovered as methane via DIET, which may not be possible via interspecies H_2/formate transfer. Mathematical modeling has shown that DIET-based interspecies electron transfer rate can be 8.6 folds higher than that of interspecies H_2 transfer rate (Storck et al., 2016). Therefore, DIET-active digesters can handle relatively higher organic loading rates (OLRs) over conventional digester (Dang et al., 2016; Zhao et al., 2015).

This review article summarizes scientific and engineering advances in promoting DIET-based syntrophy in anaerobic digestion. Particular attention is given to the developments of various non-biological conductive additives for engineering DIET. Furthermore, research gaps are highlighted to suggest directions for future studies.

2.2. DIET-Active Microbial Communities

The current knowledge of DIET in methanogenic environments has been established based on the discovery of electric syntrophy between exoelectrogenic *Geobacter* species and methanogens (Morita et al., 2011; Rotaru et al., 2014a; 2014b; Shrestha et al., 2014; Liu et al., 2012). An evidence of DIET between bacteria and methanogens was first found in upflow anaerobic sludge blanket (UASB) reactors treating brewery wastewater (Morita et al., 2011). Microbial community composition analysis showed a dominance of *Methanosaeta concilii* and *Geobacter* species in these aggregates. *Methanosaeta* species are known as strictly acetoclastic methanogen (Garcia et al., 2000); *Geobacter* species can degrade simple organic acids and extracellularly exchange

electrons with their syntrophic partners in the absence of any conductive solids or insoluble electron acceptors (Summers et al., 2010). To understand the syntrophy between these two species in brewery digester, Morita et al. (2011) incubated the UASB aggregates with different electron donors, such as ethanol, hydrogen, formate, and acetate. The highest methane production rate was observed for ethanol, although acetoclastic methanogens were dominant in the aggregates. Methane production from hydrogen and formate were trivial. This finding suggested that an unknown methanogenesis pathway could be more dominant than methanogenesis via direct acetate utilization or interspecies H_2/formate transfer. Interestingly, the aggregates were electrically more conductive than a DIET-active co-culture aggregates of two *Geobacter* species (7.2 vs. 1.4 μS/cm). Hence, it was hypothesized that *Methanosaeta* species could be the syntrophic partner of *Geobacter* species, and aggregation of these two species in UASB granule might allow direct electron transport via *Geobacter* pili (see Figure 2-1(a)). Thus, this study first provided indirect evidence that DIET could happen in methanogenic digesters.

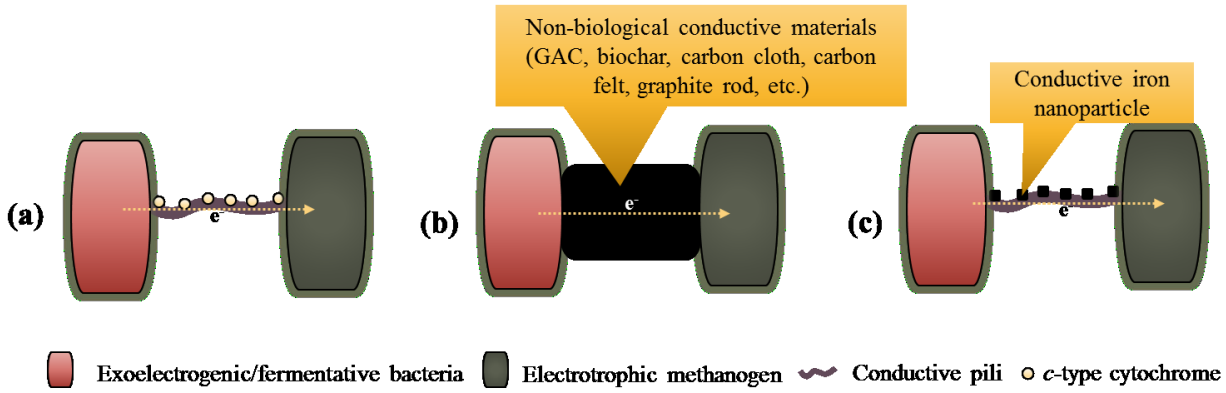

Figure 2-1. Schematic diagram showing mechanisms of direct interspecies electron transfer via: (a) conductive pili, (b) non-biological conductive materials, and (c) conductive iron nanoparticles (Note. Figures drawn with modifications after Shrestha and Rotaru (2014) and Kouzuma et al. (2015)).

Table 2-1. Summary of methanogenic communities showing direct/indirect evidence of DIET.

Electron Donor	Inoculum	Electrotrophic Methanogen	Possible Electron Donating Microorganism	Electron Conduit	Reference
Ethanol	Co-culture	*Methanosarcina barkeri*	*Geobacter metallireducens*	Conductive pili, GAC, biochar, and carbon cloth	Liu et al. (2012), Chen et al. (2014a; 2014b) and Rotaru et al. (2014b)
Ethanol	Co-culture	*Methanosaeta harundinacea*	*Geobacter metallireducens*	Conductive pili	Rotaru et al. (2014a)
Ethanol	Mixed	*Methanobacterium* and *Methanospirillum*	*Geobacter* and *Pseudomonas*	Graphene	Lin et al. (2017)
Ethanol and acetate	Mixed	*Methanosarcina* and *Methanobacterium*	*Geobacter* sp.	Hematite and Magnetite	Kato et al. (2012)
Acetate	Mixed	*Methanospirillum* and *Methanolinea*	*Geobacter* sp.	GAC	Lee et al. (2016)
Brewery wastewater and ethanol	Mixed	*Methanosaeta concilii*	*Geobacter* sp.	Conductive pili	Morita et al. (2011)
Glucose	Mixed	*Methanosaeta* and *Methanosarcina*	*Caloramator* sp.	Carbon nanotube	Yan et al. (2017)
Glucose	Mixed	*Methanosaeta, Methanospirillum,* and *Methanoregula*	*Geobacter* sp.	Graphene	Tian et al. (2017)
Butanol	Mixed	*Methanosaeata*	*Geobacter* sp.	Carbon cloth	Zhao et al. (2017)
Butyrate	Mixed	*Methanosarcinaceae*, *Methanocellales,* and *Methanobacteriales*	*Syntrophomonadaceae* and *Geobacteraceae*	Magnetite	Li et al. (2015a)
Butyrate	Mixed	*Methanosarcina*, and *Methanoregula*	*Syntrophomonas* and *Sulfurospirillum* species	Magnetite and carbon nanotube	Zhang and Lu (2017)
Butyrate and propionate	Mixed	*Methanosaeta and Methanosarcina*	*Geobacter* sp.	Conductive pili and GAC	Zhao et al. (2016a)
Propionate and acetate	Mixed	*Methanosarcina thermophila*	*Tepidoanaerobacter* sp. and *Coprothermobacter* sp.	Magnetite	Yamada et al. (2015)

Table 2-1. Continued.

Propionate	Mixed	*Methanospirillum* and *Methanosphaerula*	*Thauera sp*.	Magnetite	Jing et al. (2017)
Sucrose	Mixed	*Methanosaeta*	*Clostridium sensu stricto*	Polyaniline nanorods	Hu et al. (2017)
Benzoate	Mixed	*Methanobacterium*	*Peptococcaceae and Bacillaceae*	Hematite and Magnetite	Zhung et al. (2015)
Dog food	Mixed	*Methanosarcina*	*Sporanaerobacter*	Carbon cloth and GAC	Dang et al. (2016; 2017)
Leachate	Mixed	*Methanosarcina* and *Methanospirillum*	*Bacteroides*, *Streptococcus*, and *Syntrophomonas*	Carbon cloth	Lei et al. (2016)
Rice paddy soil	Mixed	*Methanothrix*	*Geobacter* sp.	Conductive pili	Holmes et al. (2017)

More direct evidence of DIET in methanogenic communities was found by Rotaru et al. (2014a). In their study, DIET was investigated with defined co-cultures of *Geobacter metallireducens* and *Methanosaeta harundinacea*, isolated from UASB aggregates (Rotaru et al., 2014a). *G. metallireducens* is unable to grow via interspecies H_2/formate transfer (Summers et al., 2010); *Methanosaeta harundinacea* can not utilize H_2/formate (Smith and Ingram-Smith, 2007). Despite these facts, co-cultures of these species successfully produced methane from ethanol with 96% electron recovery. A stoichiometric analysis of methane production suggested that *M. harundinacea* produced methane from both acetate and electrons released from the oxidation of methanol by *G. metallireducens*; 1.5 moles of methane produced from 1 mole of ethanol (see Figure 2-2). Metatranscriptomic analysis of co-cultures showed high expression of genes for pili and CO_2 reduction in *G. metallireducens* and *M. harundinacea*, respectively. In contrast, co-cultures of pilin-deficient *G. metallireducens* and *M. harundinacea* were unable to metabolize ethanol for methane production, which implied that conductive pili of *Geobacter* species played a major role in ethanol conversion to methane. Furthermore, radiotracer analysis with [^{14}C]-bicarbonate showed the reduction of $^{14}CO_2$ to $^{14}CH_4$, suggesting that *Methanosaeta* species could reduce CO_2 to methane by accepting electrons from *Geobacter* species (see Figure 2-2). Thus, multiple lines of evidence conclusively demonstrated that DIET could occur between these two species. A further study by Rotaru et al. (2014b) showed that acetoclastic *Methanosarcina barkeri* could also build a DIET-based syntrophic partnership with *G. metallireducens*. Recently, acetoclastic *Methanothrix* species (formerly *Methanosaeta*) have also been found to be capable of accepting electrons from *Geobacter* species (Holmes et al., 2017).

Rotaru et al. (2014a) previously found that co-cultures of *G. metallireducens* with H_2/formate utilizing *Methanospirillum hungatei* and *Methanobacterium formicicum* were unable to metabolize ethanol to methane. In contrast, recent studies have shown that the addition of non-biological conductive materials in anaerobic digester can promote DIET between exoelectrogens and hydrogenotrophic *Methanobacterium*, *Methanospirillum, Methanosphaerula,* and *Methanolinea* species (see Table 2-1). Furthermore, few studies provided indirect evidence of DIET between fermentative bacteria and methanogens in the presence of various conductive materials (Yamada et al., 2015; Dang et al., 2016; 2017; Lei et al., 2017; Hu et al., 2017). For instance, Yamada et al. (2015) reported that supplementation of magnetite in thermophilic anaerobic digester could induce DIET between acetoclastic *Methanosarcina thermophila* and

organic acids oxidizing bacteria (*Tepidoanaerobacter sp.* and *Coprothermobacter sp.*). Furthermore, studies reported DIET between various fermentative microorganisms (e.g., *Sporanaerobacter*, *Bacteroides*, *Streptococcus*, and *Syntrophomonas* species) and methanogens in the presence of GAC and carbon cloth (Dang et al., 2016; 2017; Lei et al., 2017). Although the presence of certain species on conductive additives not necessarily confirm their capability of DIET, these findings seem reasonable since several fermentative bacteria have been found to be capable of EET from their outer membrane proteins to anode electrode in microbial electrochemical systems (Wang et al., 2010; Lusk et al., 2015). To achieve more fundamental insights into DIET in complex microbial communities, further research needs to be done with defined co-cultures of these species.

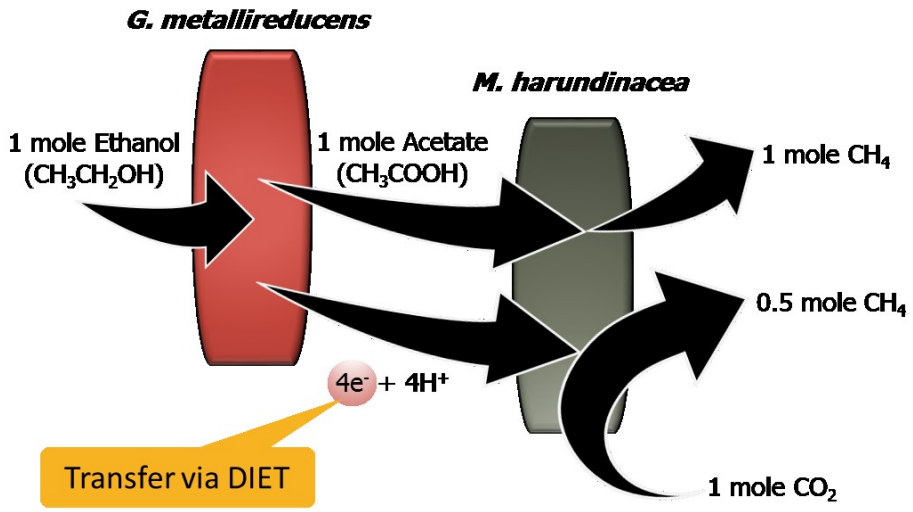

Figure 2-2. Conceptual schematic of DIET based electron transfer from *G. metallireducens* to *M. harundinacea* during ethanol conversion to methane (Note. Figure drawn with modifications after Rotaru et al. (2014a)).

2.3. Engineering DIET with Conductive Materials

DIET-active methanogenic communities seem to be abundant in some specific configuration of methanogenic digesters (e.g., UASB digester), where electrical connection between species exists due to aggregation of biomass. However, such electrical connection may not exist in other configurations of digesters, such as continuously stirred tank reactor (CSTR). Significant research

Table 2-2. Summary of different conductive materials used for engineering DIET in methanogenic bioreactor.

Conductive Material (Loading/specific surface area)	Inoculum	Mode	Temp. (°C)	Electron donor	Major Impact	Reference
GAC (25 g/L)	Co-culture[a]	Batch	37	Ethanol	Significantly decreased lag phase	Liu et al. (2012)
GAC (25 g/L)	Mixed[b]	Batch	37	Ethanol	CH_4 production rate increased by 2.5 times	Liu et al. (2012)
GAC (1 g/L)	Mixed[b]	Continuous	35	Acetate	CH_4 production rate increased by 1.8 times	Lee et al. (2016)
GAC (-)	Mixed[b]	Batch	37	Propionate and Butyrate[*]	Improved propionate and butyrate degradation and CH_4 production rates over control	Zhao et al. (2016a)
GAC (50 g/L)	Mixed[b]	Batch	37	Dog food[e]	CH_4 production rate increased by 18 times	Dang et al. (2017)
GAC (50 g/L)	Mixed[b]	Semi-continuous	37	Dog food[e]	CH_4 production rate was ~13 times at high OLR (8.5 kg COD/m^3-d)	Dang et al. (2016)
GAC (10 g/L)	Mixed[b]	Batch	55	Glucose	CH_4 production rate increased by 2.68 times	Yan et al. (2017)
GAC (0.5-5 g/L)	Mixed[b]	Batch	37	Waste activated sludge	CH_4 production increased by 17.4% at 5 g GAC/L	Yang et al. (2017)
Biochar (~28 g/L)	Co-culture[a]	Batch	37	Ethanol	No CH_4 production in the absence of biochar	Chen et al. (2014a)
Biochar (1.25 g/L)	Mixed[b]	Continuous[d]	37	Ethanol	CH_4 production rate increased by 30-45%	Zhao et al. (2015)
Biochar (5 g/L)	Mixed[b]	Continuous[d]	37	Butyrate[*]	CH_4 production rate increased by 1.25 times	Zhao et al. (2016b)
Biochar (5 g/L)	Mixed[b]	Continuous[d]	37	Propionate[*]	CH_4 production rate increased by 1.15 times	Zhao et al. (2016b)

Table 2-2. Continued.

Carbon cloth (100 cm^2/L)	Mixed[b]	Continuous[d]	37	Ethanol	CH_4 production rate increased by 30-45%	Zhao et al. (2015)
Carbon cloth (500 cm^2/L)	Mixed[b]	Semi-Continuous	37	Butanol	CH_4 production rate increased by 59%	Zhao et al. (2017)
Carbon cloth (1465 cm^2/L)	Mixed[b]	Batch	37	Dog food[e]	CH_4 production rate increased by 9.7 times	Dang et al. (2017)
Carbon cloth (1465 cm^2/L)	Mixed[b]	Semi-continuous	37	Dog food[e]	CH_4 production rate was ~13 times at high OLR (8.5 kg COD/m^3-d)	Dang et al. (2016)
Carbon cloth (833 cm^2/L)	Mixed[b]	Continuous[d]	33	Incineration leachate	CH_4 production rate increased by 1.3 times	Lei et al. (2016)
Carbon cloth (300-600 cm^2/L)	Co-culture[a]	Batch	37	Ethanol	Significantly improved ethanol degradation and CH_4 production rate	Chen et al. (2014b)
Carbon felt (1398 cm^2/L)	Mixed[b]	Semi-continuous	37	Dog food[e]	CH_4 production rate was ~13 times at high OLR (8.5 kg COD/m^3-d)	Dang et al. (2016)
Magnetite (6.4 mM as Fe)	Mixed[c]	Batch	-	Butyrate	Decreased the lag phase and CH_4 production increased by ~3 times	Li et al. (2015a)
Magnetite (25 mM as Fe)	Mixed[c]	Batch	30	Ethanol and Acetate	Decreased the lag phase and CH_4 production increased by ~1.4 times	Kato et al. (2012)
Magnetite (6.25 mM as Fe)	Mixed[b]	Batch	20-25	Propionate	CH_4 production rate increased by 1.3 times	Viggi et al. (2014)
Magnetite (10 mM as Fe)	Mixed[b]	Batch	55	Propionate and Acetate	Significantly improved propionate degradation rate	Yamada et al. (2015)
Magnetite (25 mM as Fe)	Mixed[c]	Batch	30	Benzoate	Decreased lag phase from 28 to 16 days	Zhuang et al. (2015)
Magnetite (10 mM as Fe)	Mixed[f]	Batch	30	Butyrate	CH_4 production rate increased by 34-90%	Zhang and Lu (2017)

Table 2-2. Continued.

Hematite (20 mM as Fe)	Mixed[c]	Batch	30	Ethanol and Acetate	Decreased the lag phase and CH_4 production increased by ~1.4 times	Kato et al. (2012)
Hematite (25 mM as Fe)	Mixed[c]	Batch	30	Benzoate	Decreased lag phase from 28 to 20 days	Zhuang et al. (2015)
Graphite (100 cm^2/L)	Mixed[b]	Continuous[d]	37	Ethanol	CH_4 production rate increased by 30-45%	Zhao et al. (2015)
Graphite (13,200 cm^2/L)	Mixed[b]	Semi-continuous	37	Dog food[e]	No improvement at different OLRs (1.6-10.3 kg COD/m^3-d)	Dang et al. (2016)
Graphene (30-120 mg/L)	Mixed[b]	Continuous[d]	10-20	Glucose	CH_4 production rate decreased by ~20% at 120 mg/L graphene	Tian et al. (2017)
Graphene (30-120 mg/L)	Mixed[b]	Batch	35	Glucose	CH_4 production rate increased by 51.4% at 120 mg/L graphene	Tian et al. (2017)
Graphene (0.5-2 g/L)	Mixed[b]	Batch	35	Ethanol	CH_4 production rate increased by 20% at 1 g/L	Lin et al. (2017)
Carbon nanotube (1 g/L)	Mixed[b]	Batch	55	Glucose	CH_4 production rate increased by 1.92 times	Yan et al. (2017)
Carbon nanotube (1 g/L)	Mixed[b]	Continuous[d]	35	Sucrose	CH_4 production rate increased by 2 times	Li et al. (2015b)
Carbon nanotube (5 g/L)	Mixed[f]	Batch	30	Butyrate	CH_4 production rate increased by 50%	Zhang and Lu (2016)
Polyaniline nanorod (0.3-1 g/L)	Mixed[b]	Batch	35	Sucrose	CH_4 production increased by 2 times at 0.6 g/L Polyaniline nanorod	Hu et al. (2017)
Stainless steel (0.2-0.8 g/L)	Mixed[b]	Continuous[d]	37	Acetate	CH_4 production increased by 4.5 times	Li et al. (2017)

[a]Co-culture of *Geobacter metallireducens* and *Methanosarcina barkeri;* [b]Anaerobic digester sludge; [c]Paddy field soil; [d]Upflow anaerobic sludge blanket (UASB); [e]Consisted of >26% protein, >19% fat, and <6.3% fiber; [f]Lake sediment; [*]Initially fed with

efforts to engineer DIET in methanogenic digesters have been focused on adding conductive non-biological materials, such as granular activated carbon (GAC), biochar, carbon cloth, graphite, magnetite nanoparticles, carbon-based nanomaterials, stainless steel, etc. (see Table 2-2). Results from these studies suggested that conductive materials can function as an electron conduit for the direct exchange of electrons between syntrophic partners. For instance, the addition of GAC successfully established DIET in co-culture of pilin-deficient *Geobacter metallireducens* and *Methanosarcina bakeri* (Rotaru et al., 2014b). Thus, the addition of conductive materials has shown a great potential to be a sustainable approach for engineering DIET. This section will feature performances of various conductive materials along with their fundamental roles in stimulating DIET.

2.3.1. Granular Activated Carbon (GAC)

GAC is commonly used as a support media for retention of biomass in various bioreactors (Singh and Prerna, 2009; Tao et al., 2017). GAC has been served as an efficient redox mediator for various environmental applications. For instance, GAC could accept electrons from microbial oxidation of organic acids, and could abiotically reduce recalcitrant azo dyes (Van Der Zee et al., 2003). Due to high surface area and electrical conductivity, GAC has been used as the electrode in various microbial electrochemical systems (Kumar et al., 2013; Wei et al., 2011; Liu et al., 2016). Deployment of GAC for different biocathode applications has suggested that a wide variety of microorganisms can accept electrons from GAC (Wei et al., 2011; Kalathil et al., 2012; Liu et al., 2014). Micro-porous GAC has been previously used in anaerobic digestion to adsorb toxic phenolic compounds that might inhibit methane production (Bertin et al., 2004a; 2004b; Goyal et al., 1996); while recent studies investigated GAC to stimulate DIET in methanogenic digesters (Liu et al., 2012; Lee et al., 2016; Dang et al., 2017; Yang et al., 2017; Yan et al., 2017). Liu et al. (2012) first hypothesized that GAC might facilitate DIET between bacteria and methanogens. The addition of GAC substantially reduced lag phase and enhanced methane production from ethanol in co-cultures of *G. metallireducens* and *M. barkeri* (Liu et al., 2012). Microscopic analysis of GAC-amended co-culture in their study showed that both species were tightly attached to the surface of GAC without making any aggregates for electrical connections via conductive pili. This observation suggests that the development of DIET-active microbial communities on the conductive solid surface of GAC can alleviate the role of conductive pili and outer membrane c-

type cytochromes (see Figure 2-1(b)). Zhao et al. (2015) hypothesized that biosynthesis of pili and c-type cytochromes requires a significant amount of energy investment by microbes. Thus, the presence of conductive materials may allow cells to conserve more energy, that may be the reason why DIET-active syntrophic partners attach to the surface of conductive additives.

To promote DIET, GAC has been applied in both continuous and batch anaerobic digesters fed with various organic substrates, such as ethanol, acetate, butyrate, propionate, waste activated sludge, and commercial dog food (see Table 2-2). It was evident from these studies that stimulating DIET with GAC can improve methanogenesis rate. For instance, amendments of GAC in a continuous anaerobic digester significantly increased the methane production rate by 1.8 times (Lee et al., 2016). Furthermore, the specific methane production (mL-CH_4/g VSS) from GAC attached biomass was 3.7 times higher than that of suspended biomass in their study, suggesting DIET-active microbial communities can produce a significant portion of methane. Dang et al. (2017) have reported that GAC amended digesters can perform better than carbon cloth amended digester, possibly due to the larger specific surface area provided by GAC. However, literature provides limited information on the optimum GAC loading (g/L) or specific surface area (m^2/L) required for improving DIET kinetics. As shown in Table 2-2, most of the studies were conducted with a specific GAC loading. Although Yang et al. (2017) recently reported that 5 g GAC/L could be optimum among different GAC loadings ranged from 0.5 to 5 g/L, other studies used relatively higher GAC loading from 10 to 50 g/L (Liu et al., 2012; Dang et al., 2017; Yan et al., 2017). Hence, more studies would be required to optimize the GAC loading or specific surface area for efficiently promoting DIET kinetics in anaerobic digestion.

2.3.2. Biochar

Biochar, a low-cost replacement of GAC, is produced through pyrolysis of plant and animal-based biomass (Ahmed et al., 2014). Biochar has been widely used as a sorbent for remediation of various soil and water contaminants, such as pentachlorophenol, atrazine, antibiotics, tylosin, pyrimethanil, heavy metals, etc. (Ahmed et al., 2014; Lu et al., 2017). Several studies previously used biochar as an additive to anaerobic digestion to alleviate methanogenesis inhibition by ammonia and acid stress (Lü et al., 2016; Shen et al., 2016; Luo et al., 2015; Fagbohungbe et al., 2016). It has now been shown that biochar can also promote DIET between methanogen and their syntrophic partners (Chen et al., 2014a; Zhao et al., 2015). Chen et al. (2014a) first investigated

biochar for improving DIET kinetics between *Geobacter metallireducens* and *methanosarcina barkeri*. The addition of biochar in their study resulted in 86% electrons recovery as methane from ethanol, which was comparable with 77% electron recovery previously observed with GAC (Liu et al., 2012). Based on the microscopic analysis, Chen et al. (2014a) also suggested that the mechanism of biochar-engineered DIET could be analogous to that of GAC.

2.3.3. Carbon Cloth

Carbon cloth has been proven as a very promising electrode material in microbial electrochemical systems (Wei et al., 2011; Hindatu et al., 2017). Although few studies previously used carbon cloth to improve retention of biomass in digesters (Sasaki et al., 2011; Tatara et al., 2005), the potential impact of carbon cloth in DIET has not been addressed in these studies. Chen et al. (2014b) first studied the feasibility of carbon cloth for improving DIET kinetics. They found that *Geobacter* strains lacking pili and *c*-type cytochromes could facilitate cooperative electron exchange with *Methanosarcina barkeri* in the presence of carbon cloth. Among three conductive carbon materials (carbon cloth, graphite rod, and biochar), carbon cloth showed superior performance in terms of COD removal during syntrophic conversion of ethanol to methane using mixed culture (Zhao et al., 2015). However, methane production rates at different hydraulic residence times (HRTs) were 30-45% higher for all conductive materials.

2.3.4. Iron Nanoparticles

In recent years, synthesis of iron nanoparticles, such as magnetite and hematite, has drawn significant attention due to their diverse applications in heterogeneous catalysis, drug delivery, bioseparation, and biosensing (Wu et al., 2015). These minerals are also abundant in nature, and their presence in soils and subsurface sediments can facilitate extracellular electron transport by iron-reducing microorganisms, such as *Geobacter* species (Kato et al., 2010; Liu et al., 2014). Kato et al. (2012) first found that addition of haematite and magnetite in anaerobic digesters can significantly reduce the lag time and enhance methane production rate due to a DIET-based syntropy. However, studies suggested that mechanism of stimulating DIET by iron nanoparticles would be different from other non-biological conductive materials (Viggi et al., 2014; Baek et al., 2017; 2016; Liu et al., 2015). Syntrophic microorganisms can attach to surfaces of relatively larger (mm scale) conductive materials, such as GAC, biochar, etc. Therefore, the addition of these

materials can stimulate DIET in the absence of pili (Liu et al., 2015). In comparison, iron nanoparticles (20-50 nm) attach to conductive pili, and mainly alleviate the requirement of multi-heme *c*-type cytochromes for DIET (see Figure 2-1(c)) (Liu et al., 2014). Therefore, magnetite-supplemented methanogenic biomass showed complex aggregate structure due to extensive colonization (Viggi et al., 2014; Baek et al., 2017; 2016). Thus, promoting DIET between the distant syntrophic partners may not be possible with nanoparticles (Liu et al., 2015).

To date, several studies have shown that iron nanoparticles can significantly accelerate DIET between bacteria and methanogens (see Table 2-1 & 2-2). However, most of these studies have been conducted in batch mode, and it would be an engineering challenge to retain these nanoparticles during continuous operation. Recently, Baek et al. (2017) have shown that recycling biomass can be a sustainable method for minimizing magnetite particle washout from methanogenic digester during long-term operation.

2.3.5. Stainless Steel

Li et al. (2017) recently studied the effects of stainless-steel addition in a UASB digester fed with sulfate-rich acetate medium. The addition of 0.5 g/L of stainless steel could increase methane production rate by 4.5 times over control. Microbial and electrochemical characterization of the biomass attached on stainless steel surface suggested that DIET-based syntrophy between *Geobacter* species and methanogen could outcompete microbial sulfate-reduction process that occurs via interspecies hydrogen transfer (IHT); electron transfer kinetics of DIET-based methanogenesis was 10^8 folds faster than that of sulfate-reduction via IHT. Along with affordable price and high conductivity, stainless steel can be more advantageous over carbon-based conductive materials due to their high chemical resistance and mechanical strength (Li et al., 2017). However, weak adhesion of attached biomass on stainless steel surface can be a concern (Kumar et al., 2013). Hence, the long-term sustainability of stainless steel in engineering DIET should be further investigated.

2.3.6. Carbon-Based Nanomaterials

Development of nanotechnology has introduced various carbon-based nanomaterials, such as graphene and carbon nanotubes. These nanomaterials provide various unique physicochemical properties including high electrical conductivity and larger surface area (Zhang et al., 2013).

Although antimicrobial properties (e.g., cellular oxidative stress, cell apoptosis, etc.) of these nanomaterials have been reported (Simon-Deckers et al., 2009), they are being used as electrodes in various microbial electrochemical systems (Ren et al., 2015; Mink and Hussain, 2013). Few recent studies have shown that addition of these carbon-based nanomaterials can promote DIET in anaerobic digestion (see Table 2-2). Tian et al. (2017) studied long and short-term effects of nano-graphene on methanogenesis. Short-term exposure of methanogenic communities to graphene (30 and 120 mg/L) significantly increased methane production rate. However, long-term exposure to graphene at 120 mg/L showed slight inhibition of methanogenesis, although the inhibition mechanism was unknown. In comparison, Lin et al. (2017) found that DIET between exoelectrogens and hydrogenotrophic methanogens can be engineered at a relatively high concentration of graphene (1 g/L). Zhang and Lu (2017) showed that addition of 5 g/L of multi-walled carbon nanotube (MWCNT) could increase methane production rate by 50% due to enhanced DIET kinetics. However, these studies provide limited information on how these nanomaterials facilitate DIET. Li et al. (2015b) found that extracellular polymeric substances (EPS) secreted by mesophilic methanogenic communities closely networked with single-walled carbon nanotubes (SWCNTs) and formed more densely packed aggregates. Similar aggregates were formed in digester supplemented with magnetite nanoparticles (Viggi et al., 2014; Baek et al., 2017; 2016). Thus, there is a possibility that the fundamental mechanism of promoting DIET with carbon-based nanomaterials may be analogous to that of iron nanoparticles, which has not yet been studied.

As summarized in Table 2-2, the addition of various carbon-based nanomaterials up to a certain concentration level can significantly improve DIET kinetics. Nonetheless, economic feasibility would be one of the most critical factors for carbon-based nanomaterials. Considering the price of $100/kg CNT (Zhang et al., 2013), supplementation of 1 g CNT/L would cost $100,000 per m^3 of the digester. In contrast, the approximate cost for GAC loading at 50 g/L would be $15-150 per m^3 of the digester ($300-3000/tonnes GAC; source: www.alibaba.com). Thus, the high cost of carbon-based nanomaterials may impede their widespread adoption in engineering DIET. However, a comprehensive techno-economic evaluation of various conductive materials is required to find the most feasible material for the field-scale application.

2.3.7. Conductive Polymeric Material

Application of highly conductive and biocompatible conductive polymers, such as polyaniline and polypyrrole, significantly improved biological electron transfer kinetics in various microbial electrochemical systems (Kumar et al., 2013; Luckarift et al., 2012; Yong et al., 2012). Recently, Hu et al. (2017) first studied the feasibility of polyaniline (PANI) nanorods (diameter of ~250 nm and a length of ~3000 nm) for stimulating DIET in anaerobic digestion. The addition of 0.6 g/L of PANI in batch anaerobic digester almost doubled the methane production over control; suggesting PANI can be an efficient alternative conductive material for engineering DIET between bacteria and methanogenic archaea. Microscopic analysis showed that PANI nanorods were uniformly distributed in the digester sludge. Few studies previously suggested that positively charged PANI can electrostatically interact with the negatively charged microbial cell membrane and can attach to their redox active outer membrane proteins (Yong et al., 2012; Lai et al., 2011). Furthermore, the branching structures of PANI can act as conductive nanowires like pili in facilitating EET from outer membrane proteins to conductive solids (Yong et al., 2012; Lai et al., 2011). Thus, there is a possibility that PANI may act as a substitute for pili in promoting DIET in methanogenic communities, which warrant further investigation.

2.4. Role of Electrical Conductivity in DIET

The significance of electrical conductivity in DIET has been recognized in the literature (Zhao et al., 2016a; Shrestha et al., 2014). As summarized in Table 2-3, multi-species aggerates from methanogenic digesters exhibited ohmic conductivity ranged from 0.2 to 36.7 μS/cm. Moreover, exponential increase in aggregate conductivity upon cooling from room temperature confirmed that there was no contribution from any inorganic metals or minerals in the two-electrode conductivity measurements, and conductivity was solely attributed to biological conductive materials (Morita et al., 2011). The similar conductive nature has also been observed for mixed-culture anode biofilms in microbial electrochemical systems, where *Geobacter* species were identified as the key players contributing to the electrical conductivity of anode biofilms (Malvankar et al., 2012a; Dhar et al., 2016; Lee et al., 2016). The abundance of conductive pili in *Geobacter* biofilms showed a strong relationship with biofilm conductivity (Malvankar et al., 2011; 2012a); the conductivity of an individual *G. metallireducdens* pili can be as high as 277±18.9 S/cm (Tan et al., 2017). In comparison, cytochromes showed a minimal contribution to anode

biofilm conductivity (Malvankar et al., 2012b), although they are essential for extracellular electron transport between pili and the electron acceptor or donor (Lovley, 2011a; Liu et al., 2015). Hence, it has been assumed that *Geobacter* pili would be mainly responsible for electrical conductivity of methanogenic aggregates (Morita et al., 2011; Shrestha et al., 2014). Shrestha et al. (2014) found a moderate correlation (r = 0.67) between the abundance of *Geobacter* species and UASB aggregate conductivity; while the abundance of sulfate-reducing bacteria, fermentative bacteria, and methanogens showed an insignificant relationship with aggregate conductivity. However, few studies have shown that sulfate-reducing bacteria (e.g., *Desulfovibrio* spp.) and some fermentative bacteria can produce electrically conductive nanowires like *Geobacter* pili for facilitating EET (Eaktasang et al., 2016; Gorby et al., 2006). Therefore, we can not completely rule out the fact that microorganism other than *Geobacter* species can facilitate DIET via electrically conductive nanowires. As shown in Table 2-3, methanogenic aggerates in most studies also showed higher electrical conductivity than the dual-species aggregates of *Geobacter metallireducens* and *Geobacter sulfurreducens* (1.4±0.3 μS/cm), previously reported by Morita et al. (2011). For instance, Zhao et al. (2016a) reported that aggregate conductivity could be as high as 16.5 μS/cm, where relative abundance of *Geobacter* species was only 3.03%. Furthermore, the aggregates from a UASB reactor treating leachate from municipal solid waste incineration plant also showed conductive nature (5.47 μS/cm), even when *Geobacter* species were not detected (Lei et al., 2016). Thus, the contribution of other microorganisms in aggregate conductivity is yet to be investigated in detail. There is also the possibility that various environmental parameters such as pH and temperature can influence the expression of conductive pili produced by *Geobacter* and other potential DIET-active species (Malvankar et al., 2011; 2012b; 2014; Adhikari et al., 2014). Hence, further investigation of the significance of these environmental parameters in aggregate conductivity is needed to expand fundamental understanding of DIET in anaerobic digestion.

Liu et al. (2012) previously hypothesized that addition of GAC might improve DIET kinetics due to its high electrical conductivity (3000±327 μS/cm) over that of methanogenic aggregates (0.2-36.7 μS/cm). In comparison, the electrical conductivity of biochar was significantly lower (2.11-4.41 μS/cm) than other conductive materials used for stimulating DIET (see Table 2-4). However, biochar has been found to be almost as effective as GAC in promoting DIET kinetics in co-cultures of *Geobacter metallireducens* and *methanosarcina barkeri* (Chen et

al., 2014a). Furthermore, the addition of semi-conductive haematite and conductive magnetite showed comparable methane production rates in DIET stimulated methanogenic environments, although their electrical conductivity was different (Kato et al., 2012). Thus, these results might infer that the electrical conductivity above a certain threshold would be adequate to trigger DIET-based syntrophy in methanogenic digesters.

Table 2-3. Electrical conductivity of UASB aggregates without conductive additives.

Conductivity (μS/cm)	**Electron Donor**	**Relative abundance of *Geobacter* species**	**Reference**
6.1-7.2	Brewery wastewater	25%	Morita et al. (2011)
0.8-36.7	Brewery wastewater	2.3-29%	Shrestha et al. (2014)
7.6	Propionate	2.01%	Zhao et al. (2016a)
16.5	Butyrate	3.03%	Zhao et al. (2016a)
5.47	Leachate from incineration plant	-	Lei et al. (2016)

Table 2-4. Electrical conductivity of non-biological conductive materials used for promoting DIET in methanogenic digester.

Conductive Material	**Conductivity (μS/cm)**	**Reference**
Granular activated carbon	3000	Liu et al. (2012)
Carbon cloth	4350	Lei et al. (2016)
Biochar	2.11-4.41	Chen et al. (2014a)
Single-walled carbon nanotube	>100	Yan et al. (2017)
Polyaniline nanorod	740	Hu et al. (2017)

2.5. Significance of Substrate Characteristics in DIET

To date, various electron donors have been explored for studying DIET in anaerobic digestion. However, most of these studies used simple organic acids and alcohols; while few studies used complex organic wastes, such as dog food, waste activated sludge, and leachate. Mixed-culture studies conducted with ethanol identified *Geobacter* species as a key microbial player involved in DIET with methanogens (Lin et al., 2017; Zhao et al., 2016a). The mechanisms of DIET involved

in ethanol conversion to methane is well understood from co-culture studies (Liu et al., 2012; Rotaru et al., 2014a; 2014b). However, ethanol may not be the key intermediate during fermentation of complex organic wastes in anaerobic digestion; other reduced organic compounds, such as propionate and butyrate can be primary intermediates in some methanogenic digesters (De Bok et al., 2004; Wang et al., 2016; Shin et al., 2010). A recent study has shown that co-cultures of *G. metallireducens* and *Methanosarcina barkeri* can not metabolize propionate and butyrate even in the presence of conductive materials, probably due to the metabolic constraints of these species (Wang et al., 2016). In contrast, few mixed-culture studies provided indirect evidence that addition of conductive materials might promote conversion of propionate and butyrate to methane (Cruz Viggi et al., 2014; Li et al., 2015a). However, the potential pathways and microorganisms involved in DIET coupled to methane production from propionate or butyrate were not clear from these studies. Zhao et al. (2016a) recently demonstrated that long-term enrichment of methanogenic communities with ethanol could promote syntrophic propionate or butyrate degradation. Microbial community analysis showed the presence of *Geobacter* and *Methanosaeta* or *Methanosarcina* species in the aggregates. Since some *Geobacter* species can metabolize butyrate (Prakash et al., 2010), they hypothesized that *Geobacter* species might be involved in degradation of butyrate or propionate coupled to DIET with methanogens.

Studies conducted with complex organic wastes (e.g., dog food, leachate, etc.) have suggested that fermentative microorganisms would mainly participate in DIET in the presence of conductive materials (Dang et al., 2016; 2017; Lei et al., 2016). For instance, Lei et al. (2016) found an abundance of fermentative bacteria (*Bacteroides*, *Streptococcus*, and *Syntrophomonas* species) and acetoclastic *Methanosarcina* in a digester amended with carbon cloth, and operated with leachate from incineration plant leachate. Dang et al. (2016) suggested that fermentative *Sporanaerobacter* species might use altered metabolic pathways for conversion of complex organics to acetate and carbon dioxide along with direct electron transfer to *Methanosarcina* species. Such metabolic alteration might alleviate production of butyrate, propionate, and H_2. It seems that DIET mechanisms in anaerobic digesters fed with real organic wastes can be more complex than that of simple organic substrate. Hence, further investigations would be required to confirm these possibilities suggested for DIET-based syntrophic conversion of complex organics to methane.

2.6. Influence of Organic Loading Rates

Organic loading rate (OLR) is one of the most critical process parameters for anaerobic digestion that can affect methanogenic activity and kinetics (Ferguson et al., 2016; Ziganshin et al., 2016; Gou et al., 2014). OLR is typically maintained in a digester by manipulating HRT. The operation of digesters at high OLRs is preferred due to smaller footprint of digesters and lower heating cost; while an optimum OLR primarily depends on the substrate characteristics, such as biodegradability, C/N ratio, etc. At high OLRs, fermentation rate can be faster than methanogenesis rate, which can result in process instability or complete failure due to an irreversible acidification of digester through accumulation of short-chain volatile fatty acids and alcohols (Ferguson et al., 2016; Ziganshin et al., 2016; Gou et al., 2014). For example, OLR of 8.5 kg COD/m^3/d completely inhibited methanogenesis in mesophilic co-digestion of food waste and municipal waste activated sludge (Gou et al., 2014). Studies have shown that promoting DIET-based syntrophy in the digester can significantly enhance the conversion of volatile fatty acids and alcohols to methane, which can allow the operation of digesters at high OLRs (i.e., shorter HRT) (Zhao et al., 2015; Dang et al., 2016). Zhao et al. (2015) studied the effects of different OLRs, ranged from 4.11 to 12.33 kg COD/m^3/d, in continuous UASB digesters amended with biochar, graphite, and carbon cloth. At each OLRs, the control digester (without conductive materials) showed 30-45% lower methane production rates from ethanol along with an accumulation of high concentrations of ethanol and acetate in the effluent. Dang et al. (2016) investigated the effects of various OLRs, ranged from 1.6 to 10.3 kg COD/m^3/d, in digesters fed with commercial dog food consisted of protein, fat, and fiber. Digester amended with GAC demonstrated sustained methane production with minimal accumulation of various volatile fatty acids and alcohols at a high OLR of 10.3 kg COD/m^3/d. In comparison, methane production from the control digester significantly dropped at OLRs of >6.7 kg COD/m^3/d due to the acidification of the digester; pH dropped to ~6 at OLR of 8.5 kg COD/m^3/d. Thus, it was evident that engineering DIET could reduce the acid stress in digesters operated at high OLRs. However, interestingly, both control and DIET-active digesters amended with conductive materials in their study showed comparable methane production rates at OLRs of <6.7 kg COD/m^3/d. This finding implied that engineering DIET would be more effective at higher OLRs when digesters are operated with complex feedstocks; possibly the distribution of volatile fatty acids and alcohols at higher OLRs would play a key role in structuring the DIET-active microbial communities. Hence, it would be interesting to see how

the different OLRs shifts the microbial community structure and abundance of DIET-active species.

2.7. Conclusions

Engineering DIET is an emerging strategy for improving anaerobic digestion of organic waste. Co-culture studies established the mechanisms pertaining to DIET from simple organic substrates; while much remains to be discovered regarding the DIET in anaerobic digestion of complex organic wastes. Different conductive additives have been identified that enable DIET-based syntrophy between bacteria and methanogens, although the significance of electrical conductivity and surface area of these conductive additives in accelerating DIET kinetics is not yet conclusive. Hence, further developments in fundamental understanding would be required to develop sustainable strategies for engineering DIET in anaerobic digestion.

Chapter 3

Enhanced Methanogenic Co-degradation of Propionate and Butyrate by Anaerobic Microbiome Enriched on Conductive Carbon Fibers

A version of this chapter was published in Bioresource Technology, vol. 266, pp. 259-266.

3.1. Introduction

Anaerobic methanogenesis, one of the most popular bioprocesses for organic waste and high-strength wastewater treatment, produces bio-methane that can be used to meet on-site heat and electricity needs. The process of methanogenesis relies on the microbial breakdown of complex organics. In addition to inferior kinetics, process stability issues remain ongoing challenges in the operation of the high-rate methanogenic bioreactors (Ferguson et al., 2016; Ziganshin et al., 2016). Accumulation of various organic acids and alcohols, particularly at high organic loading rates, can lead to inhibition of methanogens by irreversible acidification (Ferguson et al., 2016; Ziganshin et al., 2016).

Propionate and butyrate are key metabolites produced during anaerobic degradation of complex organic matter in waste and wastewater. The biodegradation of propionate and butyrate is thermodynamically unfavourable ($\Delta G^o > 0$) under standard conditions; hence, accumulation of these organic acids often leads to process instability or the complete failure of methanogenic bioreactors (Curz Viggi et al., 2014; Jing et al., 2017; Zhao et al., 2016a, 2016b). However, propionate and butyrate can be oxidized to acetate, bicarbonate, and hydrogen (H_2) or formate through a syntrophic partnership between propionate/butyrate-oxidizing bacteria and methanogenic archaea (Jia and Fang, 1999; Schmidt and Ahring, 1993). Acetoclastic methanogens convert acetate to methane. On the other hand, hydrogenotrophic methanogens utilize H_2 for carbon dioxide (CO_2) reduction to methane (CH_4), which is known as interspecies hydrogen transfer (IHT) (Cheng and Call, 2016). In addition to this IHT, recent studies have identified a unique syntrophic pathway for methanogenesis, known as direct interspecies electron transfer (DIET) (Barua and Dhar, 2017; Cheng and Call, 2016; Lovley, 2017; Rotaru et al., 2014a, 2014b). This unique syntropy enables cell-to-cell electron transport between bacteria and methanogen, which is coupled with CO_2 reduction to CH_4. The DIET creates thermodynamically and

metabolically favourable conditions within the anaerobic microbiome that enable the rapid conversion of various organic acids and alcohols to CH_4 (Cheng and Call, 2016; Lovley, 2017; Park et al., 2018). The DIET-active methanogenic communities can be naturally established with conductive nanowires and extracellular redox cofactors (e.g., *c*-type cytochrome) produced by electroactive bacteria, (e.g, *Geobacter* species); however, DIET can also be engineered with the addition of non-biological conductive materials, such as granular activated carbon (GAC), biochar, carbon cloth, magnetite, carbon nanomaterials, etc. (Barua and Dhar, 2017; Cheng and Call, 2016; Lovley, 2017; Park et al., 2018; Zhao et al., 2015). It has been hypothesized that conductive materials might alleviate the energy investment by electroactive bacteria for biosynthesis of nanowires or cytochromes.

To date, limited information is available on the methanogenic degradation of propionate/butyrate through DIET. Few mixed-culture studies suggested that the addition of conductive materials (e.g., GAC, magnetite, biochar), as well as the enrichment of the methanogenic communities with ethanol, can accelerate conversion of propionate and butyrate as sole electron donors by promoting DIET along with IHT (Cruz Viggi et al., 2014; Jing et al., 2017; Li et al., 2015; Zhang and Lu, 2016; Zhao et al., 2016a, 2016b). Amendment of anaerobic bioreactors with magnetite nanoparticles significantly improved methanogenesis from propionate; kinetic evaluation of methanogenesis indicated that magnetite might alter the metabolic pathways of propionate oxidizing bacteria toward acetate production coupled with direct electron transfer to electrotrophic methanogens (Cruz Viggi et al., 2014). Recently, Zhao et al. (2016b) found that initial enrichment of methanogenic communities with ethanol can accelerate syntrophic propionate or butyrate degradation. Due to the higher abundance of electroactive *Geobacter* species in the aggregates, they postulated that *Geobacter* species might build DIET-based partnerships with methanogens and, thereby, enhanced propionate/butyrate degradation. In contrast to these findings, co-cultures of *Geobacter metallireducens*/*Methanosarcina barkeri* and *Geobacter metallireducens*/*Methanosaeta harundinacea* were unable to metabolize propionate/butyrate even in the presence of conductive materials, such as magnetite and GAC (Wang et al., 2016). Thus, further studies are required to acquire more insight into the significance of DIET in the methanogenic degradation of propionate/butyrate. For example, most of the previous studies investigated the implications of DIET using propionate or butyrate as the sole electron donors, while co-degradation of propionate and butyrate has yet to be examined. In methanogenic

bioreactors, propionate and butyrate usually present as co-substrates that influence their relative degradation (Jia and Fang, 1999; Schmidt and Ahring, 1993).

In this study, methanogenic co-degradation of propionate and butyrate was investigated in an anaerobic bioreactor amended with conductive carbon fibers. To assess the significance of DIET, the methane productivity, methanogenesis kinetics, microbial communities, and electrocatalytic activities of biomass were characterized.

3.2. Materials and Method

3.2.1. Anaerobic Co-degradation Experiment

This study used four glass anaerobic bioreactors with working volumes of 0.9 L. These glass bioreactors were equipped with mechanical agitators coupled with electrical motors and reactor lids with gas and liquid sampling ports. Conductive carbon fibers comprised of 24,000 fiber filaments with a filament diameter of 7 μm (2293-A, 24A Carbon Fiber, Fibre Glast Development Corp., Brookville, OH, USA) were used as the conductive additive in the anaerobic bioreactor. The carbon fibers were pretreated with nitric acid, acetone, and ethanol (Dhar et al., 2013) and then washed with deionized water to remove any contaminants that can potentially hinder charge transfer efficiency (Wang et al., 2009; Zhu et al., 2011). Glass bioreactors were amended with pretreated carbon fibers to provide a total specific surface area of 1583 m^2/m^3 (referred to as CF); carbon fibers were fixed onto the agitator shafts of glass bioreactors using nonconductive elastic rubber bands. Bioreactors without carbon fibers were used as the control (referred to as control). Duplicate bioreactors were operated for each condition and average results were reported here.
During start-up, all bioreactors were inoculated with 400 mL of anaerobic digester sludge collected from a full-scale sewage sludge digester at the Gold Bar Wastewater Treatment Plant, Edmonton, Alberta. The total chemical oxygen demand (TCOD), soluble chemical oxygen demand (SCOD), total suspended solids (TSS), and volatile suspended solids (VSS) concentrations of the anaerobic digester sludge were 9.7, 1.4, 12, and 6.6 g/L respectively. Then, 50 mL of effluent from a lab-scale microbial electrolysis cell (MEC) fed with acetate medium was added to each bioreactor as a supplementary inoculum for the enrichment of electroactive microorganisms. After inoculation, bioreactors were fed with ethanol as an electron donor (TCOD: 4860 ± 410 mg/L) for enrichment of the DIET-active communities (Zhao et al., 2016a, 2016b). Then, the bioreactors' liquids were sparged with ultra-pure nitrogen gas (99.999%) for three minutes and capped tightly with reactor

lids. Initially, the bioreactors were operated in fed-batch mode (6.25 days of hydraulic residence time (HRT)) with ethanol. At the end of each fed-batch cycle, the mixing was stopped. After a settling period of two hours, 400 mL of supernatant was drawn from each bioreactor with a syringe and then 400 mL of fresh substrate medium was fed into each bioreactor, also using a syringe. During this process, gas bags filled with nitrogen gas were connected to gas ports to mitigate oxygen diffusion into bioreactors. After the operation of over 10 fed-batch cycles with ethanol, experiments were conducted with propionate and butyrate as co-substrates (1:1 as the ratio of COD; TCOD: 4820 ± 156 mg/L). Several studies reported production of propionate to butyrate at a ratio of 1:1 (COD basis) during anaerobic digestion of various complex feedstocks, including sewage sludge (Feng et al., 2014; Lin et al., 1986); hence, this ratio was used as a basis for co-degradation experiment. During the experiment with propionate-butyrate medium, HRT was maintained at 15 days. Both ethanol and propionate-butyrate medium were supplemented with 3.5 g/L of $NaHCO_3$ and 5 mL/L of trace element solution. The composition of the trace element solution was (g/L): $CaCl_2.2H_2O$, 15; $MgCl_2.6H_2O$, 10; H_3BO_3, 0.05; $ZnCl_2$, 0.05; $CuSO_4.5H_2O$, 0.03; $MnCl_2.4H_2O$, 0.5; $Na_2MoO_4.2H_2O$, 0.05; $AlK(SO_4)_2.12H_2O$, 0.05; $Co(NO_3)_2.6H_2O$, 0.05; $NiCl_2$, 0.05; $FeCl_2$, 0.1. Bioreactors were operated in a water bath (VWR Water bath 28L, 120V, VWR Canada, Mississauga, ON, Canada) to maintain mesophilic operating condition at 37 ± 1°C. The liquids were stirred with agitators at 300 rpm. The gas port of each bioreactor was connected to a wet-tip gas meter equipped with a closed CO_2 sequestration chamber for direct monitoring of CH_4 gas production. In these CO_2 sequestration chambers (working volume of 80 mL), 3 M NaOH with thymolphthalein indicator was used as the CO_2-absorbing solution. After each fed-batch cycle, all gas meters were re-calibrated.

3.2.2. Evaluation of Methanogenesis Kinetics and Methane Recovery

The CH_4 production from all bioreactors was monitored over time. The following equation was used to estimate methanogenesis rate from the experimental methane production data (Li et al., 2015):

$$V = V_m (1 - e^{-kt}) \qquad (1)$$

Where, V is the cumulative CH_4 volume at time t (mL), V_m is the ultimate methane production (mL), k is the methanogenesis rate constant (d^{-1}). The best-fit V_m and k were estimated using the

relative least squares method in Microsoft Excel Solver. COD recovery as methane was calculated using the following equation (Eq. 2).

$$\text{COD recovery as } CH_4(\%) = \frac{\text{COD equivalent of } CH_4 \text{ produced}}{\text{COD removed during fed-batch cycle}} \times 100\% \qquad (2)$$

3.2.3. Electrochemical Characterization of Biomass

At the end of all experiments, electrical conductivities were measured for the suspended biomass and attached biomass from the control and CF bioreactors respectively. During start-up period including first few cycles of fed-batch operation, suspended biomass was visible in the CF bioreactor. However, no visibly suspended biomass was observed after completion of all experiments (see Supplementary Material); indicating that biomass was primarily attached to the surface of carbon fibers. A study by Matsumoto et al. (2012) suggested that carbon fibers have a high capacity of adsorbing microbial cells due to less negative zeta potential and the large Hamaker constant for interaction between carbon fibers and microbial cells in the aqueous phase, which might explain why suspended biomass was absent in the CF bioreactor after long-term operation. Biomass collected from both bioreactors were centrifuged at 8000 rpm for 10 minutes and placed on gold electrode sensors (A-AD-GG-103-N, Zimmer and Peacock Ltd., Royston, UK) for conductance measurement (see Supplementary Material). For the two-probe conductance measurement (Dhar et al., 2017b, 2016a; Malvankar et al., 2011), a voltage ramp of 0 - 300 mV in steps of 100 mV was applied across working and counter electrodes using a source measurement unit (Keithley 2400, Keithley Instruments, Inc., USA) and a current-voltage (I-V) response was obtained. The current for each voltage was recorded every three seconds for over 33 seconds. The conductance of the biomass was calculated from the I-V response. The ohmic conductivity was calculated using the following equation (Eq. 3):

$$\sigma = \frac{GL}{A} \qquad (3)$$

Where, G is the conductance calculated from I-V response (S), L is the non-conductive gap between the two electrodes (0.03 cm), and A is the cross-sectional area (0.0028 cm^2). Electrocatalytic activity of the carbon fiber-attached biomass was further characterized by the low-scan cycle voltammetry (LSCV) technique (Dhar et al., 2016b). A single-chamber microbial electrolysis cell (MEC) with a working volume of 400 mL was used for the LSCV analysis. After the experiment, the carbon fiber module from the CF bioreactor was immediately removed and

integrated with a stainless-steel mesh (Type 304, McMaster Carr, Cleveland, OH, USA) to be used as the anode electrode in the MEC. A similar anode module without any biomass was used as an abiotic control anode for the LSCV analysis. In both cases, a stainless-steel mesh was used as the cathode electrode. The MEC was equipped with a reference electrode (Ag/AgCl, MF-2079, Bioanalytical System Inc., West Lafayette, IN, USA) and the distance between the anode and reference electrode was ~1 cm. For LSCV analysis, the anode potential was ramped in the range of -0.4 to 0.4 V vs. standard hydrogen electrode (SHE) at a scan rate of 1 mV/s using a multi-channel potentiostat (Squidstat Prime, Admiral Instruments, Phoenix, AZ, USA). The LSCV tests were conducted in the presence of fresh propionate-butyrate medium. These tests were completed within a couple of hours after transferring the carbon fiber module to the MEC to avoid any microbial community shift due to operation with the potentiostat.

3.2.4. Microbial Community Characterization

The characterization of the microbial communities in control and CF bioreactors was performed using high throughput 16S rRNA gene pyrosequencing. At the end of the experiments, suspended biomass from the control bioreactor and attached biomass from the CF bioreactor were collected for microbial community analysis. The genomic DNA of the biomass samples was extracted using PowerSoil® DNA Isolation Kit (MoBio Laboratories, Carlsbad, CA, USA) according to the manufacturer's protocol. The concentration, quality, and integrity of the extracted DNA samples were measured using a spectrophotometer (NanoDrop 2000C, Thermo Fisher Scientific, Waltham, MA, USA). The extracted DNA samples were stored at -70°C until Illumina Miseq Sequencing was constructed and performed by the Research and Testing Laboratory (Lubbock, TX, USA) using specific bacterial primers 357Wf: CCTACGGGNGGCWGCAG and 785R: GACTACHVGGGTATCTAATCC, and archaeal primer 517F: GCYTAAAGSRNCCGTAGC and 909R: TTTCAGYCTTGCGRCCGTAC to target 16S rRNA gene. To examine the microbial diversity, the nucleotide sequence reads were sorted using a data analysis pipeline. A denoising step and chimera detection were used to remove short sequences, noisy reads, and chimeric sequences. Then each sample was run through the analysis pipeline to determine the taxonomic information for each constituent read. Bacteria taxonomy was assigned using the Quantitative Insights Into Microbial Ecology (QIIME) pipeline (http://qiime.org; Caporaso et al., 2010). Raw data, FASTA data, and data analysis methodology for bacteria

(http://www.researchandtesting.com/docs/Data_Analysis_ Methodology.pdf) were provided by the laboratory. The genera of the electroactive bacteria and non-electroactive propionate/butyrate oxidizing bacteria (i.e., fermentative bacteria) were screened according to the previous literatures (Boone and Bryant, 1980; Freguia et al., 2010; Gulhane et al., 2017; Koch and Harnisch, 2016; Liu et al., 1999; Mei et al., 2017; Ruiz et al., 2014; A. Schmidt et al., 2013; Yamada et al., 2007).

3.2.5. Microscopic Imaging of Attached Biomass

To examine the morphology of methanogenic aggregates on carbon fibers, scanning electron microscopy (SEM) was performed at the end of all experiments. Biomass samples were fixed with 2.5% glutaraldehyde in 0.1 M phosphate buffer for up to 24 hours at 4°C, then washed 3 times in 0.1 M phosphate buffer for 10 min each, dehydrated further in an ethanol/water mixture of 50%, 70%, 90% and 100% for 20 minutes each (dehydration in 100% ethanol was done 2 times) and at last immersed in ethanol/ hexamethyldisilazane or HMDS (Sigma Aldrich, St Louis, MO, USA) mixture of 75%, 50%, 25% and 100% for 20 minutes each and leaved overnight to dry in fume hood. Carbon fibers were mounted on SEM stubs and sputter coated with gold to be imaged with Zeiss Sigma 300 VP-FESEM (Carl Zeiss, Cambridge, UK) at 10.0 KV.

3.2.6. Analytical Methods

TCOD and SCOD were measured using HACH COD reagent kit (High Range, 20 - 1500 mg/L; HACH Co., Loveland, CO, USA). The concentrations of different volatile fatty acids (e.g., acetate, propionate, butyrate, etc.) were analyzed after filtering the sample through 0.45 μm membrane filter using a gas chromatograph (Varian 430, Varian Inc., Toronto, Canada) with split/splitless injector and FID detector with a Stabilwax-DA column (30m x 0.53mm x 0.5μm). Initial temperature was held at 35°C for 3 min, then increased to 190°C at 20°C/min, and held for 4 min for a total run time of 14.75 min. The injector was run with a split ratio of 1:1 at 170°C, and 1μL of sample was injected. Helium was used as carrier gas at a constant flow of 11 mL/min.

3.3. Results and Discussion

3.3.1. Methanogenic Co-degradation of Propionate and Butyrate

Figure 3-1A shows cumulative methane production obtained from control and CF bioreactors in five consecutive fed-batch cycles; methane production data with time are provided in the

Supplementary Material. In all cycles, the CF bioreactor exhibited appreciably higher total cumulative methane production than the control bioreactor. Figure 3-1B compares average specific methane production (mL-CH_4/g $COD_{Initial}$) and methanogenesis rate (d^{-1}) from control and CF bioreactors. Specific methane production from CF (264 ± 11 mL-CH_4/g $COD_{Initial}$) was almost 2.4 times higher than control (111 ± 31 mL-CH_4/g $COD_{Initial}$). Analogous to specific methane production, the unamended control bioreactor had a substantially inferior methanogenesis rate (0.06 ± 0.02 d^{-1}) over CF (0.40 ± 0.04 d^{-1}). Previous studies have shown that the addition of biochar and magnetite could increase methanogenesis rates by 1.15 to 1.33 times from propionate or butyrate as sole electron donors (Curz Viggi et al., 2014; Zhang and Lu, 2016; Zhao et al., 2016a). The results of this study provide evidence that the addition of carbon fibers can boost methanogenesis rate up to 6.7 times higher than that of control when propionate and butyrate were present as co-substrate. Hence, carbon fibers should be considered as a potential conductive additive for boosting methane productivity and kinetics in anaerobic treatment of organic waste and wastewater.

Figure 3-2A shows the average concentrations of propionate and butyrate in the effluents from control and CF bioreactors. Butyrate was efficiently degraded in both configurations. The CF bioreactor resulted in complete degradation of propionate; while a significant portion of propionate (876 ± 60 mg COD/L) remained unmetabolized in the control effluent. Thus, enhanced propionate and butyrate co-degradation efficiencies from the CF bioreactor were positively correlated with higher methane productivity and kinetics. No accumulation of acetate was observed for either bioreactor, indicating that the acetate produced from the co-degradation of propionate and butyrate was completely metabolized by microbial communities. Syntrophic propionate degradation coupled with IHT usually requires much lower H_2 partial pressure (P_{H2}) than butyrate degradation (Jia and Fang, 1999; Schmidt and Ahring, 1993), which probably caused the high propionate accumulation in the control bioreactor. As will be discussed later, microbial community analysis also suggested that IHT was the dominant pathway for co-degradation of propionate and butyrate in the control bioreactor. Conversely, DIET as a dominant methanogenesis pathway could alleviate potential P_{H2} inhibition due to metabolic alteration (i.e., acetate/electron production instead of acetate/H_2) (Cruz Viggi et al., 2014; Jing et al., 2017). It should be noted that no accumulation of butyrate and acetate in both bioreactors does not necessarily indicate that the conversion of butyrate and acetate to methane was unaffected by the

addition of carbon fibers, as bioreactors were operated at longer HRT of 15 days. Operation of bioreactors at relatively shorter HRTs could reveal the potential effect of carbon fibers addition on methanogenic conversion of butyrate and acetate.

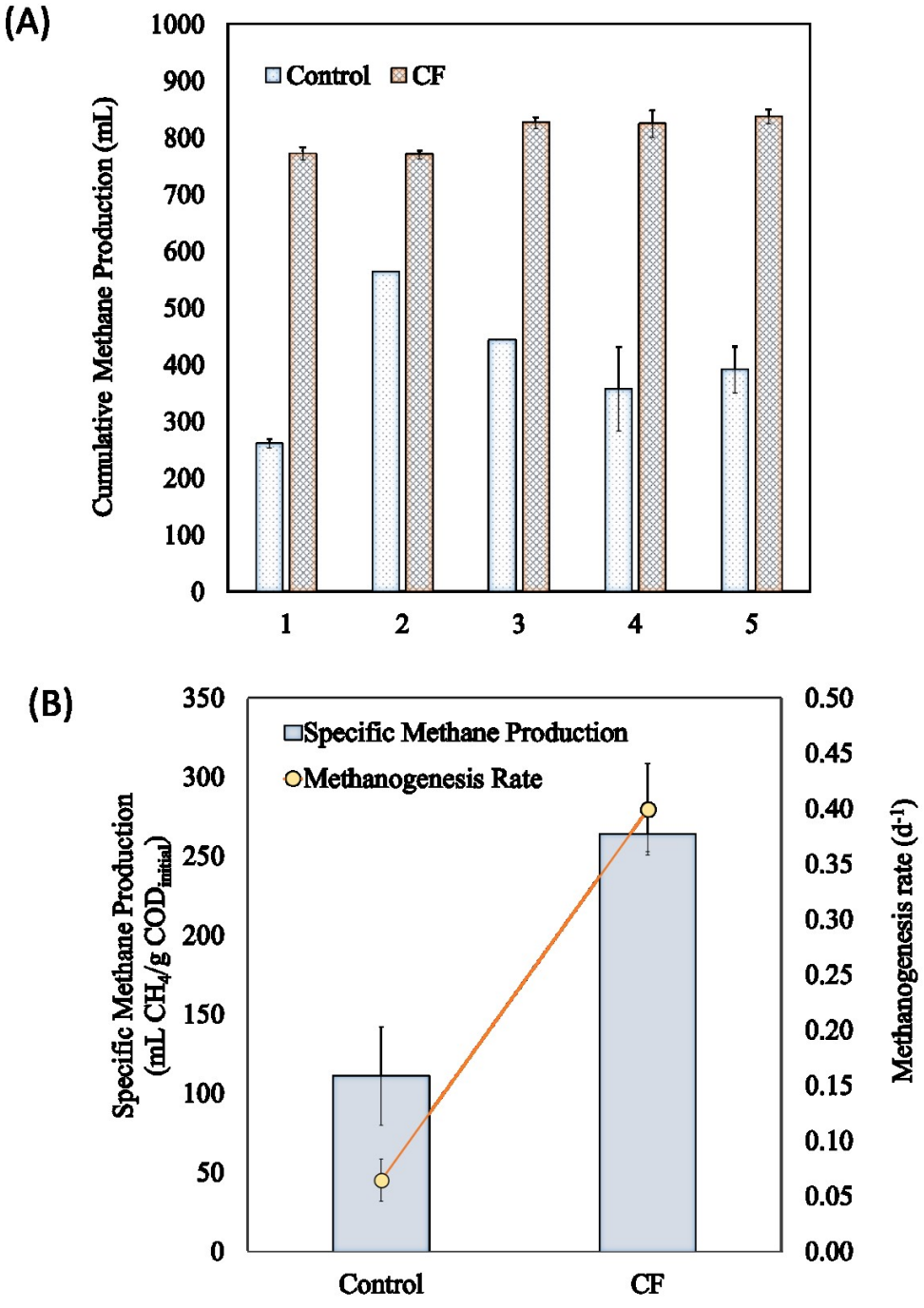

Figure 3-1. (A) Cumulative methane production from five consecutive fed-batch cycles, and (B) average specific methane production and methanogenesis rate.

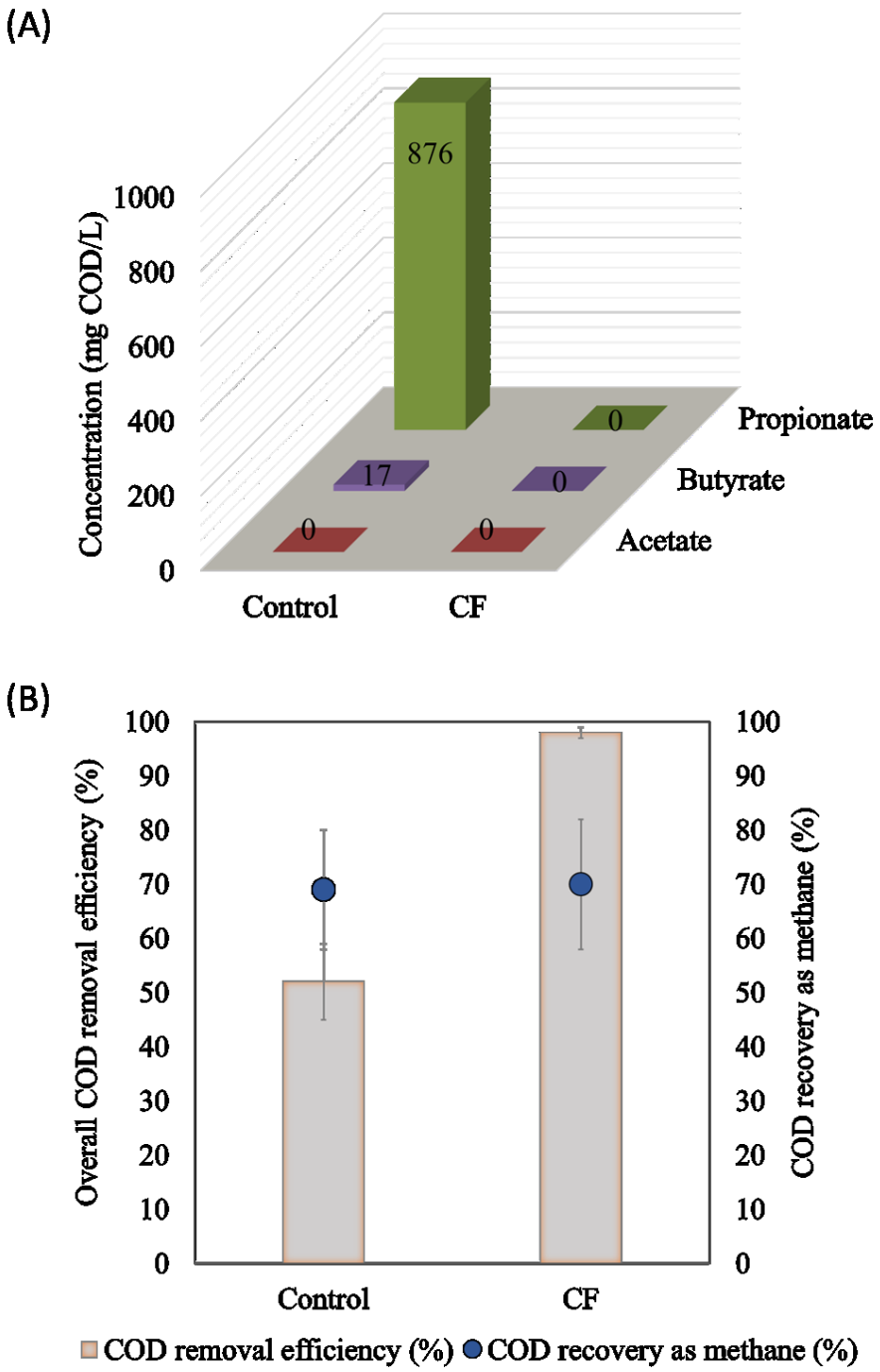

Figure 3-2. (A) Distribution of propionate, butyrate, and acetate in the effluent, (B) COD removal efficiency and COD recovery as methane in Control and CF bioreactors.

The average COD removal efficiency in control and CF bioreactors were 52 ± 7% and 98 ± 1% respectively (Figure 3-2B). The amount of removed COD recovered as CH_4 in control and CF bioreactors was 69 ± 11% and 70 ± 12% respectively (Figure 3-2B). This result is expected, as both DIET and IHT based propionate/butyrate degradation pathways can ultimately lead to similar theoretical methane yields (1. 75 mol CH_4 /mol and 2.5 mol CH_4/mol of propionate and butyrate respectively). A list of reactions involved in propionate and butyrate conversion to methane via both pathways is provided in the Supplementary Material.

3.3.2. Microbial Community: Significance of DIET

Figure 3-3A shows bacterial community structures in control and CF bioreactors. In the control, genus *Syntrophomonas* was the most predominant (14%), followed by *Longilinea* (13%) and *Azovibrio* (8%). *Syntrophomonas* and *Longilinea* genera are well-known for syntrophic butyrate and propionate degradation to acetate and H_2 respectively (A. Schmidt et al., 2013; Yamada et al., 2007). Thus, both genera are unlikely to be involved in DIET. *Azovibrio* have been reported as electrochemically active (Freguia et al., 2010; Ruiz et al., 2014) and *Azovibrio* could be involved in the DIET-based syntrophic degradation of propionate/butyrate/acetate. Other known electroactive bacterial genera present in the control bioreactor were *Pseudomonas* (3%), *Azonexus* (1%), and *Desulfuromonas* (1%). Thus, non-electroactive propionate/butyrate oxidizing bacteria accounted for about 27% of the bacterial community; while electroactive bacteria accounted for only 13% of the bacterial community in the control bioreactor (see Supplementary Material). Three genera of propionate-oxidizing bacteria identified in the CF bioreactor were *Syntrophobacter* (5%), *Longilinea* (4%), and *Smithella* (3%). The relative abundances of the butyrate-oxidizing *Syntrophomonas* and *Sedimentibacter* were 7%, and 4% respectively. Consequently, known propionate/butyrate oxidizing genera accounted for about 23% of the bacterial community in the CF, which was slightly lower than the control (27%) (see Supplementary Material). In contrast, multiple electroactive genera, including *Desulfuromonas* (19%), *Pseudomonas* (9%), *Azonexus* (3%), and *Azovibrio* (1%) were identified in the CF bioreactor. Collectively, these electroactive bacteria represent a major portion of the bacterial community in the CF bioreactor (see Supplementary Material). Microbial community analysis revealed higher abundances of known fermentative bacteria in the control bioreactor than the CF bioreactor; however, both propionate and butyrate were efficiently degraded by the methanogenic

microbiome enriched on the carbon fibers along with an appreciably higher methanogenesis rate compared to the control. Methanogenic activities in this study have shown a negative correlation with the abundances of known propionate/butyrate-oxidizing bacteria. Thus, it is evident that the co-degradation of propionate/butyrate in the CF bioreactor was less dependent on degradation to acetate and H_2 by known fermentative bacteria and more driven by multiple electroactive bacteria. Interestingly, the electroactive *Geobacter* genus was not found in either bioreactor, which is consistent with few recent studies that confirmed that *Geobacter*-deprived methanogenic communities could also facilitate DIET (Dang et al., 2017; Dubé and Guiot, 2017; Jing et al., 2017). Electroactive bacteria (e.g., *Pseudomonas*, *Azonexus*, and *Desulfuromonas*) were also present in the control bioreactor at lower levels. Therefore, DIET-based methanogenesis might also present in the unamended control possibly due to the initial enrichment of communities with ethanol but this seemed to be a non-dominant pathway.

Comparison of archaeal communities revealed a high proportion of known acetoclastic methanogens (*Methanosaeta* or *Methanosarcina*) in both bioreactors (Figure 3-3B). In the control, *Methanosarcina* was dominant (65%), while *Methanosaeta* accounted for only 9% of the archaeal community. The archaeal community in the CF bioreactor was mainly dominated by *Methanosaeta* (72%), whereas the relative abundance of *Methanosarcina* was only 11%. Several studies reported the electrotrophic activity of both *Methanosaeta* and *Methanosarcina* (Cheng and Call, 2016; Lovley, 2017; Park et al., 2018; Rotaru et al., 2014a, 2014b); hence, both could be involved in DIET. However, *Methanosarcina* species are metabolically versatile and can facilitate both the acetoclastic and hydrogenotrophic methanogenesis (Ma et al., 2013), thereby posing the possibility that the abundance of *Methanosarcina* in the control bioreactor might be associated with the IHT pathway rather than DIET. Moreover, hydrogenotrophic *Methanobacterium* accounted for 24% and 11% in control and CF bioreactors respectively. Other H_2-utilizing methanogens, such as *Methanoculleus* and *Methanospirillum*, were present at very low concentrations in both bioreactors. Overall, various hydrogenotrophic methanogens were higher in relative abundance in the control than the CF bioreactor. Thus, IHT could be the dominant pathway for methanogenesis in the control bioreactor. This speculation is also consistent with the higher abundance of known non-electroactive fermentative bacteria in the absence of carbon fibers. Nonetheless, the results suggested that both IHT and DIET pathways were involved in methanogenic co-degradation of

propionate and butyrate in control and CF bioreactors; while DIET appeared to be the dominant pathway in the presence of carbon fibers.

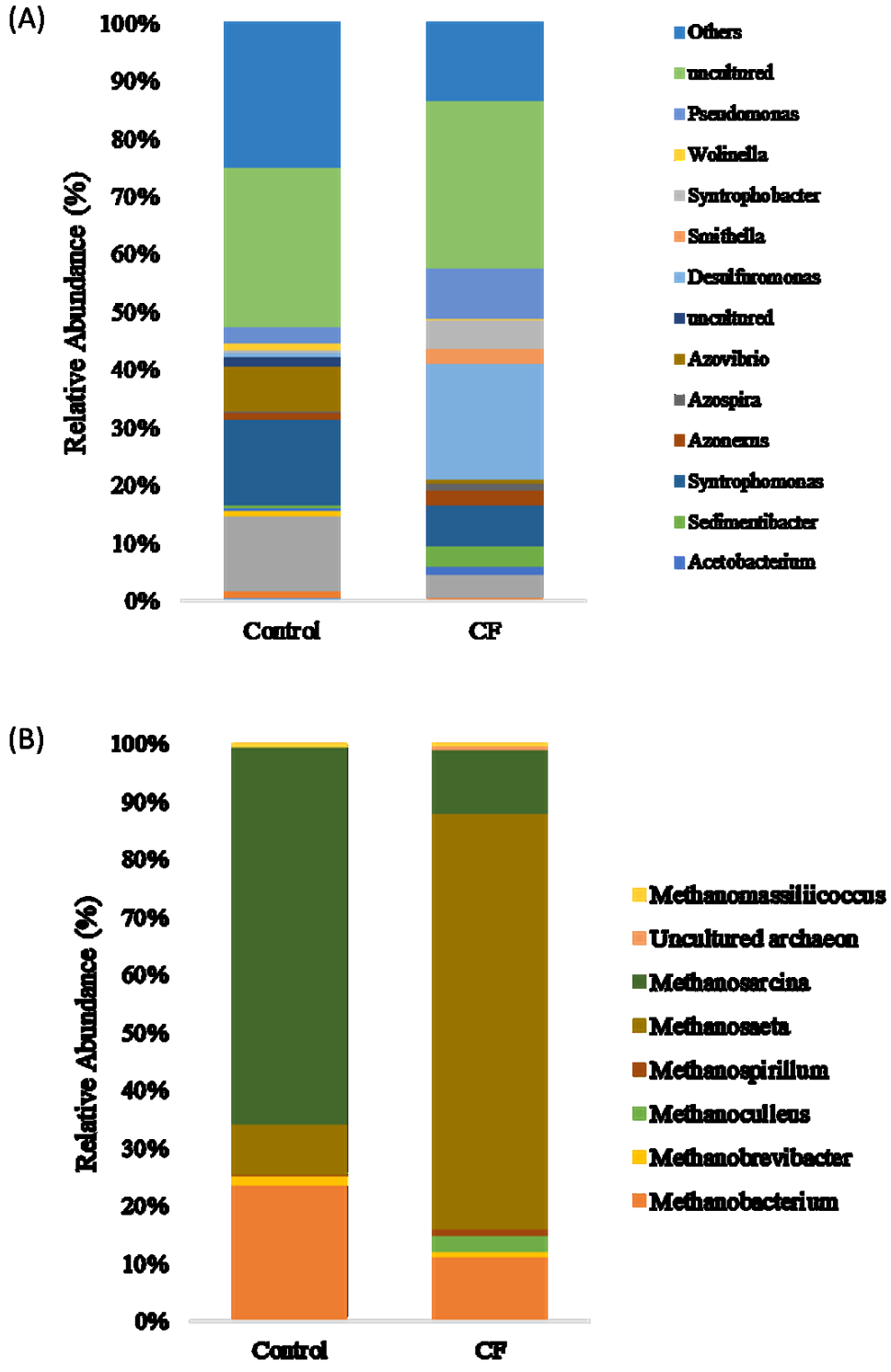

Figure 3-3. (A) Bacterial and (B) archaeal communities at the genus level.

It should be noted that carbon fibers could act as a media for biomass retention; thus, we cannot rule out the possibility that higher methanogenesis rate observed from the CF bioreactor might also be partially attributed to higher concentration of active biomass in comparison with the control (Cruz Viggi et al., 2017; Park et al., 2018). Nonetheless, the variations in bacterial and archaeal communities in control and CF bioreactors conclusively inferred that the role of carbon fibers was not just as a simple means for biomass retention but also as an electrical conduit for DIET-based co-degradation of propionate and butyrate.

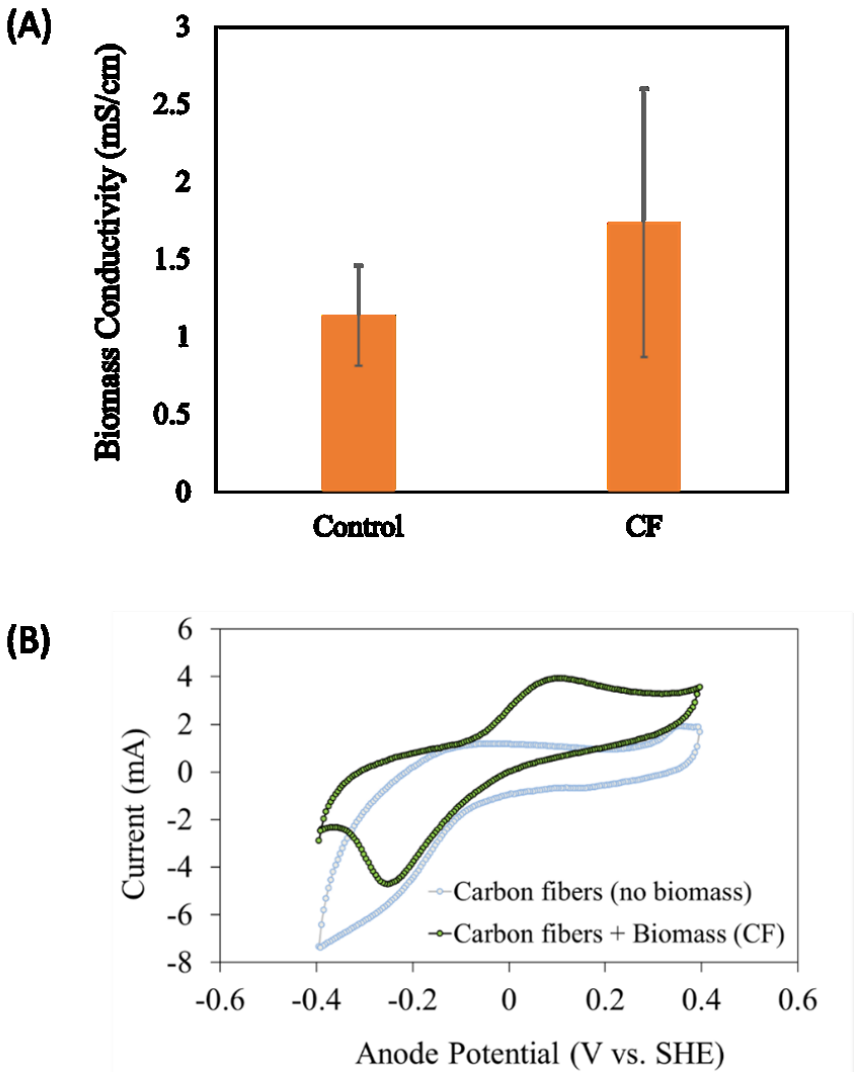

Figure 3-4. (A) Electrical conductivities of biomass, (B) low-scan cyclic voltammogram of carbon fibers with and without biomass.

3.3.3. Electrocatalytic Activity of Biomass: Impact of Carbon Fibers

Figure 3-4A presents electrical conductivities of biomass from the control and CF bioreactors. Electrical conductivities of biomass from the control (1.14 ± 0.32 µS/cm) and the CF (1.74 ± 0.86 µS/cm) were comparable. It should be noted that the biomass conductivity was measured according to a two-probe method previously reported in the literature (Morita et al., 2011; Shrestha et al., 2014; Zhao et al., 2016b); high standard deviation in measured conductivity values indicates the requirement of a more accurate method. Previous studies have shown that the conductivity of methanogenic aggregates is usually attributable to the abundance of *Geobacter* species due to the production of conductive nanowires and/or *c*-type cytochromes OmcS (Morita et al., 2011; Shrestha et al., 2014; Zhao et al., 2016b). Electrical conductivities observed in this study were slightly lower than those previously reported (7.5 - 16.5 µS/cm) for ethanol-stimulated methanogenic communities utilizing propionate or butyrate as sole electron donors (Zhao et al., 2016b), where the relative abundance of *Geobacter* species was 2.01% (propionate) to 3.03% (butyrate). The *Geobacter* genus was almost undetected in this study. Moreover, SEM images of the carbon fibers-attached biomass (see Supplementary Material) did not reveal any of the nanowire-like filaments typically observed in electrochemically active methanogenic biomass (Lin et al., 2017). A few studies have reported that some electroactive species belonging to the *Desulfuromonas* and *Pseudomonas* genera can express conductive nanowires like the *Geobacter* species but these may not be highly conductive (Maruthupandy et al., 2015; Reimers et al., 2017). Both genera were also present in the control bioreactor at very low relative levels (*Desulfuromonas*, 1%; *Pseudomonas*, 3%); however, electrical conductivities were similar. These observations indicate that the electroactive bacteria primarily utilized carbon fibers instead of producing any conductive filaments or cytochromes for facilitating DIET to their syntrophic partners. This finding is contrary to that observed by Lei et al. (2016) on the methanogenesis of leachate in the presence of carbon cloth, where the electrical conductivity of the carbon cloth-attached biomass was higher than the control but is in agreement with another study (Yang et al., 2017). These differences can be attributed to the various physical and electrical properties of conductive additives that can influence their interactions with microbes as well as their electrocatalytic activity (Barua and Dhar, 2017; Cruz Viggi et al., 2017; Park et al., 2018). To further probe electroactivity of the CF-attached biomass, the LSCV (1 mV/s) test was performed. As shown in Figure 3-4B, the peak current from the carbon fibers-attached biomass (3.94 mA) was

almost two times higher than that of bare carbon fibers (1.94 mA), clear evidence of the electrocatalytic activity of methanogenic communities grown on carbon fibers.

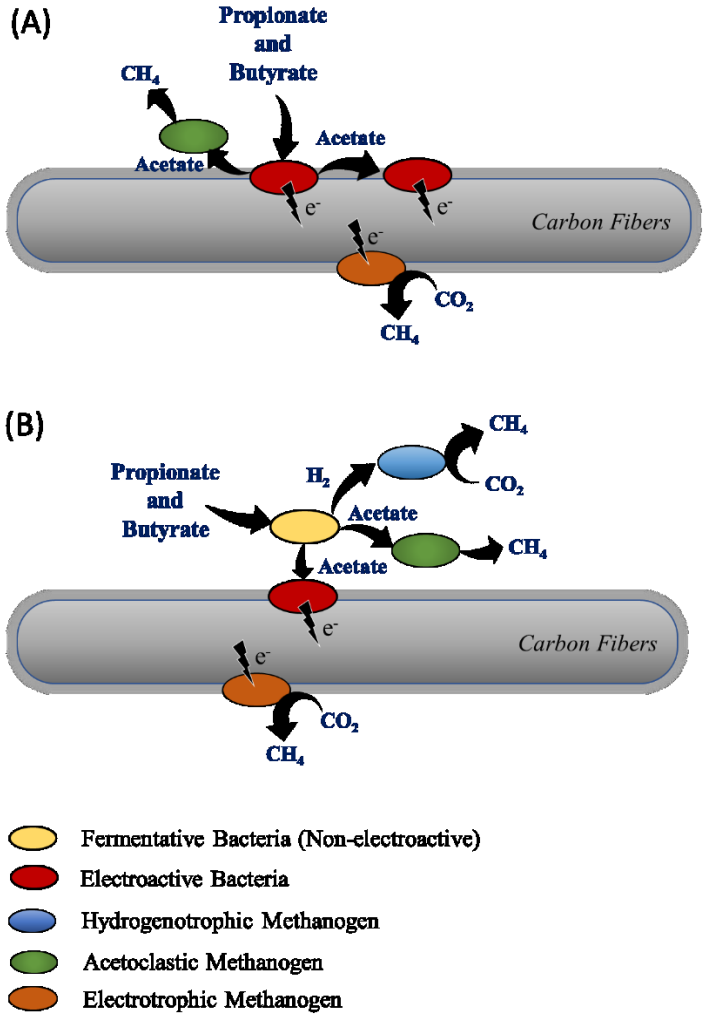

Figure 3-5. Possible pathways for methanogenic degradation of propionate and butyrate through (A) DIET, and (B) IHT in the presence of carbon fibers.

3.3.4. Possible Pathways for DIET: Role of Electroactive Bacteria

Both electroactive bacteria and known propionate/butyrate oxidizing bacteria were present in the CF bioreactor; hence, it can be hypothesized that enhanced co-degradation of propionate/butyrate was achieved by a combination of IHT and DIET-based pathways. Based on the results of this

study, Figure 3-5 summarizes the possible routes for DIET- and IHT-based methanogenesis from propionate/butyrate in the presence of conductive carbon fibers. As shown in Figure 3-5A, some electroactive bacteria can oxidize propionate/butyrate to acetate and electrons (Cruz Viggi et al., 2014; Jing et al., 2017; Zhao et al., 2016b); electrons are transferred to the conductive additive by extracellular electron transport (EET). Electrotrophic methanogens (e.g., *Methanosaeta*) utilize the transferred electrons from a conductive material for CO_2 reduction to CH_4. Conversely, non-electroactive propionate/butyrate oxidizing bacteria (i.e., known fermentative bacteria) can facilitate IHT through the production of acetate and H_2 (Figure 3-5B). Hydrogenotrophic methanogens can consume H_2, which also facilitates CO_2 reduction to CH_4. Either acetoclastic methanogens utilize the acetate produced by both electroactive and non-electroactive fermentative bacteria for methane production or some acetate-utilizing electroactive bacteria can transfer electrons to the conductive material through EET (Cruz Viggi et al., 2014; Jing et al., 2017). Transferred electrons then can be utilized by electrotrophic methanogen for CH_4 production. As various electroactive genera (e.g., *Desulfuromonas*, *Pseudomonas*, etc.) were more abundant in the CF bioreactor, it can be hypothesized that enhanced propionate/butyrate co-degradation was primarily accomplished through the DIET-based pathway (Figure 3-5A). However, further investigation is required to acquire more insights into the specific roles of these microbes as well as their relative substrate affinities among propionate, butyrate, and acetate.

3.4. Conclusions

Conductive carbon fibers have a significant positive impact on the co-degradation of propionate and butyrate. In comparison, butyrate was degraded efficiently in the unamended control. The bacterial community enriched on carbon fibers primarily consisted of various electroactive bacteria rather than known propionate/butyrate oxidizing bacteria, indicating that a significant portion of propionate/butyrate was degraded through DIET. Moreover, *Methanosaeta* was dominant in the CF bioreactor and might be involved in DIET. No significant differences in electrical conductivities of the biomass from control and CF bioreactor propose the possibility that the DIET-active syntrophic communities primarily utilized carbon fibers as an electrical conduit.

Chapter 4

Syntrophic Degradation of Propionate with GAC and Magnetite Doped GAC

A version of this chapter will be submitted for publication in a peer-reviewed journal.

4.1. Introduction

Anaerobic digestion (AD) is one of the most popular and sustainable bioprocesses in waste diversion from landfills, and bioenergy recovery from various organic wastes (Mezzullo et al., 2013; Vasco-Correa et al., 2018). AD process produces bio-methane that can be used for on-site heat and energy production, or can be upgraded into more value-added biofuels, such as bio-CNG (compressed natural gas) and methanol (Vasco-Correa et al., 2018). Thus, deployment of AD process simultaneously mitigate greenhouse gas emissions by replacing fossil fuels and enabling energy positive waste treatment process (Vasco-Correa et al., 2018). Fundamentally in AD process, fermentative bacteria convert intermediates, such as volatile fatty acids (VFAs) and alcohols (e.g., propionate, butyrate, ethanol, etc.) into various simple substrates (e.g., acetate, CO_2/H_2, methanol and formate) which is utilized by methanogens to produce methane (Cheng and Call, 2016). These simple substrates serve as electron carriers between fermentative bacteria and methanogens. This syntropy can be interrupted due to accumulation of VFAs or at high H_2 partial pressure (P_{H2}) (Jia and Fang, 1999; Schmidt and Ahring, 1993). For instance, high concentration of VFAs, such as acetate, propionate, and butyrate, can acidify the digester which leads to the inhibition of microbiome of bacteria and methanogens (Boone and Xun, 1987). Among various VFAs, propionate has often been detected as the major organic acids in the acidified digester (Jia and Fang, 1999; Schmidt and Ahring, 1993). On the other hand, high P_{H2} increases Gibbs free energy (ΔG) of VFAs degradation which inhibits the fermentative bacteria, and thus results in accumulation of VFAs, such as propionate. Biodegradation of propionate is thermodynamically unfavourable and therefore, requires low P_{H2} ($< 10^{-4}$ atm) under standard condition (Jia and Fang, 1999; Schmidt and Ahring, 1993). Syntrophic interspecies H_2 transfer (IHT) between fermentative bacteria and methanogens was believed to be thermodynamically more important in maintaining low P_{H2} to keep the balance of this syntropy (Amani et al., 2010; Cruz Viggi et al., 2014). However, the interspecies distance between the syntrophic partners often results in diffusion limitation of H_2

transfer that increases local P_{H2} (Schmidt and Ahring, 1995). Additionally, anaerobic respiration is always less efficient than aerobic respiration due to less positive reduction potential of available electron acceptors (e.g., nitrate, sulfate, CO_2, etc.) as compared with oxygen (Amani et al., 2010). Therefore, close aggregation of the syntrophic partners, such as anaerobic granulation, enables microbiome to utilize the extracellular proton translocation which ultimately boost the efficacy of IHT pathway (Amani et al., 2010). Recent investigation of microbial aggregates from an up flow anaerobic sludge blanket (UASB) reactor discloses the unique capability of some bacteria that transfer electron along with CO_2/H^+ directly to methanogenic archaea instead of CO_2/H_2 for IHT pathway (Morita et al., 2011). This unique cell-to-cell electron transfer pathway is called direct interspecies electron transfer (DIET) (Barua and Dhar, 2017; Cheng and Call, 2016; Lovley, 2017). Electron transfer through DIET pathway is thermodynamically favoured, and more faster than IHT which ultimately increases the robustness of digester at high organic loading rate through faster methanogenesis (Barua and Dhar, 2017; Cheng and Call, 2016; Lovley, 2017; Morita et al., 2011; Summers et al., 2010). Bacteria that can transfer electron via extracellular electron transfer (EET) are named "exoelectrogen" or "electrochemically active bacteria (EAB)" and methanogenic archaea capable of accepting electrons are named "electrotrophic methanogen" (Logan, 2009; Lovley, 2011a, 2011b). EAB can transfer electron towards electrotrophic methanogen via conductive nanowires (pili) and extracellular redox cofactors (e.g., *c*-type cytochrome) when close aggregation of biomass occurred in some specific configuration of anaerobic bioreactors, e.g., UASB reactors (Lovley, 2017, 2011b; Morita et al., 2011). Nonetheless, various non-biological conductive materials (e.g., GAC, biochar, carbon cloth, carbon fiber, magnetite, etc.) enable microbiome to transfer electron through these conductive materials that can boost methane production in some engineered bioreactors, including continuous stirred tank reactors (CSTRs). Furthermore, these non-biological conductive additives mitigate the energy investment by microbes for conductive nanowires or extracellular redox cofactors production, and provide metabolically more favoured condition to conserve more energy (Zhao et al., 2015).

Geobacter species is well known for its EET transport towards methanogens from various types of reduced organic carbons such as, ethanol, acetate etc. (Barua and Dhar, 2017; Cheng and Call, 2016; Lovley, 2017; Morita et al., 2011; Summers et al., 2010). Few recent batch or fed-batch studies postulated the role of *Geobacter* species under supplementation of conductive materials in improving propionate degradation (Viggi et al., 2014; Jing et al., 2017; Li et al., 2015;

Zhang and Lu, 2016; Zhao et al., 2016a, 2016b). In contrast to these findings, some recent studies have emerged the possibility of *Geobacter* species deprived methanogenic propionate degradation (Barua et al., 2018; Jing et al., 2017; Xu et al., 2018). However, to date limited information is reported in syntrophic propionate biodegradation through DIET pathway in the long-term study of fed-batch bioreactors.

Various conductive materials, such as GAC, biochar, carbon cloth, carbon fibers, magnetite, stainless steel, etc., are examined in promoting DIET (Barua et al., 2018; Barua and Dhar, 2017; Cheng and Call, 2016; Park et al., 2018). For instance, supplementation of magnetite nanoparticles can facilitate enrichment of DIET active syntrophic microbiome, and hence reduce the lag phase and enhance methane production rate (Cruz Viggi et al., 2014; Kato et al., 2012). Small size magnetite nanoparticle (20-150 nm) can attach to the pili and enhance electron transport through DIET pathway (Barua and Dhar, 2017; Cruz Viggi et al., 2014). In comparison, DIET mechanism under larger size non-biological conductive materials, such as GAC, biochar, etc., is different from small particles, such as magnetite. DIET active syntrophic microbiome attach on the surface of these big particles and use them as the route for syntrophic electron transport which is more efficient than electron transport through pili (Barua and Dhar, 2017; Zhao et al., 2015). Among the non-biological conductive materials, GAC has received the most attention in DIET study possibly due to its low cost and high conductivity along with high surface area. GAC is also used as anode electrode in various microbial electrochemical systems (Yasri and Nakhla, 2017; Zhang et al., 2013). Studies have shown that GAC doped with functional groups (e.g., iron, calcium, sulfur, nitrogen, etc.) can further enhance its conductivity and biocompatibility, and thereby promote enrichment of various electroactive bacteria in microbial electrochemical systems (Baudler et al., 2015; Santoro et al., 2015; Yasri and Nakhla, 2017). Based on extensive literature search, no studies could be found on the impact of doped GAC particles on anaerobic digestion process.

To address the abovementioned research gap, this study investigated the effects of magnetite doped GAC particles on anaerobic biodegradation of propionate as a sole substrate. We compared the performance of bioreactors amended with GAC, magnetite doped GAC, and unamended control in terms of methane productivity from propionate, and accumulation of propionate and acetate. Furthermore, microbial communities established in different bioreactors

were compared. The results of this study first demonstrate that GAC particles can be further tailored though doping with magnetite for anaerobic digestion application.

4.2. Materials and Methods

4.2.1. Doping of GAC Particles

Granular activated carbon (GAC) particles were doped as previously described with slight modification (Yasri and Nakhla, 2016). GAC (mesh size: 8−20, BET surface area: 600−800 m^2/g, conductivity: ~3000 μS/cm) was purchased from Sigma Aldrich, Canada. Before doping, GAC particles were washed thoroughly with deionized water and dried at 105±5 ºC. 6.5 gm magnetite particles (95%, powder size < 5 μm; Sigma Aldrich, Canada) was suspended into 150 mL of deoxygenated water. Then, 100 gm dried GAC particles was added into the suspension and gently mixed for 12 hours at 300 rpm. Finally, the liquid was vacuum dried at 120 ºC. The doped GAC particles were analysed with scanning electron microscopy (SEM) and energy dispersive spectrometry (EDS); 27.38 and 6.85 mass% Fe was detected on the surface of the magnetite doped GAC particles before and after the anaerobic digestion experiment, respectively which confirmed the success and effectiveness of the doping procedure (see Supplementary Information). Here, GAC particles doped with magnetite are referred as "magnetite doped GAC" and GAC particles received the same treatment as described above except magnetite, are referred as "GAC".

4.2.2. Evaluation of Anaerobic Biodegradability of Propionate

Nine glass anaerobic bioreactors (working volume of 0.8 L) equipped with mechanical agitators and coupled with electrical motors and reactor lids along with gas and liquid sampling ports were used in this study. Bioreactors supplemented with 18 grams of GAC and magnetite doped GAC are referred as "GAC" and "MDGAC", respectively. Bioreactors without any GAC served as the unamended control. Triplicate bioreactors were operated for each condition and the average results are reported here. A mixture of anaerobic digester sludge and effluent from microbial electrolysis cell (MEC) was used as inoculum for the start-up of each bioreactor, as previously described in the literature (Barua et al., 2018). The volume ratio of digested sludge to MEC effluent was 8:1. The MEC effluent was collected from a mother reactor operated with 25 mM sodium acetate medium for over one year. The anaerobic digester sludge was collected from a full-scale sewage sludge digester at the Gold Bar Wastewater Treatment Plant, Edmonton, Alberta. The total

suspended solids (TSS), volatile suspended solids (VSS), total chemical oxygen demand (TCOD) and soluble chemical oxygen demand (SCOD) concentrations of the sludge were 12.4±0.05, 6.4±0.03, 9.6±0.06 and 1.5±0.09 g/L, respectively. Initially, 400 mL of inoculum and 400 mL of substrate medium were added into each bioreactor. Ethanol (TCOD: 4860 ± 410 mg/L) was used as the substrate to stimulate enrichment of DIET-active communities as previously described in the literature (Barua et al., 2018; Zhao et al., 2016a, 2016b). Then, we switched the substrate from ethanol to a mixture of ethanol and propionate, and later on switched to propionate as a sole substrate to gradually adopt the microbial communities (see Supplementary Information). Finally, the anaerobic biodegradability of propionate was assessed in consecutive fed-batch operation with propionate medium (TCOD: 13280±90 mg/L). The medium was always supplemented with 3.5 g/L of $NaHCO_3$ and 5 mL/L of trace element solution as described elsewhere (Barua et al., 2018). At the end of each cycle, mixing was stopped for three hours and supernatant was replaced with fresh substrate medium as summarized in Table B-1. During this time, a gas bag filled with nitrogen was used to alleviate oxygen diffusion into the bioreactors. The bioreactors' temperature was maintained at 37 ± 1°C using a water bath (VWR Water bath 28L, 120V, VWR Canada, Mississauga, ON, Canada) and liquid medium was stirred at 300 rpm.

4.2.3. Analytical Methods

Liquid samples were filtered using 0.45 µm and 0.2 µm membrane filter for analysis of SCOD and short-chain volatile fatty acids (acetate, and propionate), respectively. SCOD were measured using HACH COD reagent kit (High Range, 20 - 1500 mg/L; HACH Co., Loveland, CO, USA). The concentrations of various VFAs were analysed using ion chromatograph (Dionex ICS-2100, Dionex, Sunnyvale, CA) equipped with an electrochemical detector (ECD) and microbore AS19 column. Dried magnetite doped GAC and GAC particles, after proper washing, were mounted on SEM stubs followed by sputter coating with gold. Then, the elemental composition of magnetite doped GAC and GAC were examined with scanning electron microscopy (SEM) and energy dispersive spectrometry (EDS) (Zeiss Sigma 300 VP-FESEM, Carl Zeiss, Cambridge, UK). For measurement of methane gas production from various bioreactors, the gas sampling port of each bioreactor was connected to a CO_2 sequestration bottle (80 mL; 3 M NaOH with thymolphthalein indicator) followed by a 1L gas bag to separate CO_2 and directly collect CH_4 gas (Barua et al., 2018; Fagbohungbe et al., 2016).

4.2.4. Evaluation of Propionate Degradation Kinetics

First order propionate degradation rate (k) was calculated according to the following equation at the end of Cycle #5.

$$ln\frac{C_0}{C_t} = kt \qquad (1)$$

Here, C_0 is initial propionate concentration (mg/L), C_t is propionate concentration (mg/L) at time t (d) and k is the first order rate constant (d^{-1}).

4.2.5. Statistical Analysis

All the statistical analyses were performed with JMP 11 (SAS Institute Inc., NC, USA). The Analysis of Variance (ANOVA) and student's t-test at a 95% confidence level was conducted, and $p < 0.05$ was considered statistically significant.

4.2.6. Microbial Community Characterization

Microbial community of the control, GAC and MDGAC bioreactors were performed through high throughput 16S rRNA gene sequencing at the end of Cycle #5. All the bioreactors were stirred at 300 rpm to collect the suspended and attached biomass samples together from triplicate reactors and a composite sample was used for DNA extraction for each condition (control, GAC and MDGAC). The genomic DNA of the biomass samples were extracted according to the manufacturer's protocol using PowerSoil® DNA Isolation Kit (MoBio Laboratories, Carlsbad, CA, USA). The properties of the extracted DNA samples (e.g., concentration, quality, and integrity) were measured using a spectrophotometer (NanoDrop 2000C, Thermo Fisher Scientific, Waltham, MA, USA). The extracted DNA samples were stored immediately at -70°C prior to performing Illumina Miseq Sequencing at the Research and Testing Laboratory (Lubbock, TX, USA) using the specific primers 357Wf: CCTACGGGNGGCWGCAG and 785R: GACTACHVGGGTATCTAATCC to target the 16S rRNA gene. The demultiplexed sequencing data were processed and analysed using the Quantitative Insights Into Microbial Ecology (QIIME v2) software (Caporaso et al., 2010). The sequences were denoised (dada2) to remove and/or correct noisy reads, remove chimeric sequences and singletons, and join denoised paried-end reads (Callahan et al., 2016). The denoised sequences were assigned to species-equivalent operational taxonomic units (OTUs) at a 97% sequence similarity level using the open-reference OTU picking method (2013-08 Greengenes database) (Rideout et al., 2014). The distribution of major bacterial

and archaea genera (each represented by >0.1% of their population) was further analysed using heatmap with a double hierarchical dendrogram (Babicki et al., 2016). The genera of the electroactive bacteria and non-electroactive propionate oxidizing bacteria (i.e., fermentative bacteria) were screened according to the previous literatures (Boone and Bryant, 1980; Freguia et al., 2010; Gulhane et al., 2017; Koch and Harnisch, 2016; Liu et al., 1999; Mei et al., 2017; Ruiz et al., 2014; A. Schmidt et al., 2013; Yamada et al., 2007).

4.3. Results and Discussion

4.3.1. Methane Production and COD Removal Efficiency

Figure 4-1A illustrates methane productivities from control, GAC, and MDGAC bioreactors in four consecutive fed-batch cycles; the time course cumulative methane production for each condition is provided in the Supplementary Information (Figure B-1). Addition of GAC and MDGAC led to significantly higher methane production over the control. The MDGAC showed 1.52- and 1.21-times higher methane production as compared with control and GAC bioreactors ($p<0.05$), respectively. On the other hand, GAC showed 1.25 times higher methane production than the control during four consecutive fed-batch cycles. Biodegradation of propionate under micro-size magnetite particles supplementation increased methane production rate by 1.33-times in batch experiment (Cruz Viggi et al., 2014). Furthermore, biochar was found to improve methane production rate by 1.16 times higher in UASB reactors from propionate (Zhao et al., 2016a). There is no significant difference in the ultimate methane production from MDGAC in four consecutive cycles ($p>0.05$), while methane production from both control and GAC gradually decreased ($p<0.05$) after each fed-batch cycle. As shown in Figure 4-1B, MDGAC exhibited 1.5- and 1.2-times higher COD removal efficiency than that of control and GAC, respectively while GAC provided 1.29 times higher COD removal efficiency over the control. Analogous to methane production, COD removal efficiency in MDGAC-amended reactors remained almost constant during all cycles ($p = 0.7092$). In addition to that, COD removal efficiency in the GAC and control decreased from Cycle #1 to 4 (GAC: 62±1% vs 47±8% and control: 50±8% vs 36±2%). Based on the methane productivity and COD removal efficiency, the following ranking could be established: MDGAC > GAC > control. The positive impact of GAC addition is consistent with several studies that suggested GAC addition could boost the methane productivity and COD removal efficiencies in methanogenesis from both synthetic and complex organic feedstocks (Barua and Dhar, 2017;

Jing et al., 2017; Park et al., 2018). Notably, the results of this study first demonstrated that doping of GAC particles with magnetite could offer further improvement of methanogenesis from propionate, a substrate that is not readily degradable by methanogenic microbiome. Few studies have previously suggested that the surface modification of GAC with conductive/semi-conductive iron-oxide particles could stimulate enrichment of electroactive bacteria on its surface due to increased electrical conductivity, which could improve current density in microbial electrochemical systems (Yasri and Nakhla, 2017, 2016). Thus, the observed improvement could be attributed to the enrichment of electroactive methanogenic microbiome due to a decrease in charge transfer resistance of doped GAC, which warrants further investigation.

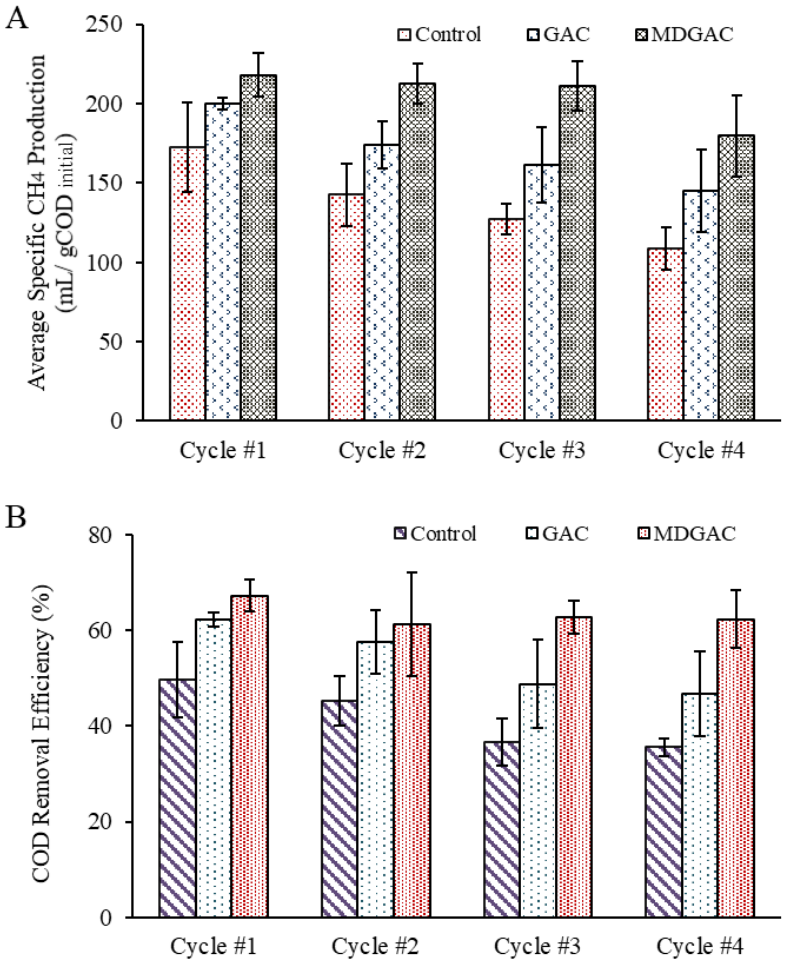

Figure 4-1. (A) Average specific methane production, and (B) COD removal efficiencies in four consecutive fed-batch cycles.

4.3.2. VFA Degradation

Accumulation of VFAs (acetate and propionate) was monitored to evaluate the performance of the bioreactors (Figure 4-2 and Table B-1), and Figure 4-2A represents average effluent acetate concentration during four consecutive fed-batch cycles. Addition of MDGAC successfully maintained lowest acetate concentration ($p=0.1366$) during the observed cycles, as compared with GAC and control. Acetate concentration in GAC increased gradually from Cycle #1 to 4 (1168±86 vs 1759±288 mg COD/L) however GAC was able to maintain lower acetate accumulation over control while acetate accumulated in the control expeditiously ($p<0.05$). The trend of the bioreactors in maintaining low acetate concentration in the effluent was MDGAC > GAC > control; this accumulated acetate in control and GAC influenced the influent and effluent acetate concentration in all the subsequent cycles (Table B-1). At the end of Cycle #4, the effluent acetate concentration in control and GAC was 1.74- and 1.34-times higher, respectively than that of MDGAC. This significant portion of unmetabolized acetate in control can lower the metabolism of methanogens (Boone and Xun, 1987; Jia and Fang, 1999). Furthermore, this slow methanogenic metabolism can increase the P_{H2} which can also decrease the syntrophic propionate degradation through IHT pathway because low P_{H2} provides thermodynamically feasible environment for syntrophic propionate degradation through IHT pathway (Jia and Fang, 1999; Schmidt and Ahring, 1993). This higher P_{H2} probably caused lower biodegradation of propionate which results in unmetabolized propionate accumulation in the effluent of control and GAC from Cycle #1 to 4. Analogous to maintaining lowest acetate accumulation, MDGAC was also able to maintain lowest propionate accumulation in the bioreactors (Figure 4-2B). At the end of Cycle #4, control and GAC experienced 3.3- and 2.3-times higher propionate accumulation, respectively as compared with MDGAC.

Figure 4-3 demonstrates time course degradation profiles of VFAs in the control, GAC and MDGAC as observed during Cycle #5. Initial acetate and propionate concentration in Control was highest as compared with GAC and MDGAC, that could be attributed to the accumulation of VFAs at the end of Cycle #4. Comparable trend in acetate production was observed regardless of the difference in the concentration among the sets of bioreactors; acetate concentration reached plateau quickly. However, propionate degradation rate constant was highest in the MDGAC (Figure B-7) that can be positively correlated with the highest methane production, COD removal efficiency, and VFA degradation, as compared with control and GAC. As will be discussed later, microbial

community analysis also suggests the effectiveness of GAC particles doped with magnetite in shaping the DIET active communities to accelerate methanogenic degradation of propionate.

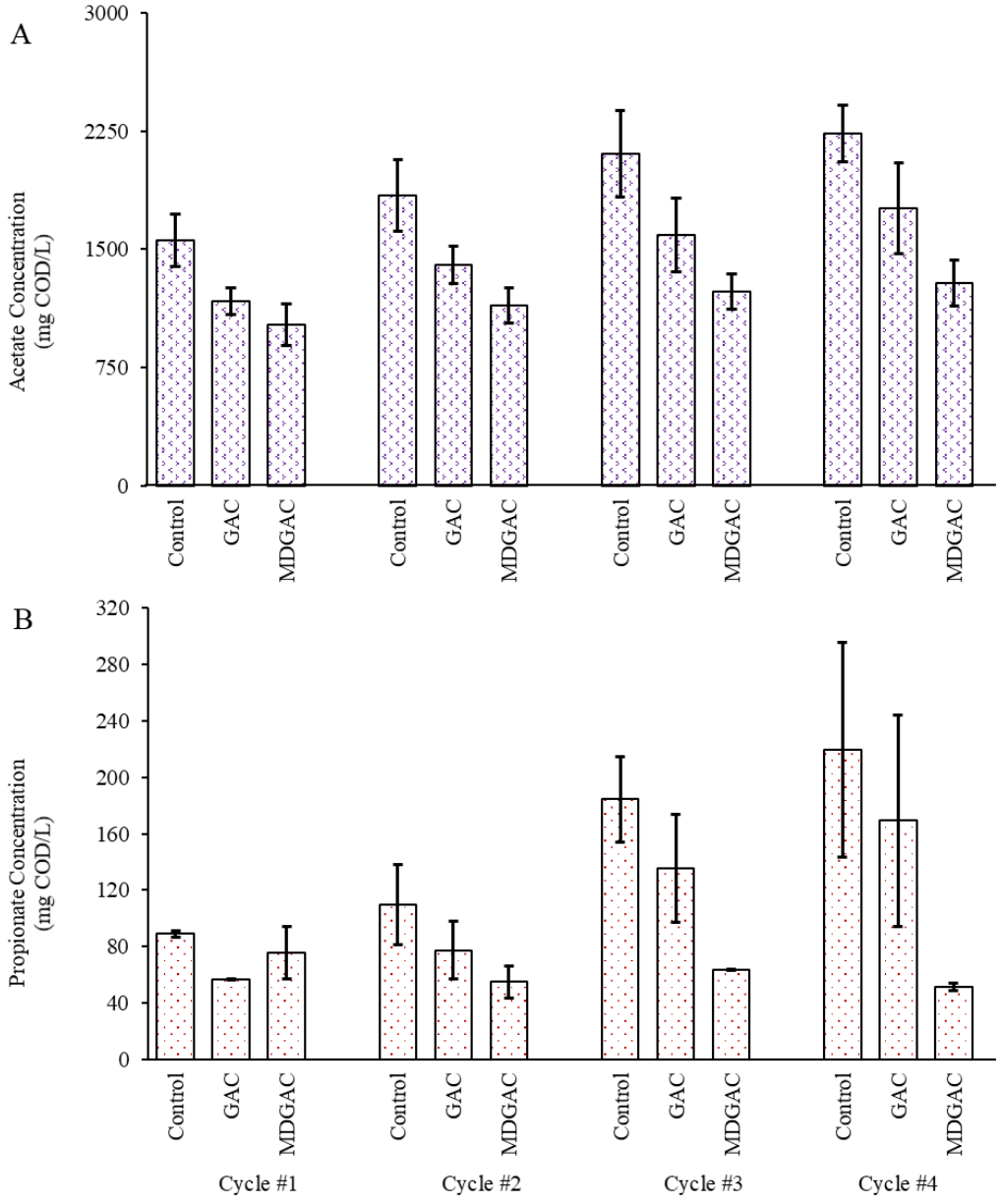

Figure 4-2. Average effluent (A) acetate, and (B) propionate concentrations during four consecutive fed-batch cycles.

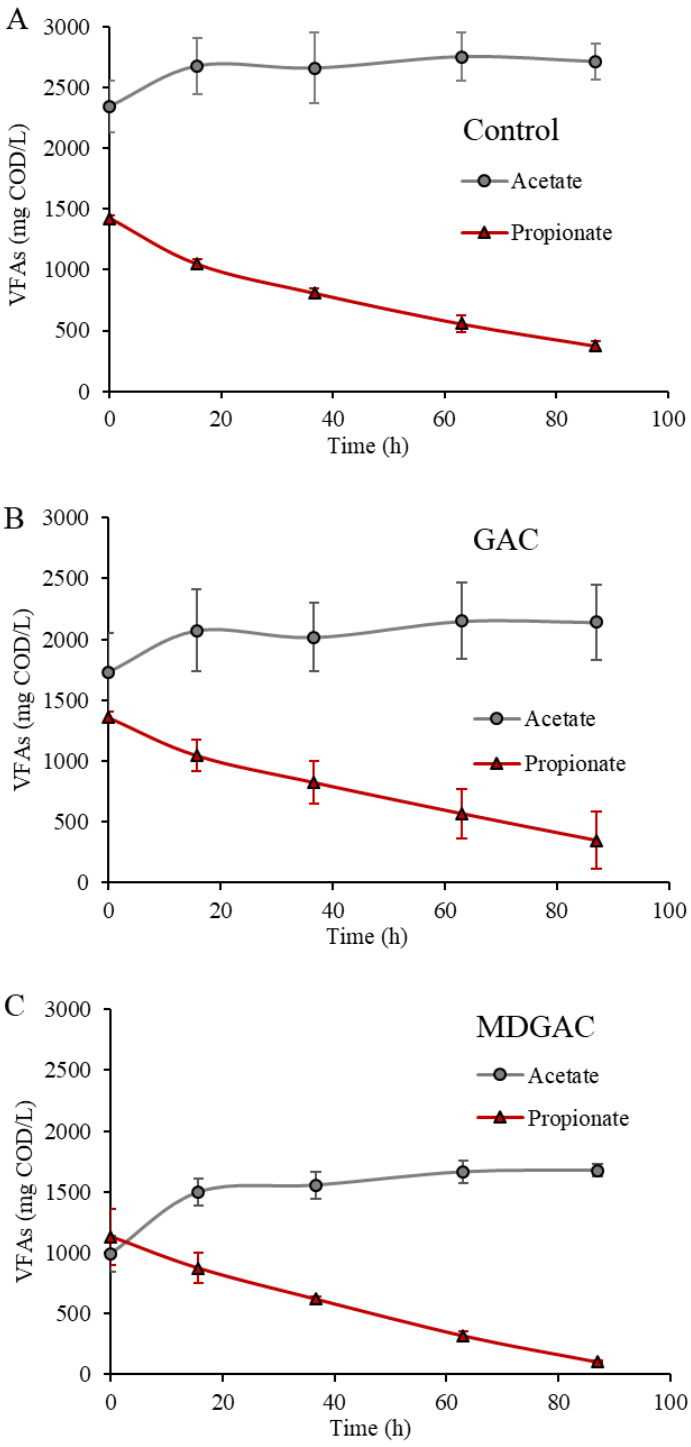

Figure 4-3. Degradation profiles of VFAs in (A) control, (B) GAC, and (C) MDGAC bioreactors during Cycle #5.

4.3.3. Microbiome Responsible for Syntrophic Degradation of Propionate

4.3.3.1. Bacterial Community

Figure 4-4A shows the relative abundance of bacterial communities at phylum level. The two most predominant phyla in all bioreactors were *Proteobacteria* and *Chloroflexi*; both accounting for ~60% of the bacterial community. In the control, *Chloroflexi* (34%) was dominant, whereas *Proteobacteria* (37-40%) prevailed in the reactors amended with GAC and MDGAC. It should be noted that, most of the well-known electroactive bacteria (e.g., *Geobacter*, *Shewanella*, etc.) reported in literature belongs to *Proteobacteria* phylum (Koch and Harnisch, 2016; Lovley, 2011a, 2006). Additionally, *Firmicutes* (7% vs. 16-18%) was lower while *Bacteroidetes* (14% vs. 5-7%) was higher in the control as compared with the amended bioreactors (GAC and MDGAC). *Firmicutes* contains various fermentative bacteria, such as *Clostridium* and *Syntrophomonas*. Notably, the bacterial communities were similar in GAC and MDGAC reactors regarding bacterial phylum structure. The distribution of the major bacterial genera was further analysed using heatmap (Figure 4-5). Results showed GAC and MDGAC addition substantially altered the bacterial community in comparison to control. Group I contains three genera (*Syntrophobacter*, candidate genus T78 and HA73) that prevailed in all three bioreactors. *Syntrophobacter* is well-known for syntrophic propionate oxidation to acetate/H_2 and the candidate genus T78 belongs to the family *Anaerolinaceae* (phylum *Chloroflexi*). Notably, group IIa contains genera that were almost undetected in the control, while increased to 1-4 folds in the detected sequence number of GAC and MDGAC amended bioreactors. Most of these genera belongs to *Proteobacteria*, and are known as electroactive bacteria (*Shewanella*, *Pseudomonas*, *Geobacter*, and *Desulfuromonas*). The total relative abundance of these genera was substantially higher in GAC and MDGAC amended reactors (11-12%) than that of the control (0.7%). Previous study on propionate degradation have also reported the dominance of *Pseudomonas* and *Desulfuromonas* with the addition of carbon fibers (Barua et al., 2018). Another genus *Pelotomaculum* (phylum *Firmicutes*) in group IIa contains well-known syntrophic propionate-oxidizing bacteria (e.g., *P. propionicicum*) (Imachi et al., 2007). Group IIb contains very diverse bacteria; most of them were present in all the bioreactors with similar abundance, such as *Syntrophomonas* and *Acetobacterium*, while some were considerably lower in GAC and MDGAC as compared to control, such as *Clostridium*. The genera *Clostridium* and *Syntrophomonas* contain various well-

known syntrophic hydrogen-producing bacteria (Guo et al., 2014). *Acetobacterium* is well known homoacetogen (typically convert H_2 and CO_2 to acetate) and no literature reported EET capability of these genera, which suggest that they were not likely to be involved in the DIET to methanogens. Briefly, the results showed that multiple electroactive bacteria (*Shewanella*, *Pseudomonas*, *Geobacter*, and *Desulfuromonas*) were selectively enriched in the GAC and MDGAC bioreactors as compared with control, which suggests that they might be involved in DIET with methanogens. Analogous to the significantly higher methane production in GAC and MDGAC amended bioreactors as compared with control, it is possible that the degradation of propionate in the GAC and MDGAC amended bioreactors was less dependent on known fermentative bacteria (acetate/H_2 for IHT pathway) and more driven by multiple electroactive bacteria through DIET pathway (acetate/H^+).

4.3.3.2. Archaeal Community

Figure 4-4B shows the relative abundance of methanogens at genus level. Interestingly, *Methanosaeta* was the most dominant genus in all the bioreactors, and its proportion was highest in the MDGAC (85%), followed by GAC (49%) and control bioreactors (43%). Hydrogenotrophic methanogens including *Methanobacterium* and *Methanoculleus* accounted for 46% of archaeal community in control, whereas 44% in GAC and only 13% in MDGAC. Other H_2 utilizing methanogens such as *Methanolinea* were present at low proportion in all bioreactors and decreased in relative abundance with the addition of GAC and MDGAC. Clearly, various hydrogenotrophic methanogens were higher in relative abundance in the control and GAC bioreactors than that of the MDGAC bioreactors. On the other hand, *Methanosarcina* was also present at low relative abundance in all the bioreactors; 3% and 4% in the control and GAC, respectively whereas only 1% in the MDGAC. Comparable to this finding, previous studies have also reported the dominance of *Methanosaeta* with conducive additives for methanogenic degradation of various simple and complex substrate (Barua et al., 2018; Lin et al., 2018; Xu et al., 2018; Zhao et al., 2017). Several studies confirmed the electrotrophic activity of *Methanosaeta*, suggesting its potential to be involved in DIET. Since no apparent electroactive bacteria were detected in the control, IHT could be the primary pathway for propionate degradation to acetate/H_2, followed by acetoclastic methanogenesis and hydrogenotrophic methanogenesis. In contrast, considering the selective enrichment of multiple electroactive bacteria in GAC and MDGAC, both DIET and IHT pathways

were involved in propionate degradation. Although the contributions of each pathway were not confirmative, DIET appear to be the more dominant pathway in MDGAC than GAC amended bioreactors as indicated by the substantially higher proportions of electroactive bacteria along with *Methanosaeta* and lower proportions of hydrogenotrophic methanogens.

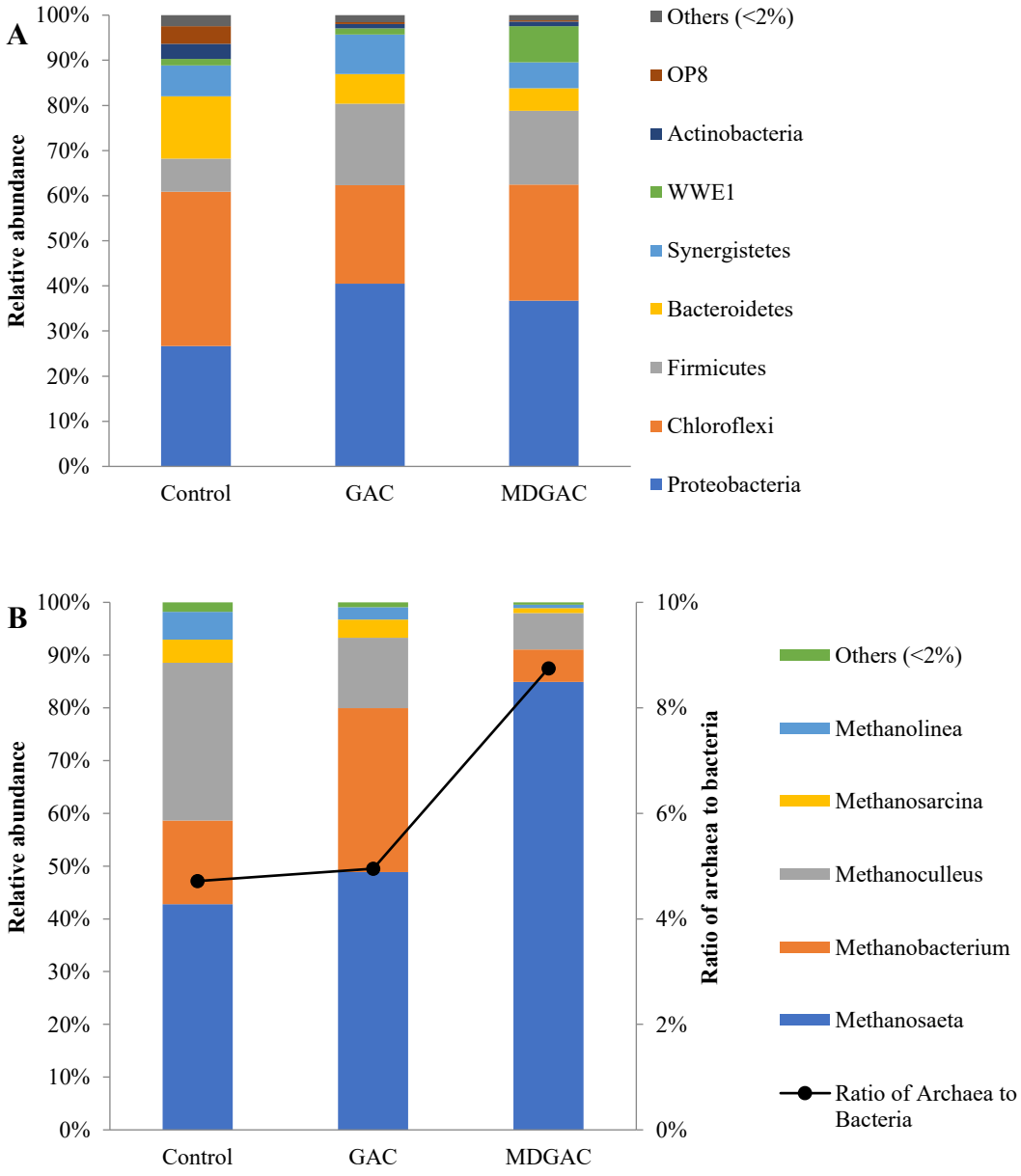

Figure 4-4. Relative abundance of (A) bacterial community at phylum level, and (B) archaeal community at genus level and ratio of archaea to bacteria. Note: sequences that accounted for less than 2% of their population were grouped into "Others".

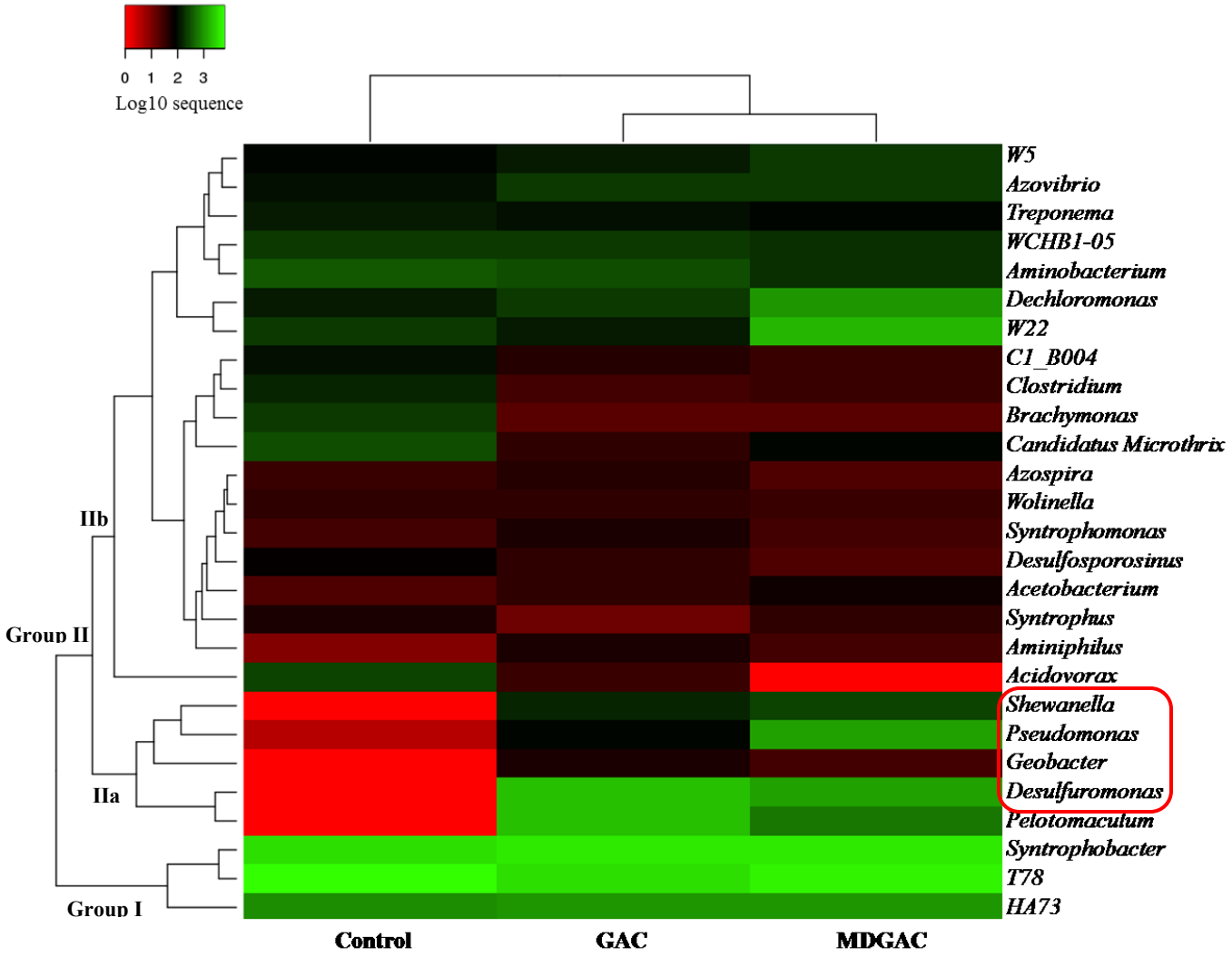

Figure 4-5. Double hierarchical dendrogram based on log sequence number of bacterial genera that were assigned a genus name (each represented >0.1% of their population).

Additionally, the ratio of archaea to bacteria was also calculated (Figure 4-4B). Interestingly, the ratio was the highest in MDGAC (9%), followed by GAC (5%) and control (4.7%) bioreactors. Higher ratio of methanogens to bacteria in MDGAC can be positively correlated with the highest reactor performances as compared with the control and GAC bioreactors. The possible reason could be the washout of slow-growing acetoclastic methanogens than hydrogenotrophic methanogens, especially from the unamended control (Asztalos and Kim, 2015; T. Schmidt et al., 2013b). It is widely recognized that there are two classes of acetoclastic

methanogens. Genus *Methanosaeta* is known to have a high affinity for acetate however they have relatively low maximum specific growth rate as compared with *Methanosarcina* (maximum specific growth rate 0.1/d vs. 0.3/d) (Conklin et al., 2006; Mladenovska and Ahring, 2000; Tatara et al., 2005). Therefore, we may speculate that the acetoclastic methanogens were partially washed out from the control with fed-batch operation (3.6 days/batch) at 20 days of HRT, and thus accumulation of acetate occurred. Use of GAC and MDGAC appears to be advantageous for attaching microbes because microbes with slow growth rates, such as acetoclastic methanogens, have hydrophobic membranes and can easily attach themselves to these materials (Asztalos and Kim, 2015; T. Schmidt et al., 2013b).

4.4. Conclusions

Magnetite doped GAC particles significantly enhanced syntrophic degradation of propionate as sole substrate over undoped GAC particles; specific methane production and COD removal efficiency were ~1.2 times higher. Bacterial community analysis suggests the efficacy of GAC/magnetite doped GAC for the enrichment of various electroactive bacteria rather than known propionate fermenting bacteria. Furthermore, higher archaea to bacteria ratio along with higher abundance of electroactive *Methanosaeta* can be positively correlated with the higher robustness (acetate and propionate degradation, methane productivity, and COD removal efficiency) of the bioreactors amended with magnetite doped GAC particles, which indicates the possibility of DIET between electroactive bacteria and *Methanosaeta* as the dominant pathway for syntrophic propionate degradation besides the IHT between propionate fermenting bacteria and archaea.

Chapter 5

Conclusions and Recommendations

5.1. Conclusions

Understanding and engineering DIET based syntropy in anaerobic digestion process is vital for the development of the next generation digester. Conductive carbon fibers and magnetite doped GAC particles showed a positive impact in stimulating DIET kinetics from propionate/butyrate as substrate. Various DIET active microbiome was enriched rather than known propionate/butyrate oxidizing bacteria on the surface of carbon fibers, and *Methanosaeta* was the dominant electroactive archaea in the CF bioreactor. The biomass conductivity of the CF amended, and unamended control was comparable which implies the possibility of using CF as the primary route for electron transfer. On the other hand, magnetite doped GAC particles retained more DIET-active bacteria and *Methanosaeta* than the GAC amended bioreactor that results in ~ 1.2 times higher methane production and COD removal efficiency form propionate. The findings of this study can provide significant knowledge in search of the suitable non-biological conductive materials in stimulating methanogenesis of complex organics through enhancing the growth of the DIET active communities.

5.2. Recommendation for Future Work

Based on the findings of this study, the following recommendations can be suggested to dig the insight of the DIET potential using carbon fibers and magnetite doped GAC particles:

- This study only focused on methanogenic degradation of propionate/butyrate in the fed-batch mode of operation. Further study is required to find the efficacy of carbon fibers and magnetite doped GAC particles in stimulating methanogenesis of more complex substrates (e.g., food waste, activated sludge, source-separated black water, etc.) in continuous operating mode.
- Fundamental study is required to observe the effect of material properties (e.g., surface area, pore size distribution, surface functional groups, hardness, conductivity, etc.) on the enrichment of DIET active microbiome.

- Further studies would be required to confirm the function of individual microbes responsible in DIET/IHT pathways because 16S rRNA gene sequencing can't provide the exact roles of the individual microbe.

References

Adhikari, R.Y., Malvankar, N.S., Tuominen, M.T. and Lovley, D.R., 2016. *Conductivity of individual Geobacter pili.* RSC Adv. 6, 8354-8357.

Ahmad, M., Rajapaksha, A.U., Lim, J.E., Zhang, M., Bolan, N., Mohan, D., Vithanage, M., Lee, S.S. and Ok, Y.S., 2014. *Biochar as a sorbent for contaminant management in soil and water: a review.* Chemosphere 99, 19-33.

Amani, T., Nosrati, M., Sreekrishnan, T.R., 2010. *Anaerobic digestion from the viewpoint of microbiological, chemical, and operational aspects — a review.* Environ. Rev. 18, 255–278.

Appels, L., Lauwers, J., Degrève, J., Helsen, L., Lievens, B., Willems, K., Van Impe, J., Dewil, R., 2011. *Anaerobic digestion in global bio-energy production: Potential and research challenges*. Renew. Sustain. Energy Rev. 15, 4295–4301.

Asztalos, J.R., Kim, Y., 2015. *Enhanced digestion of waste activated sludge using microbial electrolysis cells at ambient temperature.* Water Res. 87, 503–512.

Babicki, S., Arndt, D., Marcu, A., Liang, Y., Grant, J.R., Maciejewski, A., Wishart, D.S., 2016. *Heatmapper: web-enabled heat mapping for all.* Nucleic Acids Res. 44, W147–W153.

Baek, G., Jung, H., Kim, J. and Lee, C., 2017. *A long-term study on the effect of magnetite supplementation in continuous anaerobic digestion of dairy effluent–Magnetic separation and recycling of magnetite.* Bioresour. Technol. 241, 830-840.

Baek, G., Kim, J. and Lee, C., 2016. *A long-term study on the effect of magnetite supplementation in continuous anaerobic digestion of dairy effluent–Enhancement in process performance and stability.* Bioresour. Technol. 222, 344-354.

Barua, S., Dhar, B.R., 2017. *Advances towards understanding and engineering direct interspecies electron transfer in anaerobic digestion.* Bioresour. Technol. 244, 698–707.

Barua, S., Zakaria, B.S., Dhar, B.R., 2018. *Enhanced methanogenic co-degradation of propionate and butyrate by anaerobic microbiome enriched on conductive carbon fibers.* Bioresour. Technol. 266, 259–266.

Baudler, A., Schmidt, I., Langner, M., Greiner, A., Schröder, U., 2015. *Does it have to be carbon? Metal anodes in microbial fuel cells and related bioelectrochemical systems.* Energy Environ. Sci. 8, 2048–2055.

Bertin, L., Berselli, S., Fava, F., Petrangeli-Papini, M. and Marchetti, L., 2004a. *Anaerobic digestion of olive mill wastewaters in biofilm reactors packed with granular activated carbon and "Manville" silica beads.* Water Res. 38, 3167-3178.

Bertin, L., Colao, M.C., Ruzzi, M. and Fava, F., 2004b. *Performances and microbial features of a granular activated carbon packed-bed biofilm reactor capable of an efficient anaerobic digestion of olive mill wastewaters.* FEMS Microbiol. Ecol. 48, 413-423.

Boone, D.R., Bryant, M.P., 1980. *Propionate-Degrading Bacterium, Syntrophobacter wolinii sp. nov. gen. nov., from Methanogenic Ecosystems.* Appl. Environ. Microbiol. 40, 626–32.

Boone, D.R., Johnson, R.L. and Liu, Y., 1989. *Diffusion of the interspecies electron carriers H2 and formate in methanogenic ecosystems and its implications in the measurement of Km for H2 or formate uptake.* Appl. Environ. Microbiol. 55, 1735-1741.

Boone, D.R., Xun, L., 1987. *Effects of pH, Temperature, and Nutrients on Propionate Degradation by a Methanogenic Enrichment Culture.* Appl. Environ. Microbiol. 53, 1589–92.

Bouallagui, H., Touhami, Y., Ben Cheikh, R., Hamdi, M., 2005. *Bioreactor performance in anaerobic digestion of fruit and vegetable wastes.* Process Biochem. 40, 989–995.

Butti, S.K., Velvizhi, G., Sulonen, M.L.K., Haavisto, J.M., Oguz Koroglu, E., Yusuf Cetinkaya, A., Singh, S., Arya, D., Annie Modestra, J., Vamsi Krishna, K., Verma, A., Ozkaya, B., Lakaniemi, A.-M., Puhakka, J.A., Venkata Mohan, S., 2016. *Microbial electrochemical technologies with the perspective of harnessing bioenergy: Maneuvering towards upscaling.* Renew. Sustain. Energy Rev. 53, 462–476.

Callahan, B.J., McMurdie, P.J., Rosen, M.J., Han, A.W., Johnson, A.J.A., Holmes, S.P., 2016. *DADA2: high-resolution sample inference from Illumina amplicon data.* Nat. Methods 13, 581.

Caporaso, J.G., Kuczynski, J., Stombaugh, J., Bittinger, K., Bushman, F.D., Costello, E.K., Fierer, N., Peña, A.G., Goodrich, J.K., Gordon, J.I., Huttley, G.A., Kelley, S.T., Knights, D., Koenig, J.E., Ley, R.E., Lozupone, C.A., McDonald, D., Muegge, B.D., Pirrung, M., Reeder, J., Sevinsky, J.R., Turnbaugh, P.J., Walters, W.A., Widmann, J., Yatsunenko, T., Zaneveld, J., Knight, R., 2010. *QIIME allows analysis of high-throughput community sequencing data.* Nat. Methods 7, 335–336.

Carrere, H., Antonopoulou, G., Affes, R., Passos, F., Battimelli, A., Lyberatos, G., Ferrer, I., 2016. *Review of feedstock pretreatment strategies for improved anaerobic digestion: From lab-scale research to full-scale application.* Bioresour. Technol. 199, 386–397.

Cavinato, C., Bolzonella, D., Pavan, P., Fatone, F. and Cecchi, F., 2013. *Mesophilic and thermophilic anaerobic co-digestion of waste activated sludge and source sorted biowaste in pilot- and full-scale reactors.* Renew. Energ. 55, 260-265.

Chang, I.S., Moon, H.S., Bretschger, O., Jang, J.K., Park, H.I., Nealson, K.H. and Kim, B.H., 2006. *Electrochemically active bacteria (EAB) and mediator-less microbial fuel cells.* J. Microbiol. Biotechnol. 16, 163-177.

Chen, S., Rotaru, A.E., Liu, F., Philips, J., Woodard, T.L., Nevin, K.P. and Lovley, D.R., 2014b. *Carbon cloth stimulates direct interspecies electron transfer in syntrophic co-cultures.* Bioresour. Technol. 173, 82-86.

Chen, S., Rotaru, A.E., Shrestha, P.M., Malvankar, N.S., Liu, F., Fan, W., Nevin, K.P. and Lovley, D.R., 2014a. *Promoting interspecies electron transfer with biochar.* Sci. Rep. 4, 5019.

Cheng, Q., Call, D.F., 2016. *Hardwiring microbes via direct interspecies electron transfer: mechanisms and applications.* Env. Sci. Process. Impact 18, 968-980.

Cherubini, F., 2010. *The biorefinery concept: Using biomass instead of oil for producing energy and chemicals.* Energy Convers. Manag. 51, 1412–1421.

Conklin, A., Stensel, H.D., Ferguson, J., 2006. *Growth kinetics and competition between Methanosarcina and Methanosaeta in mesophilic anaerobic digestion.* Water Environ. Res. 78, 486–96.

Cruz Viggi, C., Rossetti, S., Fazi, S., Paiano, P., Majone, M., Aulenta, F., 2014a. *Magnetite Particles Triggering a Faster and More Robust Syntrophic Pathway of Methanogenic Propionate Degradation.* Environ. Sci. Technol. 48, 7536–7543.

Cruz Viggi, C., Simonetti, S., Palma, E., Pagliaccia, P., Braguglia, C., Fazi, S., Baronti, S., Navarra, M.A., Pettiti, I., Koch, C., Harnisch, F., Aulenta, F., 2017. *Enhancing methane production from food waste fermentate using biochar: the added value of electrochemical testing in pre-selecting the most effective type of biochar.* Biotechnol. Biofuels 10, 303.

Dang, Y., Holmes, D.E., Zhao, Z., Woodard, T.L., Zhang, Y., Sun, D., Wang, L.Y., Nevin, K.P. and Lovley, D.R., 2016. *Enhancing anaerobic digestion of complex organic waste with carbon-based conductive materials.* Bioresour. Technol. 220, 516-522.

Dang, Y., Sun, D., Woodard, T.L., Wang, L.Y., Nevin, K.P. and Holmes, D.E., 2017. *Stimulation of the anaerobic digestion of the dry organic fraction of municipal solid waste (OFMSW) with carbon-based conductive materials.* Bioresour. Technol. 238, 30-38.

De Bok, F.A.M., Plugge, C.M. and Stams, A.J.M., 2004. *Interspecies electron transfer in methanogenic propionate degrading consortia.* Water Res. 38, 1368-1375.

De Corato, U., De Bari, I., Viola, E., Pugliese, M., 2018. *Assessing the main opportunities of integrated biorefining from agro-bioenergy co/by-products and agroindustrial residues into high-value added products associated to some emerging markets: A review.* Renew. Sustain. Energy Rev. 88, 326–346.

Dhar, B.R., Gao, Y., Yeo, H., Lee, H.-S., 2013. *Separation of competitive microorganisms using anaerobic membrane bioreactors as pretreatment to microbial electrochemical cells.* Bioresour. Technol. 148, 208–214.

Dhar, B.R., Nakhla, G., Ray, M.B., 2012. *Techno-economic evaluation of ultrasound and thermal pretreatments for enhanced anaerobic digestion of municipal waste activated sludge.* Waste Manag. 32, 542–549.

Dhar, B.R., Park, J.-H., Park, H.-D., Lee, H.-S., 2019. *Hydrogen-based syntrophy in an electrically conductive biofilm anode.* Chem. Eng. J. 359, 208–216.

Dhar, B.R., Ryu, H., Ren, H., Domingo, J.W.S., Chae, J., Lee, H.-S., 2016a. *High Biofilm Conductivity Maintained Despite Anode Potential Changes in a Geobacter -Enriched Biofilm.* ChemSusChem 9, 3485–3491.

Dhar, B.R., Ryu, H., Santo Domingo, J.W., Lee, H.-S., 2016b. *Ohmic resistance affects microbial community and electrochemical kinetics in a multi-anode microbial electrochemical cell.* J. Power Sources 331, 315–321.

Dhar, B.R., Sim, J., Ryu, H., Ren, H., Santo Domingo, J.W., Chae, J., Lee, H.-S., 2017a. *Microbial activity influences electrical conductivity of biofilm anode.* Water Res. 127, 230–238.

Dubé, C.-D., Guiot, S.R., 2017. *Ethanol-to-methane activity of Geobacter-deprived anaerobic granules enhanced by conductive microparticles.* Process Biochem. 63, 42–48.

Dubé, C.-D., Guiot, S.R., 2015. *Direct Interspecies Electron Transfer in Anaerobic Digestion: A Review.* Springer, Cham, pp. 101–115.

Eaktasang, N., Kang, C.S., Lim, H., Kwean, O.S., Cho, S., Kim, Y. and Kim, H.S., 2016. *Production of electrically-conductive nanoscale filaments by sulfate-reducing bacteria in the microbial fuel cell.* Bioresour. Technol. 210, 61-67.

Fagbohungbe, M.O., Herbert, B.M., Hurst, L., Li, H., Usmani, S.Q. and Semple, K.T., 2016. *Impact of biochar on the anaerobic digestion of citrus peel waste.* Bioresour. Technol. 216, 142-149.

Ferguson, R.M., Coulon, F. and Villa, R., 2016. *Organic loading rate: A promising microbial management tool in anaerobic digestion.* Water Res. 100, 348-356.

Freguia, S., Teh, E.H., Boon, N., Leung, K.M., Keller, J., Rabaey, K., 2010. *Microbial fuel cells operating on mixed fatty acids.* Bioresour. Technol. 101, 1233–1238.

Garcia, J.L., Patel, B.K. and Ollivier, B., 2000. *Taxonomic, phylogenetic, and ecological diversity of methanogenic Archaea.* Anaerobe 6, 205-226.

Gorby, Y.A., Yanina, S., McLean, J.S., Rosso, K.M., Moyles, D., Dohnalkova, A., Beveridge, T.J., Chang, I.S., Kim, B.H., Kim, K.S. and Culley, D.E., 2006. *Electrically conductive bacterial nanowires produced by Shewanella oneidensis strain MR-1 and other microorganisms.* Proc. Natl. Acad. Sci. U.S.A. 103, 11358-11363.

Gou, C., Yang, Z., Huang, J., Wang, H., Xu, H. and Wang, L., 2014. *Effects of temperature and organic loading rate on the performance and microbial community of anaerobic co-digestion of waste activated sludge and food waste.* Chemosphere 105, 146-151.

Goyal, S.K., Seth, R. and Handa, B.K., 1996. *Diphasic fixed-film biomethanation of distillery spentwash.* Bioresour. Technol. 56(2-3), 239-244.

Gujer, W. and Zehnder, A.J., 1983. *Conversion processes in anaerobic digestion.* Wat. Sci. Tech. 15, 127-167.

Gulhane, M., Pandit, P., Khardenavis, A., Singh, D., Purohit, H., 2017. *Study of microbial community plasticity for anaerobic digestion of vegetable waste in Anaerobic Baffled Reactor.* Renew. Energy 101, 59–66.

Guo, X., Wang, C., Sun, F., Zhu, W., Wu, W., 2014. *A comparison of microbial characteristics between the thermophilic and mesophilic anaerobic digesters exposed to elevated food waste loadings.* Bioresour. Technol. 152, 420–428.

Hansen, K.H., Angelidaki, I., Ahring, B.K., 1998. *Anaerobic digestion of swine manure: inhibition by ammonia.* Water Res. 32, 5–12.

Hindatu, Y., Annuar, M.S.M. and Gumel, A.M., 2017. *Mini-review: Anode modification for improved performance of microbial fuel cell. Renew.* Sustainable Energy Rev. 73, 236-248.

Holmes, D.E., Shrestha, P.M., Walker, D.J., Dang, Y., Nevin, K.P., Woodard, T.L. and Lovley, D.R., 2017. *Metatranscriptomic evidence for direct interspecies electron transfer between Geobacter and Methanothrix species in methanogenic rice paddy soils.* App. Environ. Microbiol. 83, 00223-17.

Hu, Q., Sun, D., Ma, Y., Qiu, B. and Guo, Z., 2017. *Conductive polyaniline enhanced methane production from anaerobic wastewater treatment.* Polymer 120, 236–243.

Iannotti, E.L., Kafkewitz, I.D., Wolin, M.J., Bryant, M.P., 1973. *Glucose Fermentation Products of Ruminococcus albus Grown in Continuous Culture with Vibrio succinogenes: Changes Caused by Interspecies Transfer of H2.* J. Bacterol. 114, 1231–1240.

Imachi, H., Sakai, S., Ohashi, A., Harada, H., Hanada, S., Kamagata, Y., Sekiguchi, Y., 2007. *Pelotomaculum propionicicum sp. nov., an anaerobic, mesophilic, obligately syntrophic, propionate-oxidizing bacterium.* Int. J. Syst. Evol. Microbiol. 57, 1487–1492.

Jia, X.-S., Fang, H.H.P., 1999. *Substrate Degradation of Propionate-Utilizing Sludge.* Environ. Technol. 20, 1103–1108.

Jing, Y., Wan, J., Angelidaki, I., Zhang, S. and Luo, G., 2017. *iTRAQ quantitative proteomic analysis reveals the pathways for methanation of propionate facilitated by magnetite.* Water Res. 108, 212-221.

Kalathil, S., Lee, J. and Cho, M.H., 2012. *Efficient decolorization of real dye wastewater and bioelectricity generation using a novel single chamber biocathode-microbial fuel cell.* Bioresour. Technol. 119, 22-27.

Kato, S., Hashimoto, K. and Watanabe, K., 2012. *Methanogenesis facilitated by electric syntrophy via (semi) conductive iron-oxide minerals.* Environ. Microbiol. 14, 1646-1654.

Koch, C., Harnisch, F., 2016. *Is there a Specific Ecological Niche for Electroactive Microorganisms?* ChemElectroChem 3, 1282–1295.

Kouzuma, A., Kato, S. and Watanabe, K., 2015. *Microbial interspecies interactions: recent findings in syntrophic consortia.* Front. Microbiol. 6, 477.

Kumar, G., Sarathi, V.S. and Nahm, K.S., 2013. *Recent advances and challenges in the anode architecture and their modifications for the applications of microbial fuel cells.* Biosens. Bioelectron. 43, 461-475.

Lai, B.; Tang, X.; Li, H.; Du, Z.; Liu, X.; Zhang, Q., 2011. *Power Production Enhancement with a Polyaniline Modified Anode in Microbial Fuel Cells.* Biosens. Bioelectron. 28, 373–377

Lee, H.S., Dhar, B.R., An, J., Rittmann, B.E., Ryu, H., Santo Domingo, J.W., Ren, H. and Chae, J., 2016. *The Roles of Biofilm Conductivity and Donor Substrate Kinetics in a Mixed-Culture Biofilm Anode.* Environ. Sci. Technol. 50, 12799-12807.

Lee, H.-S., Dhar, B.R., Hussain, A., 2019. *Electron Transfer Kinetics in Biofilm Anodes*, in: Microbial Electrochemical Technology. Elsevier, pp. 339–351.

Lee, J.Y., Lee, S.H. and Park, H.D., 2016. *Enrichment of specific electro-active microorganisms and enhancement of methane production by adding granular activated carbon in anaerobic reactors.* Bioresour. Technol. 205, 205-212.

Lei, Y., Sun, D., Dang, Y., Chen, H., Zhao, Z., Zhang, Y. and Holmes, D.E., 2016. *Stimulation of methanogenesis in anaerobic digesters treating leachate from a municipal solid waste incineration plant with carbon cloth.* Bioresour. Technol. 222, 270-276.

Li, H., Chang, J., Liu, P., Fu, L., Ding, D. and Lu, Y., 2015a. *Direct interspecies electron transfer accelerates syntrophic oxidation of butyrate in paddy soil enrichments.* Environ. Microbiol. 17, 1533-1547.

Li, L.L., Tong, Z.H., Fang, C.Y., Chu, J. and Yu, H.Q., 2015b. *Response of anaerobic granular sludge to single-wall carbon nanotube exposure.* Water Res. 70, 1-8.

Li, Y., Zhang, Y., Yang, Y., Quan, X. and Zhao, Z., 2017. *Potentially direct interspecies electron transfer of methanogenesis for syntrophic metabolism under sulfate reducing conditions with stainless steel.* Bioresour. Technol. 234, 303-309.

Lin, C.-Y., Sato, K., Noike, T., Matsumoto, J., 1986. *Methanogenic digestion using mixed substrate of acetic, propionic and butyric acids.* Water Res. 20, 385–394.

Lin, R., Cheng, J., Ding, L., Murphy, J.D., 2018. *Improved efficiency of anaerobic digestion through direct interspecies electron transfer at mesophilic and thermophilic temperature ranges.* Chem. Eng. J. 350, 681–691.

Lin, R., Cheng, J., Zhang, J., Zhou, J., Cen, K. and Murphy, J.D., 2017. *Boosting biomethane yield and production rate with graphene: The potential of direct interspecies electron transfer in anaerobic digestion.* Bioresour. Technol. 239, 345-352.

Liu, B., Williams, I., Li, Y., Wang, L., Bagtzoglou, A., McCutcheon, J. and Li, B., 2016. *Towards high power output of scaled-up benthic microbial fuel cells (BMFCs) using multiple electron collectors.* Biosens. Bioelectron. 79, 435-441.

Liu, F., Rotaru, A.E., Shrestha, P.M., Malvankar, N.S., Nevin, K.P. and Lovley, D.R., 2012. *Promoting direct interspecies electron transfer with activated carbon.* Energy Environ. Sci. 5, 8982-8989.

Liu, F., Rotaru, A.E., Shrestha, P.M., Malvankar, N.S., Nevin, K.P. and Lovley, D.R., 2015. *Magnetite compensates for the lack of a pilin-associated c-type cytochrome in extracellular electron exchange.* Environ. Microbiol. 17, 648-655.

Liu, S., Song, H., Wei, S., Yang, F. and Li, X., 2014. *Bio-cathode materials evaluation and configuration optimization for power output of vertical subsurface flow constructed wetland—Microbial fuel cell systems.* Bioresour. Technol. 166, 575-583.

Liu, Y., Balkwill, D.L., Aldrich, H.C., Drake, G.R., Boone, D.R., 1999. *Characterization of the anaerobic propionate-degrading syntrophs Smithella propionica gen. nov., sp. nov. and Syntrophobacter wolinii.* Int. J. Syst. Bacteriol. 49, 545–556.

Logan, B.E., 2009. *Exoelectrogenic bacteria that power microbial fuel cells.* Nature Rev. Microbiol. 7, 375-381.

Lovley, D.R., 2017. *Syntrophy Goes Electric: Direct Interspecies Electron Transfer.* Annu. Rev. Microbiol. 71, 643–664.

Lovley, D.R., 2011a. *Live wires: direct extracellular electron exchange for bioenergy and the bioremediation of energy-related contamination.* Energy Environ. Sci. 4, 4896-4906.

Lovley, D.R., 2011b. *Powering microbes with electricity: direct electron transfer from electrodes to microbes.* Environ. Microbiol. Rep. 3, 27-35.

Lovley, D.R., 2006. *Bug juice: harvesting electricity with microorganisms.* Nat. Rev. Microbiol. 4, 497–508.

Lü, F., Luo, C., Shao, L. and He, P., 2016. *Biochar alleviates combined stress of ammonium and acids by firstly enriching Methanosaeta and then Methanosarcina.* Water Res. 90, 34-43.

Lu, K., Yang, X., Gielen, G., Bolan, N., Ok, Y.S., Niazi, N.K., Xu, S., Yuan, G., Chen, X., Zhang, X. and Liu, D., 2017. *Effect of bamboo and rice straw biochars on the mobility and redistribution of heavy metals (Cd, Cu, Pb and Zn) in contaminated soil.* J. Environ. Manage.186, 285-292.

Luckarift, H.R., Sizemore, S.R., Farrington, K.E., Roy, J., Lau, C., Atanassov, P.B. and Johnson, G.R., 2012. *Facile fabrication of scalable, hierarchically structured polymer/carbon architectures for bioelectrodes.* ACS Appl. Mater. Interfaces 4, 2082-2087.

Luo, C., Lü, F., Shao, L. and He, P., 2015. *Application of eco-compatible biochar in anaerobic digestion to relieve acid stress and promote the selective colonization of functional microbes.* Water Res. 68, 710-718.

Lusk, B.G., Khan, Q.F., Parameswaran, P., Hameed, A., Ali, N., Rittmann, B.E. and Torres, C.I., 2015. *Characterization of electrical current-generation capabilities from thermophilic bacterium Thermoanaerobacter pseudethanolicus using xylose, glucose, cellobiose, or acetate with fixed anode potentials.* Environ. Sci. Technol. 49, 14725-14731.

Ma, J., Zhao, B., Frear, C., Zhao, Q., Yu, L., Li, X., Chen, S., 2013. *Methanosarcina domination in anaerobic sequencing batch reactor at short hydraulic retention time.* Bioresour. Technol. 137, 41–50.

Malvankar, N.S., Lau, J., Nevin, K.P., Franks, A.E., Tuominen, M.T. and Lovley, D.R., 2012a. *Electrical conductivity in a mixed-species biofilm.* Appl. Environ. Microbiol. 78, 5967-5971.

Malvankar, N.S., Tuominen, M.T. and Lovley, D.R., 2012b. *Lack of cytochrome involvement in long-range electron transport through conductive biofilms and nanowires of Geobacter sulfurreducens.* Energy Environ. Sci. 5, 8651-8659.

Malvankar, N.S., Vargas, M., Nevin, K.P., Franks, A.E., Leang, C., Kim, B.C., Inoue, K., Mester, T., Covalla, S.F., Johnson, J.P. and Rotello, V.M., 2011. *Tunable metallic-like conductivity in microbial nanowire networks.* Nat. Nanotechnol. 6, 573-579.

Maruthupandy, M., Anand, M., Maduraiveeran, G., Beevi, A.S.H., Priya, R.J., 2015. *Electrical conductivity measurements of bacterial nanowires from Pseudomonas aeruginosa.* Adv. Nat. Sci. Nanosci. Nanotechnol. 6, 045007.

Matsumoto, S., Ohtaki, A., Hori, K., 2012. *Carbon Fiber as an Excellent Support Material for Wastewater Treatment Biofilms.* Environ. Sci. Technol. 120828132236002.

Mei, X., Xing, D., Yang, Y., Liu, Q., Zhou, H., Guo, C., Ren, N., 2017. *Adaptation of microbial community of the anode biofilm in microbial fuel cells to temperature.* Bioelectrochemistry 117, 29–33.

Mezzullo, W.G., McManus, M.C., Hammond, G.P., 2013. *Life cycle assessment of a small-scale anaerobic digestion plant from cattle waste.* Appl. Energy 102, 657–664.

Mink, J.E. and Hussain, M.M., 2013. *Sustainable design of high-performance microsized microbial fuel cell with carbon nanotube anode and air cathode.* ACS Nano 7, 6921-6927.

Mladenovska, Z., Ahring, B.K., 2000. *Growth kinetics of thermophilic Methanosarcina spp. isolated from full-scale biogas plants treating animal manures.* FEMS Microbiol. Ecol. 31, 225–229.

Morita, M., Malvankar, N.S., Franks, A.E., Summers, Z.M., Giloteaux, L., Rotaru, A.E., Rotaru, C. and Lovley, D.R., 2011. *Potential for direct interspecies electron transfer in methanogenic wastewater digester aggregates.* mBio 2, 00159-11.

Park, J.-H., Kang, H.-J., Park, K.-H., Park, H.-D., 2018. *Direct interspecies electron transfer via conductive materials: A perspective for anaerobic digestion applications.* Bioresour. Technol. 254, 300–311.

Prakash, O.M., Gihring, T.M., Dalton, D.D., Chin, K.J., Green, S.J., Akob, D.M., Wanger, G. and Kostka, J.E., 2010. *Geobacter daltonii sp. nov., an Fe (III)-and uranium (VI)-reducing bacterium isolated from a shallow subsurface exposed to mixed heavy metal and hydrocarbon contamination.* Int. J. Syst. Evol. Microbiol. 60, 546-553.

Rajendran, K., Surendra, K.C., Tomberlin, J.K., Khanal, S.K., 2018. *Insect-Based Biorefinery for Bioenergy and Bio-Based Products,* in: Waste Biorefinery. Elsevier, pp. 657–669.

Reimers, C.E., Li, C., Graw, M.F., Schrader, P.S., Wolf, M., 2017. *The Identification of Cable Bacteria Attached to the Anode of a Benthic Microbial Fuel Cell: Evidence of Long Distance Extracellular Electron Transport to Electrodes.* Front. Microbiol. 8, 2055.

Ren, H., Pyo, S., Lee, J.I., Park, T.J., Gittleson, F.S., Leung, F.C., Kim, J., Taylor, A.D., Lee, H.S. and Chae, J., 2015. *A high power density miniaturized microbial fuel cell having carbon nanotube anodes.* J. Power Sources 273, 823-830.

Ren, Y., Yu, M., Wu, C., Wang, Q., Gao, M., Huang, Q., Liu, Y., 2018. *A comprehensive review on food waste anaerobic digestion: Research updates and tendencies.* Bioresour. Technol. 247, 1069–1076.

Rideout, J.R., He, Y., Navas-Molina, J.A., Walters, W.A., Ursell, L.K., Gibbons, S.M., Chase, J., McDonald, D., Gonzalez, A., Robbins-Pianka, A., Clemente, J.C., Gilbert, J.A., Huse, S.M., Zhou, H.-W., Knight, R., Caporaso, J.G., 2014. *Subsampled open-reference clustering creates consistent, comprehensive OTU definitions and scales to billions of sequences.* PeerJ 2, e545.

Rotaru, A.-E., Shrestha, P.M., Liu, F., Markovaite, B., Chen, S., Nevin, K.P., Lovley, D.R., 2014a. *Direct interspecies electron transfer between Geobacter metallireducens and Methanosarcina barkeri.* Appl. Environ. Microbiol. 80, 4599–605.

Rotaru, A.-E., Shrestha, P.M., Liu, F., Shrestha, M., Shrestha, D., Embree, M., Zengler, K., Wardman, C., Nevin, K.P., Lovley, D.R., 2014b. *A new model for electron flow during anaerobic digestion: direct interspecies electron transfer to Methanosaeta for the reduction of carbon dioxide to methane.* Energy Environ. Sci. 7, 408–415.

Ruiz, V., Ilhan, Z.E., Kang, D.-W., Krajmalnik-Brown, R., Buitrón, G., 2014. *The source of inoculum plays a defining role in the development of MEC microbial consortia fed with acetic and propionic acid mixtures.* J. Biotechnol. 182–183, 11–18.

Santoro, C., Babanova, S., Artyushkova, K., Cornejo, J.A., Ista, L., Bretschger, O., Marsili, E., Atanassov, P., Schuler, A.J., 2015. *Influence of anode surface chemistry on microbial fuel cell operation.* Bioelectrochem. 106, 141-149.

Sasaki, K., Morita, M., Hirano, S.I., Ohmura, N. and Igarashi, Y., 2011. *Decreasing ammonia inhibition in thermophilic methanogenic bioreactors using carbon fiber textiles.* Appl. Microbiol. Biotechnol. 90, 1555.

Sasaki, K., Sasaki, D., Kamiya, K., Nakanishi, S., Kato, S., 2018. *Electrochemical biotechnologies minimizing the required electrode assemblies.* Curr. Opin. Biotechnol. 50, 182–188.

Sauvée, L., Viaggi, D., 2016. *Biorefineries in the bio-based economy: opportunities and challenges for economic research.* Bio - Based Appl. Econ. 5, 1–4.

Schmidt, A., Müller, N., Schink, B., Schleheck, D., 2013a. *A Proteomic View at the Biochemistry of Syntrophic Butyrate Oxidation in Syntrophomonas wolfei.* PLoS One 8, e56905.

Schmidt, J.E., Ahring, B.K., 1995. *Interspecies Electron Transfer during Propionate and Butyrate Degradation in Mesophilic, Granular Sludge.* Appl. Environ. Microbiol. 61, 2765–7.

Schmidt, J.E., Ahring, B.K., 1993. *Effects of hydrogen and formate on the degradation of propionate and butyrate in thermophilic granules from an upflow anaerobic sludge blanket reactor.* Appl. Environ. Microbiol. 59, 2546–51.

Schmidt, T., Pröter, J., Scholwin, F., Nelles, M., 2013b. *Anaerobic digestion of grain stillage at high organic loading rates in three different reactor systems.* Biomass and Bioenergy 55, 285–290.

Shen, Y., Linville, J.L., Ignacio-de Leon, P.A.A., Schoene, R.P. and Urgun-Demirtas, M., 2016. *Towards a sustainable paradigm of waste-to-energy process: Enhanced anaerobic digestion of sludge with woody biochar.* J. Clean. Prod. 135, 1054-1064.

Shin, S.G., Han, G., Lim, J., Lee, C. and Hwang, S., 2010. *A comprehensive microbial insight into two-stage anaerobic digestion of food waste-recycling wastewater.* Water Res. 44, 4838-4849.

Shrestha, P.M., Malvankar, N.S., Werner, J.J., Franks, A.E., Elena-Rotaru, A., Shrestha, M., Liu, F., Nevin, K.P., Angenent, L.T. and Lovley, D.R., 2014. *Correlation between microbial community and granule conductivity in anaerobic bioreactors for brewery wastewater treatment.* Bioresour. Technol. 174, 306-310.

Shrestha, P.M. and Rotaru, A.E., 2014. *Plugging in or going wireless: strategies for interspecies electron transfer.* Front. Microbiol. 5, 237.

Simon-Deckers, A., Loo, S., Mayne-L'hermite, M., Herlin-Boime, N., Menguy, N., Reynaud, C., Gouget, B. and Carriere, M., 2009. *Size-, composition-and shape-dependent toxicological impact of metal oxide nanoparticles and carbon nanotubes toward bacteria.* Environ. Sci. Technol. 43, 8423-8429.

Singh, S.P. and Prerna, P., 2009. *Review of recent advances in anaerobic packed-bed biogas reactors.* Renew. Sustainable Energy Rev.13, 1569-1575.

Smith, K.S. and Ingram-Smith, C., 2007. *Methanosaeta, the forgotten methanogen?* Curr. Trends Microbiol. 15, 150-155.

Storck, T., Virdis, B. and Batstone, D.J., 2016. *Modelling extracellular limitations for mediated versus direct interspecies electron transfer.* ISME J. 10, 621-631.

Summers, Z.M., Fogarty, H.E., Leang, C., Franks, A.E., Malvankar, N.S. and Lovley, D.R., 2010. *Direct exchange of electrons within aggregates of an evolved syntrophic coculture of anaerobic bacteria.* Science 330, 1413-1415.

Tan, Y., Adhikari, R.Y., Malvankar, N.S., Ward, J.E., Woodard, T.L., Nevin, K.P. and Lovley, D.R., 2017. *Expressing the Geobacter metallireducens PilA in Geobacter sulfurreducens Yields Pili with Exceptional Conductivity.* mBio 8, 02203-16.

Tao, J., Qin, L., Liu, X., Li, B., Chen, J., You, J., Shen, Y. and Chen, X., 2017. *Effect of granular activated carbon on the aerobic granulation of sludge and its mechanism.* Bioresour. Technol. 236, 60-67.

Tatara, M., Yamazawa, A., Ueno, Y., Fukui, H., Goto, M. and Sode, K., 2005. *High-rate thermophilic methane fermentation on short-chain fatty acids in a down-flow anaerobic packed-bed reactor.* Bioprocess Biosyst. Eng. 27, 105-113.

Thauer, R.K., 1998. *Biochemistry of methanogenesis: A tribute to Marjory Stephenson: 1998 Marjory Stephenson prize lecture.* Microbiology 144, 2377-2406.

Thiele, J.H., Zeikus, J.G., 1988. *Control of Interspecies Electron Flow during Anaerobic Digestion: Significance of Formate Transfer versus Hydrogen Transfer during Syntrophic Methanogenesis in Flocs.* Appl. Environ. Microbiol. 54, 20–29.

Tian, T., Qiao, S., Li, X., Zhang, M. and Zhou, J., 2017. *Nano-graphene induced positive effects on methanogenesis in anaerobic digestion.* Bioresour. Technol. 224, 41-47.

Van Der Zee, F.P., Bisschops, I.A., Lettinga, G. and Field, J.A., 2003. *Activated carbon as an electron acceptor and redox mediator during the anaerobic biotransformation of azo dyes.* Environ. Sci. Technol. 37, 402-408.

Vasco-Correa, J., Khanal, S., Manandhar, A., Shah, A., 2018. *Anaerobic digestion for bioenergy production: Global status, environmental and techno-economic implications, and government policies.* Bioresour. Technol. 247, 1015–1026.

Wang, A., Liu, L., Sun, D., Ren, N. and Lee, D.J., 2010. *Isolation of Fe (III)-reducing fermentative bacterium Bacteroides sp. W7 in the anode suspension of a microbial electrolysis cell (MEC).* Int. J. Hydrogen Energy 35, 3178-3182.

Wang, L.Y., Nevin, K.P., Woodard, T.L., Mu, B.Z. and Lovley, D.R., 2016. *Expanding the diet for DIET: electron donors supporting direct interspecies electron transfer (DIET) in defined co-cultures.* Front. Microbiol. 7, 236.

Wei, J., Liang, P. and Huang, X., 2011. *Recent progress in electrodes for microbial fuel cells.* Bioresour. Technol. 102, 9335-9344.

Wu, W., Wu, Z., Yu, T., Jiang, C. and Kim, W.S., 2015. *Recent progress on magnetic iron oxide nanoparticles: synthesis, surface functional strategies and biomedical applications.* Sci. Tech. Adv. Mater.16, 023501.

Xu, S., Han, R., Zhang, Y., He, C., Liu, H., 2018. *Differentiated stimulating effects of activated carbon on methanogenic degradation of acetate, propionate and butyrate.* Waste Manag. 76, 394–403.

Yamada, C., Kato, S., Ueno, Y., Ishii, M. and Igarashi, Y., 2015. *Conductive iron oxides accelerate thermophilic methanogenesis from acetate and propionate.* J. Biosci. Bioeng.119, 678-682.

Yamada, T., Imachi, H., Ohashi, A., Harada, H., Hanada, S., Kamagata, Y., Sekiguchi, Y., 2007. *Bellilinea caldifistulae gen. nov., sp. nov. and Longilinea arvoryzae gen. nov., sp. nov., strictly anaerobic, filamentous bacteria of the phylum Chloroflexi isolated from methanogenic propionate-degrading consortia.* Int. J. Syst. Evol. Microbiol. 57, 2299–2306.

Yan, W., Shen, N., Xiao, Y., Chen, Y., Sun, F., Tyagi, V.K. and Zhou, Y., 2017. *The role of conductive materials in the start-up period of thermophilic anaerobic system.* Bioresour. Technol. 239, 336-344.

Yang, Y., Zhang, Y., Li, Z., Zhao, Z., Quan, X. and Zhao, Z., 2017. *Adding granular activated carbon into anaerobic sludge digestion to promote methane production and sludge decomposition.* J. Clean Prod. 149, 1101-1108.

Yasri, N.G., Nakhla, G., 2017. *The performance of 3-D graphite doped anodes in microbial electrolysis cells.* J. Power Sources 342, 579–588.

Yasri, N.G., Nakhla, G., 2016. *Electrochemical Behavior of Anode-Respiring Bacteria on Doped Carbon Electrodes.* ACS Appl. Mater. Interfaces 8, 35150–35162.

Yong, Y.C., Dong, X.C., Chan-Park, M.B., Song, H. and Chen, P., 2012. *Macroporous and monolithic anode based on polyaniline hybridized three-dimensional graphene for high-performance microbial fuel cells.* ACS Nano 6, 2394-2400.

Yue, Z.R., Jiang, W., Wang, L., Gardner, S.D., Pittman, C.U., 1999. *Surface characterization of electrochemically oxidized carbon fibers.* Carbon N. Y. 37, 1785–1796.

Zhang, C., Jiang, Y., Li, Y., Hu, Z., Zhou, L., Zhou, M., 2013. *Three-dimensional electrochemical process for wastewater treatment: A general review.* Chem. Eng. J. 228, 455–467.

Zhang, J. and Lu, Y., 2016. *Conductive Fe3O4 Nanoparticles Accelerate Syntrophic Methane Production from Butyrate Oxidation in Two Different Lake Sediments.* Front. Microbiol. 7, 1316.

Zhang, Q., Huang, J.Q., Qian, W.Z., Zhang, Y.Y. and Wei, F., 2013. *The road for nanomaterials industry: A review of carbon nanotube production, post-treatment, and bulk applications for composites and energy storage.* Small 9, 1237-1265.

Zhao, Z., Zhang, Y., Holmes, D.E., Dang, Y., Woodard, T.L., Nevin, K.P., Lovley, D.R., 2016a. *Potential enhancement of direct interspecies electron transfer for syntrophic metabolism of propionate and butyrate with biochar in up-flow anaerobic sludge blanket reactors.* Bioresour. Technol. 209, 148–156.

Zhao, Z., Zhang, Y., Li, Y., Dang, Y., Zhu, T. and Quan, X., 2017. *Potentially shifting from interspecies hydrogen transfer to direct interspecies electron transfer for syntrophic metabolism to resist acidic impact with conductive carbon cloth.* Chem. Eng. J. 313, 10-18.

Zhao, Z., Zhang, Y., Woodard, T.L., Nevin, K.P. and Lovley, D.R., 2015. *Enhancing syntrophic metabolism in up-flow anaerobic sludge blanket reactors with conductive carbon materials.* Bioresour. Technol. 191, 140-145.

Zhao, Z., Zhang, Y., Yu, Q., Dang, Y., Li, Y., Quan, X., 2016b. *Communities stimulated with ethanol to perform direct interspecies electron transfer for syntrophic metabolism of propionate and butyrate.* Water Res. 102, 475–484.

Zhuang, L., Tang, J., Wang, Y., Hu, M. and Zhou, S., 2015. *Conductive iron oxide minerals accelerate syntrophic cooperation in methanogenic benzoate degradation.* J. Hazard. Mater. 293, 37-45.

Ziganshin, A.M., Schmidt, T., Lv, Z., Liebetrau, J., Richnow, H.H., Kleinsteuber, S. and Nikolausz, M., 2016. *Reduction of the hydraulic retention time at constant high organic loading rate to reach the microbial limits of anaerobic digestion in various reactor systems.* Bioresour. Technol. 217, 62-71.

Appendix A

Supplementary Information for Chapter 3

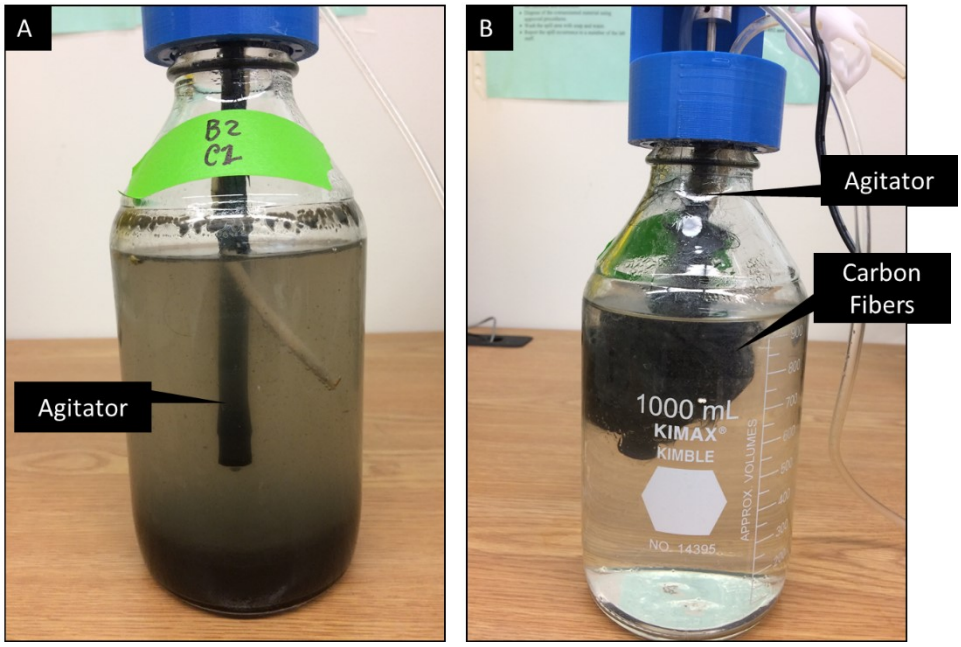

Figure A-1. Photograph of the (A) control, and (B) CF bioreactors. The photographs were taken after the completion of all experiments.

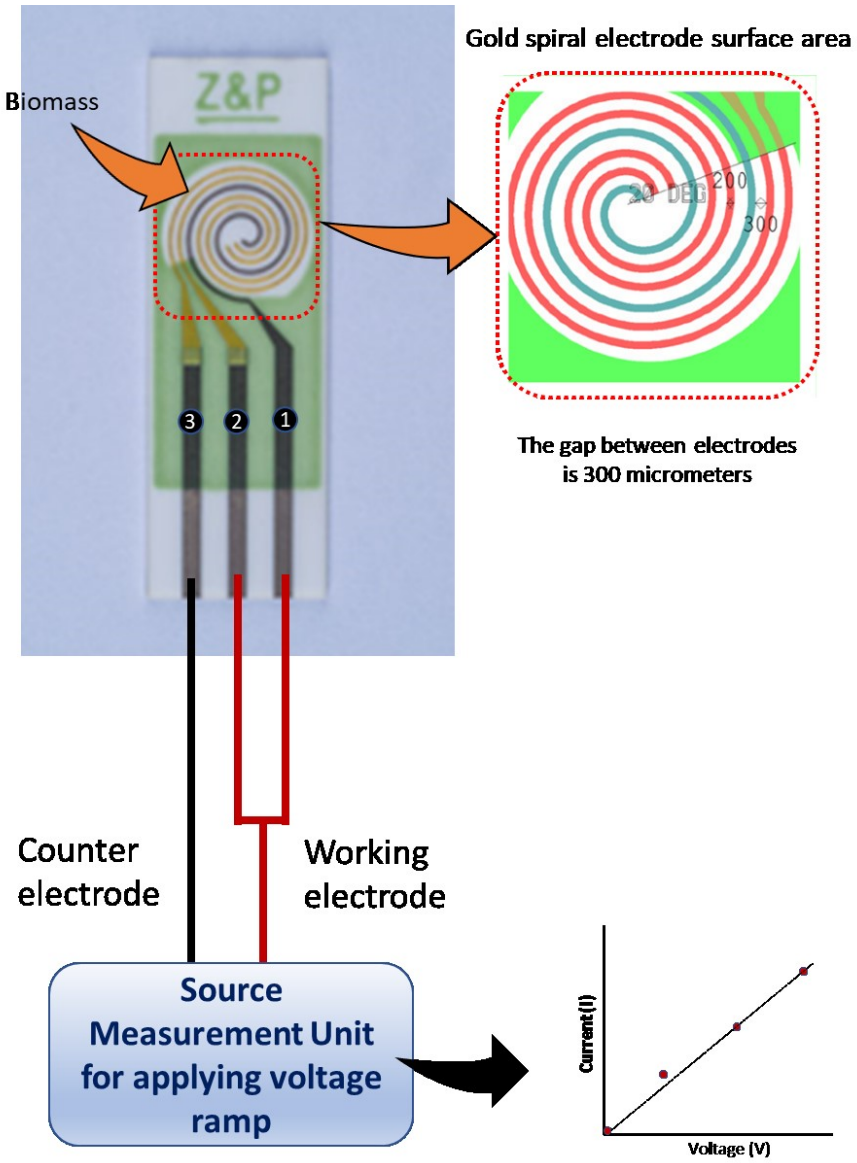

Figure A-2. Schematic of the set-up for biomass conductance measurement (Photograph of the sensor and schematic of spiral electrode surface area are adopted from the sensor manufacturer's website: *www.zimmerpeacocktech.com*).

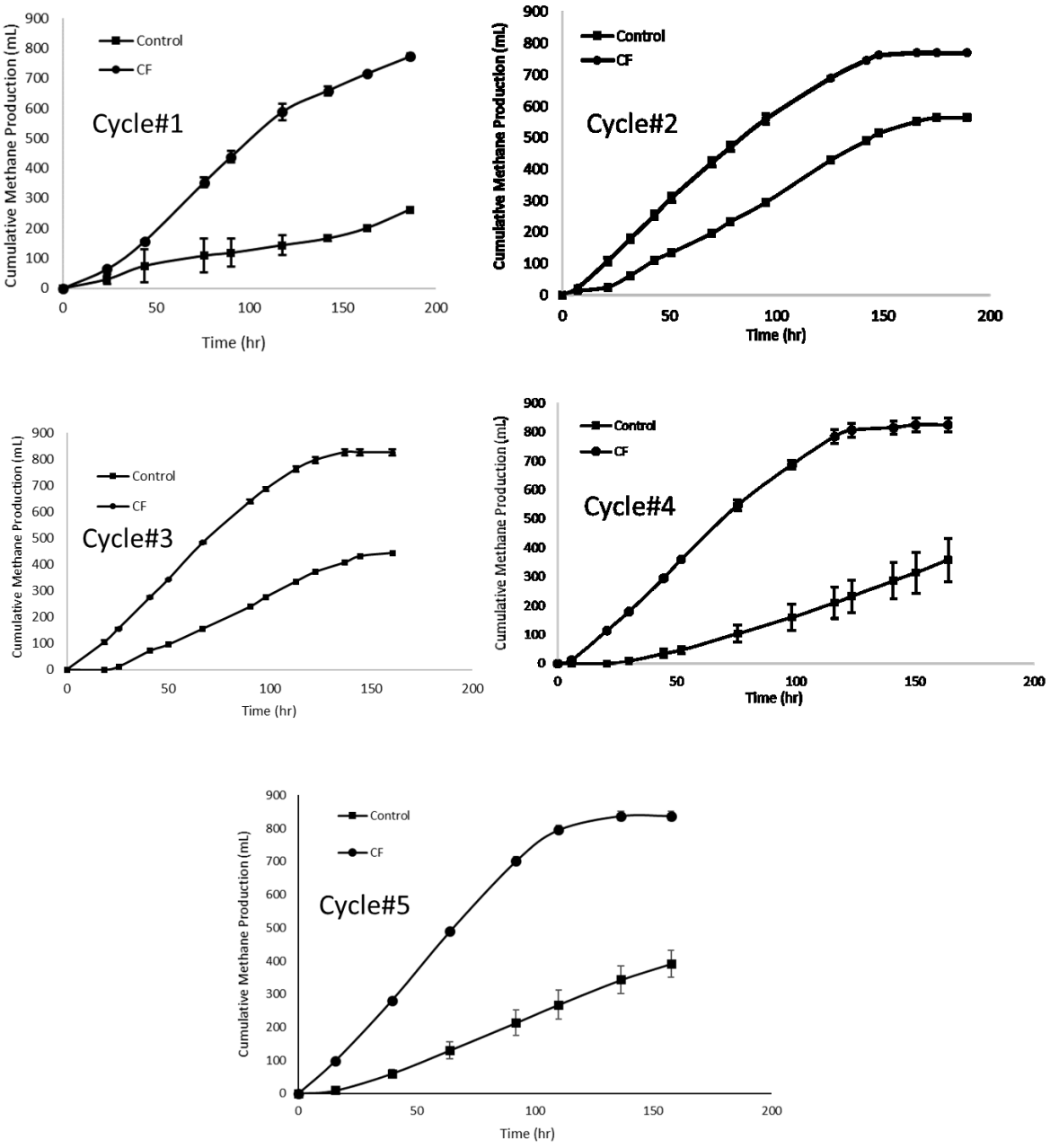

Figure A-3. Time course of methane production in five consecutive fed-batch cycles.

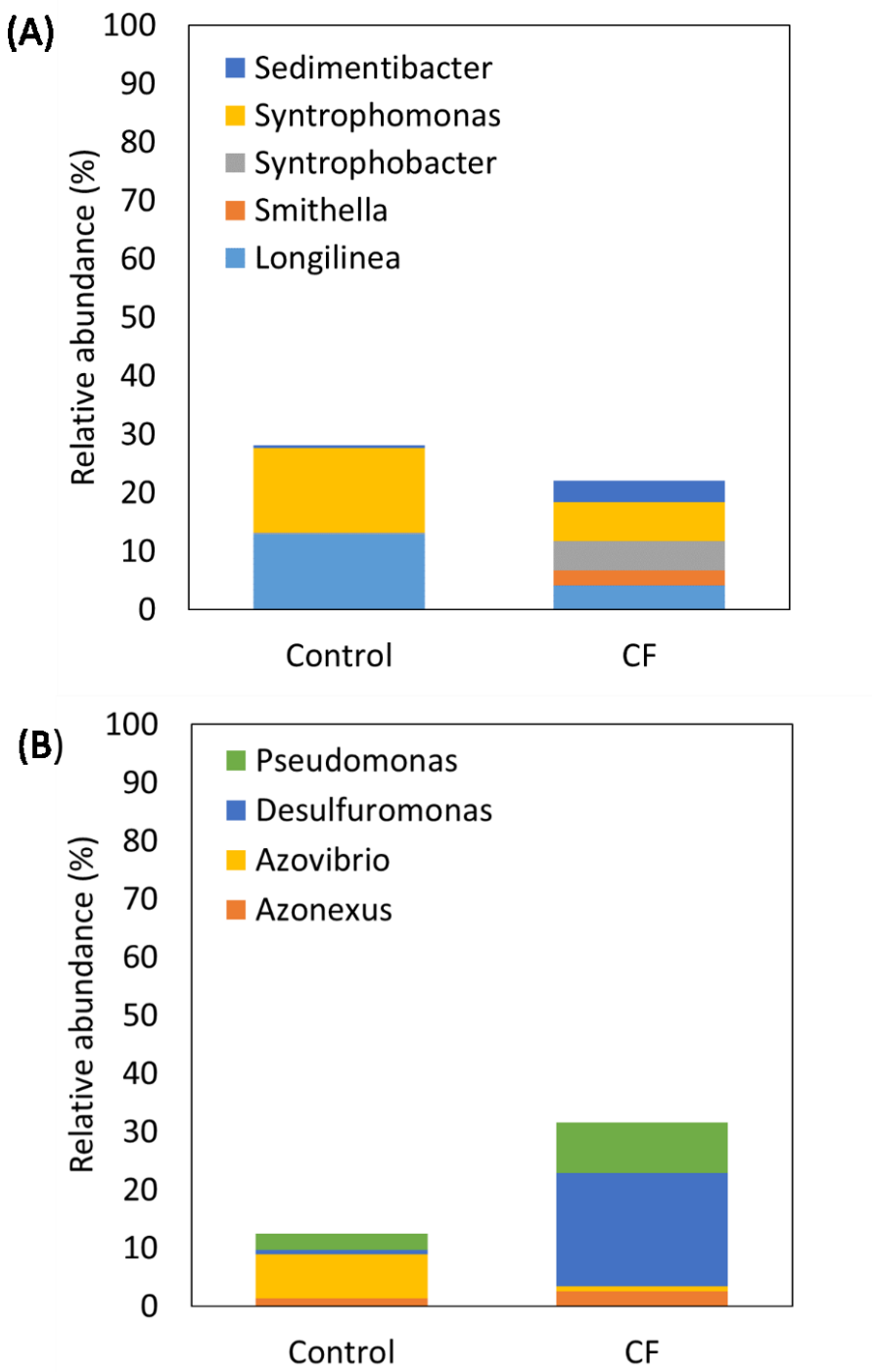

Figure A-4. Relative abundances of (A) non-electroactive propionate/butyrate oxidizing bacteria, and (B) electroactive bacteria at the genus level. The genera were screened according to the previous literatures (Boone and Bryant, 1980; Freguia et al., 2010; Gulhane et al., 2017; Koch and Harnisch, 2016; Liu et al., 1999; Mei et al., 2017; Ruiz et al., 2014; A. Schmidt et al., 2013; Yamada et al., 2007).

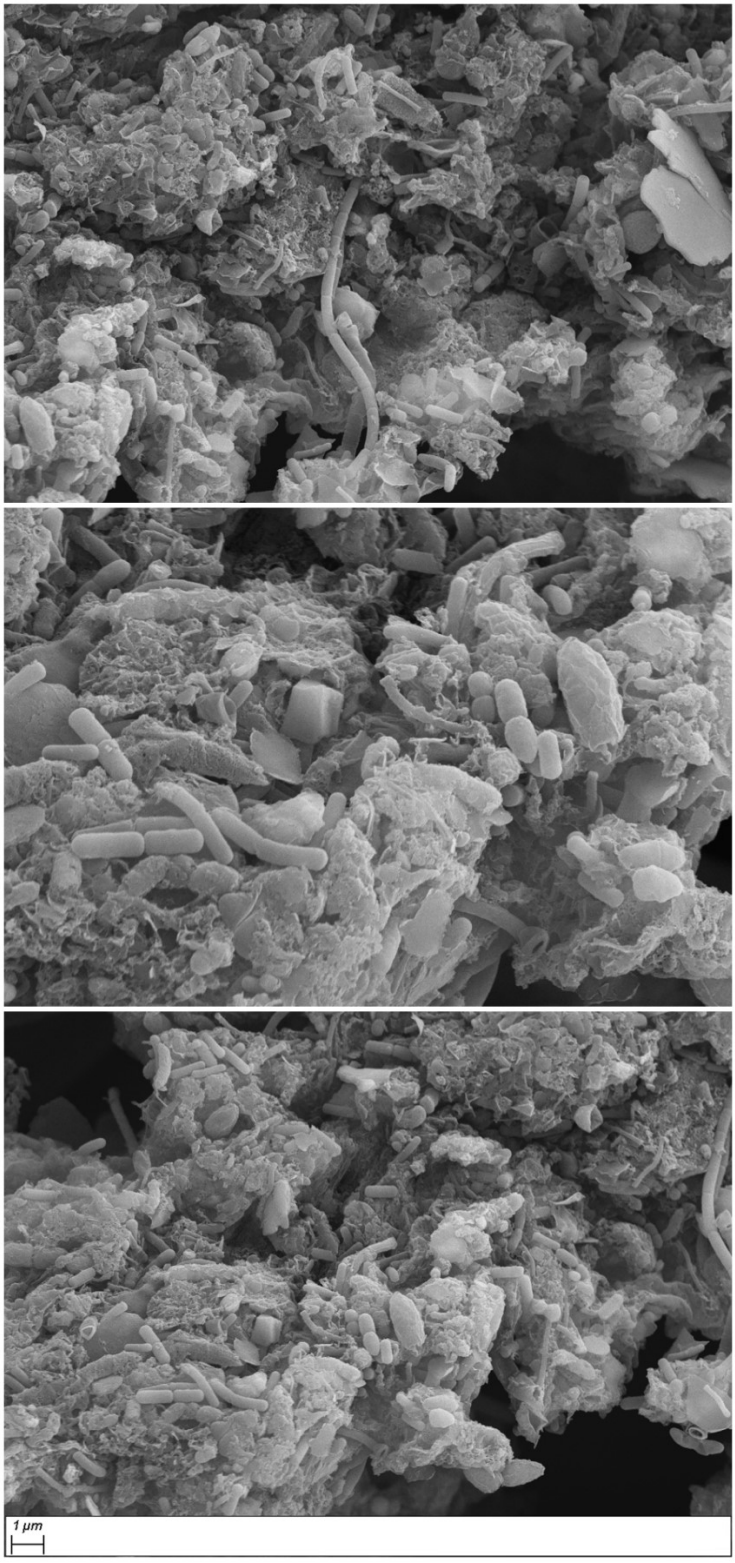

Figure A-5. SEM imaging of biomass in CF bioreactor.

Table A-1. Possible reactions involved in propionate and butyrate conversion to methane through direct interspecies electron transfer (DIET) and interspecies hydrogen transfer (IHT) based pathways.

	Direct interspecies electron transfer (DIET)	**Interspecies hydrogen transfer (IHT)**
Propionate	$4CH_3CH_2COO^- + 8H_2O \rightarrow 4CH_3COO^- + 4CO_2 + 24H^+ + 24e^-$ $4CH_3COO^- + 4H^+ \rightarrow 4CH_4 + 4CO_2$ $3CO_2 + 24e^- + 24H^+ \rightarrow 3CH_4 + 6H_2O$ Overall reaction: $4CH_3CH_2COO^- + 4H^+ + 2H_2O \rightarrow 7CH_4 + 5CO_2$	$4CH_3CH_2COO^- + 8H_2O \rightarrow 4CH_3COO^- + 4CO_2 + 12H_2$ $4CH_3COO^- + 4H^+ \rightarrow 4CH_4 + 4CO_2$ $12H_2 + 3CO_2 \rightarrow 3CH_4 + 6H_2O$ Overall reaction: $4CH_3CH_2COO^- + 4H^+ + 2H_2O \rightarrow 7CH_4 + 5CO_2$
Butyrate	$4CH_3CH_2CH_2COO^- + 8H_2O \rightarrow 8CH_3COO^- + 20H^+ + 16e^-$ $8CH_3COO^- + 8H^+ \rightarrow 8CH_4 + 8CO_2$ $2CO_2 + 16e^- + 16H^+ \rightarrow 2CH_4 + 4H_2O$ Overall reaction: $4CH_3CH_2CH_2COO^- + 4H^+ + 4H_2O \rightarrow 10CH_4 + 6CO_2$	$4CH_3CH_2CH_2COO^- + 8H_2O \rightarrow 8CH_3COO^- + 4H^+ + 8H_2$ $8CH_3COO^- + 8H^+ \rightarrow 8CH_4 + 8CO_2$ $8H_2 + 2CO_2 \rightarrow 2CH_4 + 4H_2O$ Overall reaction: $4CH_3CH_2CH_2COO^- + 4H^+ + 4H_2O \rightarrow 10CH_4 + 6CO_2$

Appendix B

Supplementary Information for Chapter 4

Detail Start-up and enrichment procedure

All the bioreactors were fed with ethanol, ethanol-propionate and propionate medium as summarized in Table B-2 and methane production was monitored to track the overall enrichment procedure. Initially, all the bioreactors were run in batch mode for 117 hour using ethanol as sole substrate to enrich DIET active communities (Phase #1). The time required for any set of bioreactors to reach plateau was used to determine the hydraulic residence time (HRT) of fed-batch operation of bioreactors during Phase #2 (Boone and Xun, 1987). During Phase #2, each bioreactor's supernatant was replaced with 400mL of ethanol medium (TCOD: 4860 ± 410 mg/L) to maintain HRT of 6 days to enrich DIET active communities. Later during Phase #3, the bioreactors were fed with propionate and ethanol as co-substrate (1:1 as of COD ratio; TCOD: 4822 ± 132 mg/L) in batch mode to ensure enrichment of fermentative and electroactive bacteria (Barua et al., 2018; Zhao et al., 2016a, 2016b). During Phase #4, substrate medium was switched to propionate as sole substrate (TCOD: 4830 ± 156 mg/L) in batch mode for 236 ± 2 hours (n=2) for further enrichment of propionate fermentative bacteria. Later, all the bioreactors were operated at batch mode (Phase #5) for 115 hours replacing 150mL of supernatant with fresh propionate medium (TCOD: 4820 ± 163 mg/L). The objective to reduce fresh substrate volume during Phase #5 was to reduce the cumulative methane production time to reach plateau and to reduce the HRT of Phase #6. During Phase #6, three fed-batch cycles were operated at 20 days of HRT and last two fed-batch cycles (referred as Cycle #E1 and E2) were monitored for CH_4 production, and influent and effluent liquid were analysed to ensure stable performance of each bioreactor at low propionate concentration. The objective of Phase #6 was to ensure comparable performance ($p>0.05$) of all sets of bioreactors because DIET pathway has less effect at low propionate concentration (Xu et al., 2018). After Phase #6, propionate medium concentration was gradually increased through four fed-batch cycles (Phase #7, 8, 9 and 10) at 20 days of HRT to study the biodegradability of propionate through DIET pathway at high propionate concentration. During Phase #7 to 10, only cumulative methane production was monitored and the height propionate medium concentration (TCOD: 13280 ± 90 mg/L) was selected when significantly different cumulative methane production among the bioreactors was observed (control, GAC, MDGAC).

Table B-1. Summary of VFAs during fed-batch experiment (average ± standard deviation; n=3).

Cycle	Feed Condition	Control		GAC		MDGAC	
		Acetate (mg COD/L)	Propionate (mg COD/L)	Acetate (mg COD/L)	Propionate (mg COD/L)	Acetate (mg COD/L)	Propionate (mg COD/L)
Cycle #1	Inlet	997±124	1194±19	653±60	1263±16	520±18	1337±18
	Outlet	1555±165	89±2	1168±86	57±0	1022±130	76±18
Cycle #2	Inlet	1470±210	1268±23	1101±19	1263±43	862±29	1323±47
	Outlet	1838±227	110±28	1402±118	77±20	1142±114	55±11
Cycle #3	Inlet	1869±250	1270±13	1336±161	1285±27	1006±31	1275±45
	Outlet	2103±275	185±30	1589±234	135±38	1230±113	63±1
Cycle #4	Inlet	2132±235	1362±21	1633±140	1382±31	1109±42	1336±11
	Outlet	2234±178	219±76	1759±288	169±75	1286±147	51±3

Table B-2. Summary of start-up and enrichment stage (average ± standard deviation; n=3×number of cycles).

Phases	Mode of Operation	Substrate	COD (mg/L)	HRT (day)	Number of Cycles	Volume of Liquid Replaced (mL)	Cumulative Methane Production (mL)		
							Control	GAC	MDGAC
Phase #1	Batch	Ethanol	4860 ± 410	-	1	-	1362 ± 205	1212 ± 37	1144 ± 63
Phase #2	Fed-batch	Ethanol	4860 ± 410	06	4	400	586 ± 61	586 ± 11	600 ± 33
Phase #3	Batch	Ethanol: Propionate (1:1 COD ratio)	4822 ± 132	-	2	400	525 ± 78	506 ± 18	583 ± 72
Phase #4	Batch	Propionate	4830 ± 156	-	2	400	570 ± 51	667 ± 132	755 ± 83
Phase #5	Batch	Propionate	4820 ± 163	-	1	150	324 ± 44	330 ± 20	371 ± 14
Phase #6	Fed-batch	Propionate	4820 ± 163	20	3	150	376 ± 41	359 ± 6	395 ± 14
Phase #7	Fed-batch	Propionate	6650 ± 120	20	1	150	449 ± 18	427 ± 10	504 ± 30
Phase #8	Fed-batch	Propionate	8210 ± 155	20	1	150	473 ± 22	504 ± 54	551 ± 5
Phase #9	Fed-batch	Propionate	9982 ± 115	20	1	150	505 ± 32	590 ± 58	590 ± 36
Phase #10	Fed-batch	Propionate	13280 ± 90	20	1	150	550 ± 70	609 ± 39	643 ± 18

Table B-3. Summary of Student's t-test.

Bioreactors		Specific Methane Production ($mL\ CH_4/\ g\ COD_{initial}$)		COD Removal Efficiency (%)	
		95% CI	p-value	95% CI	p-value
MDGAC	GAC	(13.7, 57.13)	0.0022	(3.34, 16.16)	0.004
MDGAC	Control	(45.79, 89.21)	0.0001	(15.01, 27.82)	0.0001
GAC	Control	(10.37, 53.79)	0.005	(5.26, 18.07)	0.0008

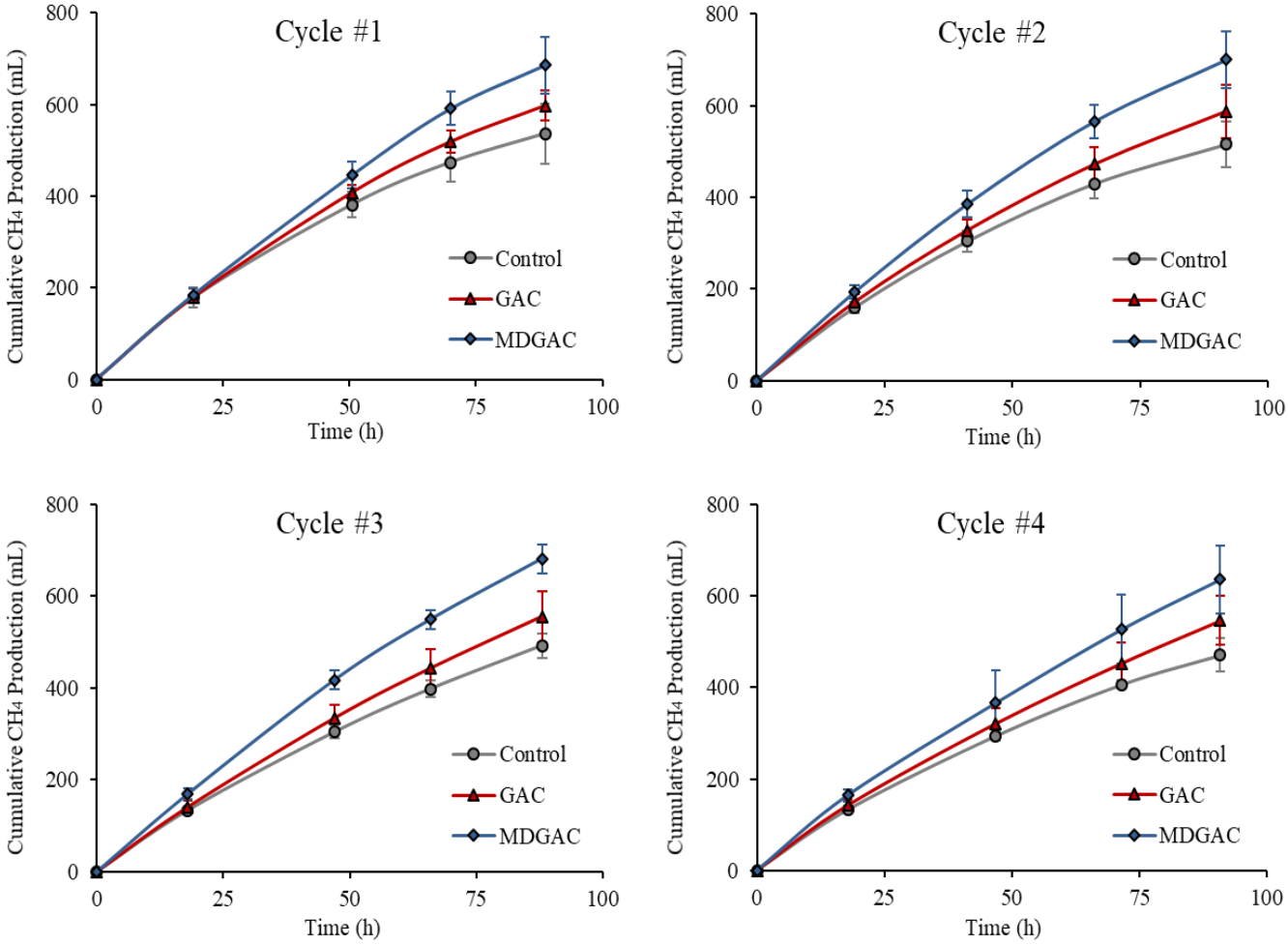

Figure B-1. Time course of methane production of four consecutive fed-batch cycles.

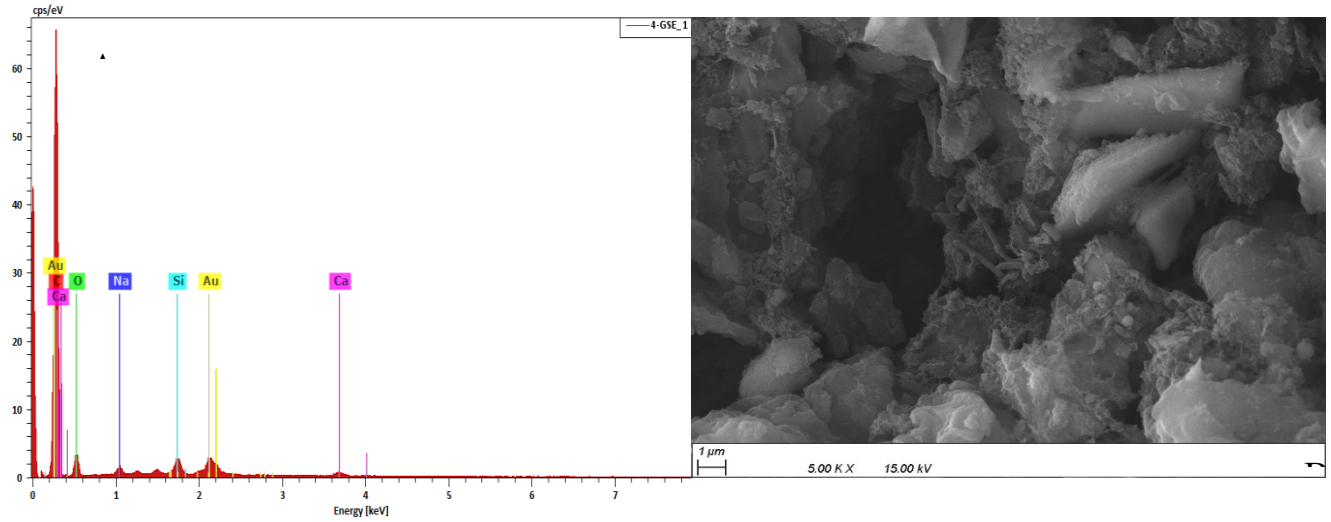

Figure B-2. (A) SEM-EDS spectrum, and (B) SEM imaging of biomass on GAC surface at the end of cycle #5.

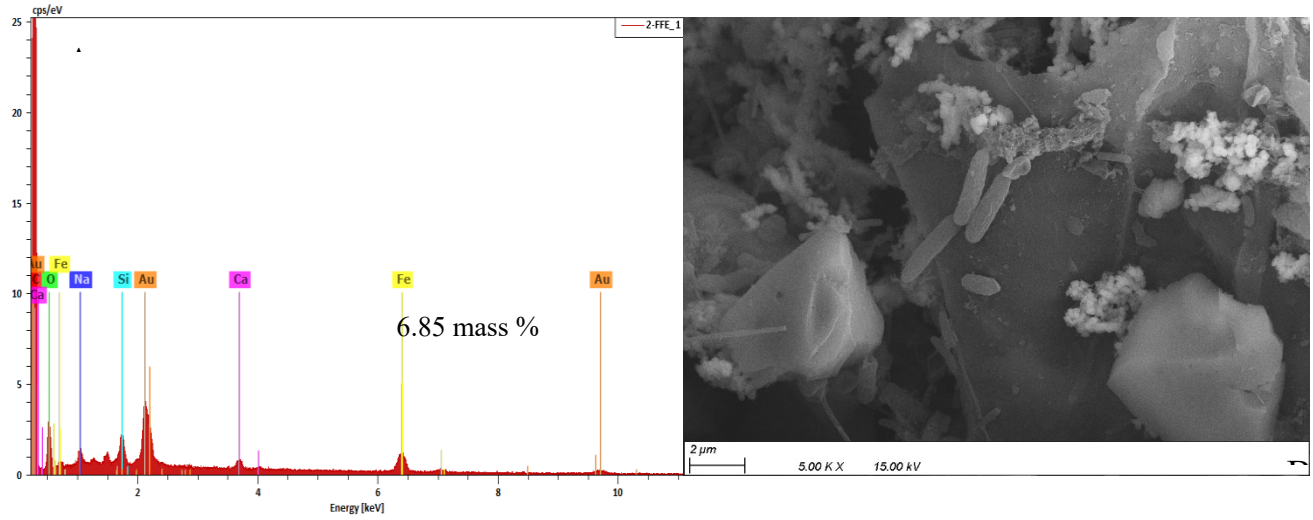

Figure B-3. (A) SEM-EDS spectrum, and (B) SEM imaging of biomass on magnetite doped GAC surface at the end of Cycle #5.

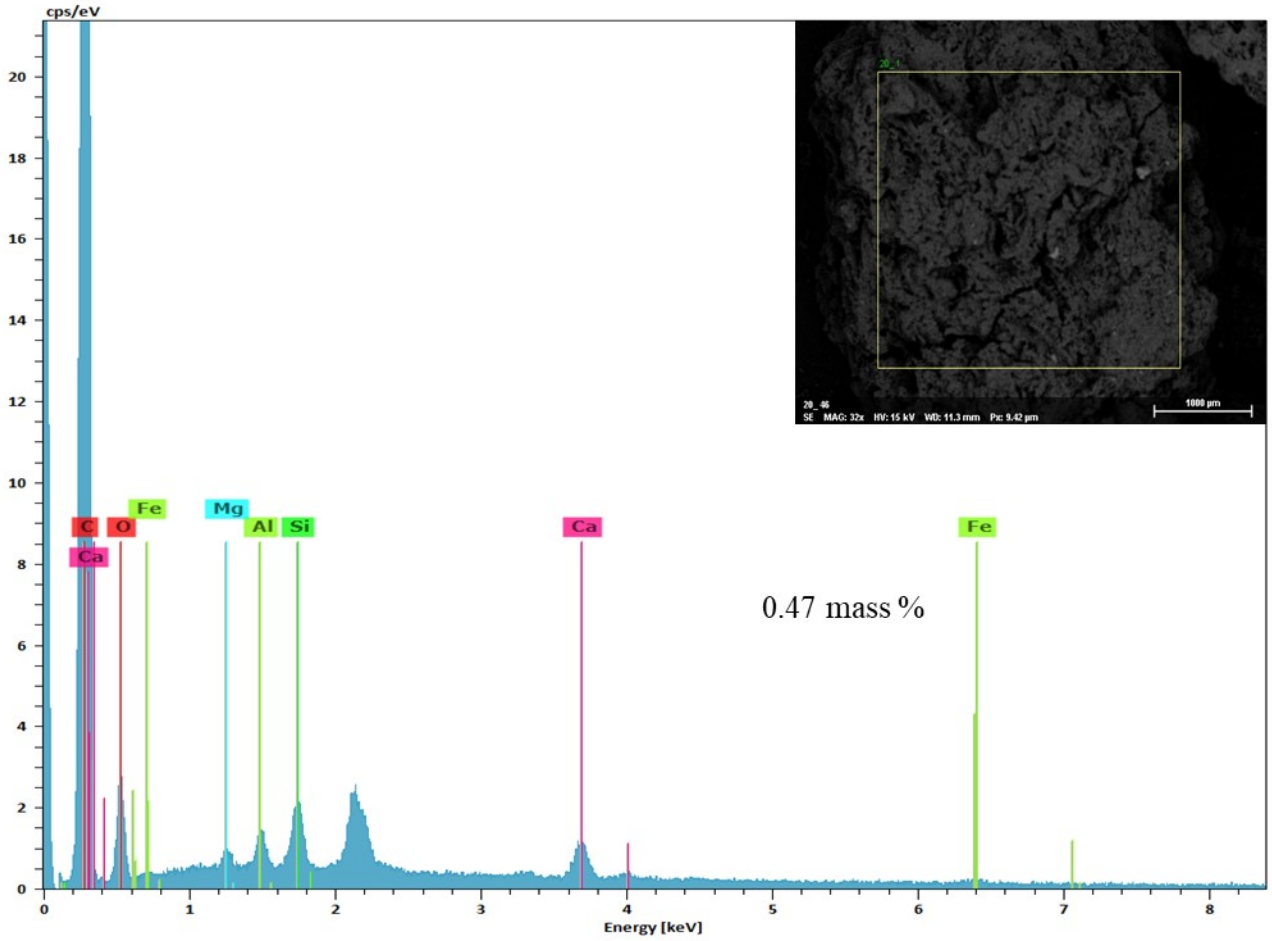

Figure B-4. SEM-EDS spectrum of undoped GAC surface.

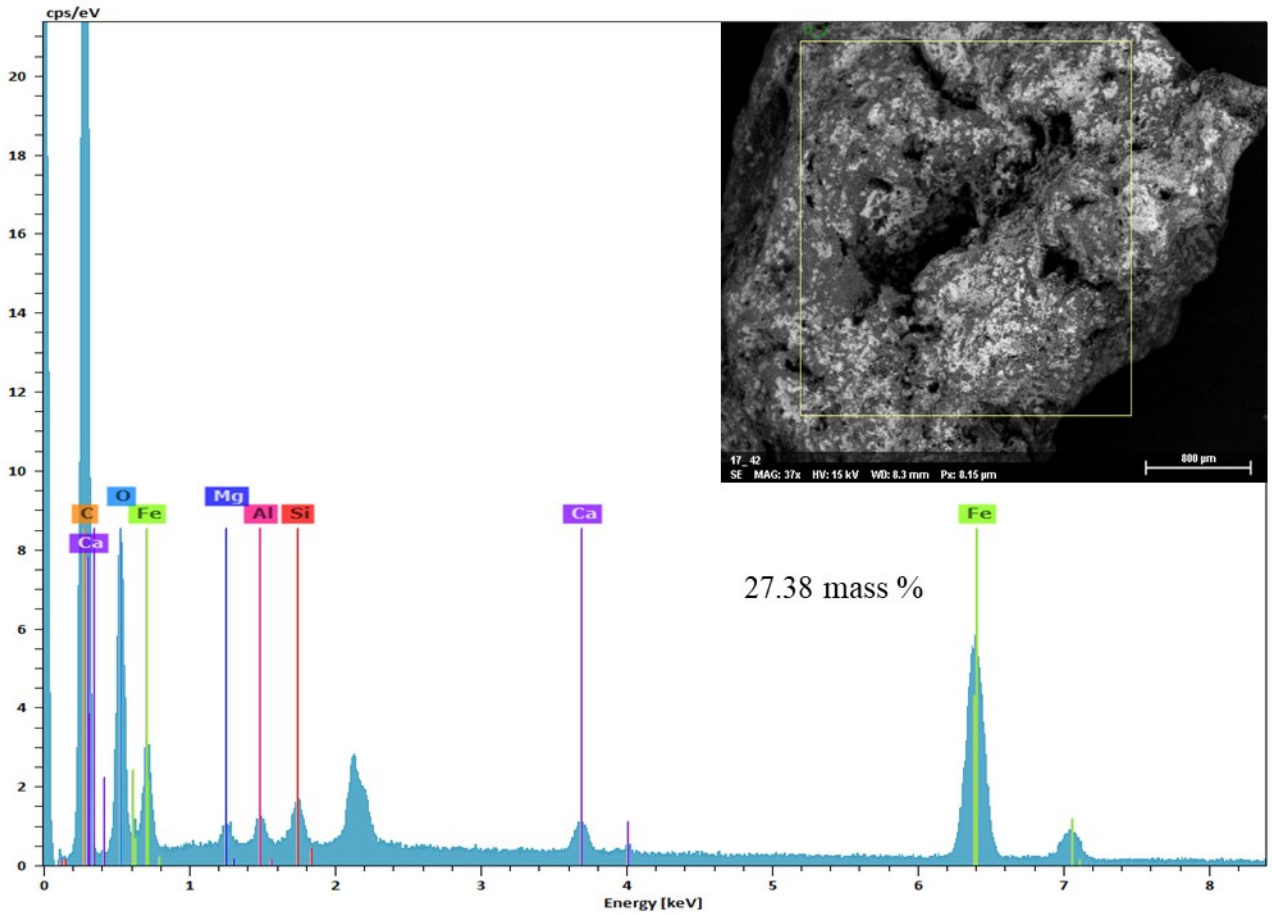

Figure B-5. SEM-EDS spectrum of magnetite doped GAC surface after doping.

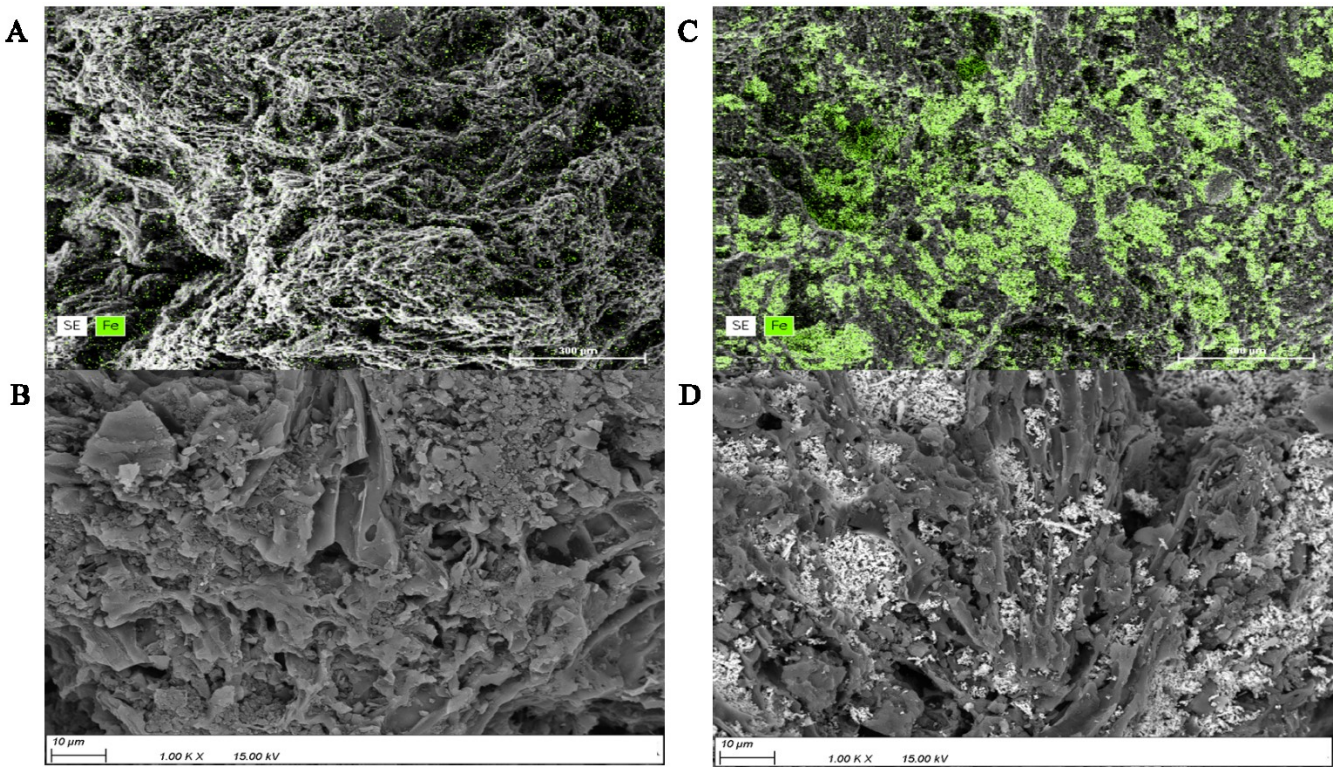

Figure B-6. SEM images of (A, B) undoped GAC surface, and (C, D) magnetite doped GAC surface.

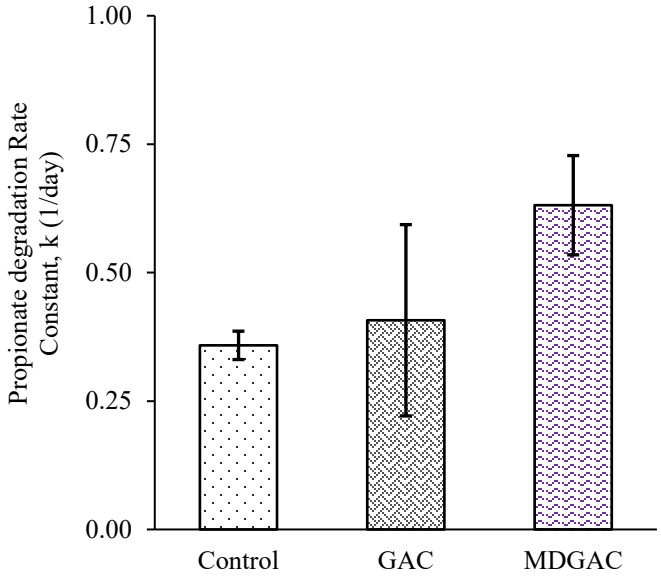

Figure B-7. Propionate degradation rate constant during Cycle #5.